Diploma Thesis
Biomedical Engineering

Monodisperse Oligo(ethylene glycols): Synthesis and Application

performed at the

Institute of Applied Synthetic Chemistry

of the

Technische Universität Wien

under the supervision of

Univ. Prof. Dipl.-Ing. Dr. techn. Johannes FRÖHLICH

and

Ass. Prof. Dipl.-Ing. Dr. techn. Christian HAMETNER

by

Dipl.-Ing. Dr. techn. Daniel LUMPI

0426601

No.555, Jin Feng Road, Min Hang District
5B, Building 3R, Shanghai Racquet Club
Shanghai 201107, China

28. August 2018

DEDICATION & ACKNOWLEDGEMENT

DEDICATION

… Gewidmet meiner geliebten Familie,

Alexandra, Emilia und Noah.

ACKNOWLEDGEMENT

Allen voran möchte ich mich bei Johannes Fröhlich aufrichtig für die Unterstützung während des Studiums „Biomedical Engineering" sowie für die Möglichkeit der Durchführung der dargelegten Diplomarbeit bedanken. Herzlichen Dank für die Freiheit und das Vertrauen, welches Du mir hierbei entgegengebracht hast!

Mein spezieller Dank gilt Christian Braunshier und Christian Hametner für die Unterstützung im Zuge der praktischen Laborarbeit und des Verfassens beider Manuskripte sowie der Diplomarbeit. Unter euer beider Betreuung hat mein wissenschaftliches Arbeiten begonnen, welches mir später so viel Freude bereitet hat – vielen Dank für den guten Einstieg!

Ernst Horkel und Hannes Mikula danke ich für die super Zusammenarbeit innerhalb und außerhalb des Labors. Vielen Dank, Ernstl und Hannes, für die große Unterstützung über so viele Jahre und die lustigen Stunden auch an diversen Partys und Konferenzen!

Meinen Studienkolleginnen Brigitte Holzer und Barbara Pokorny möchte ich natürlich auch herzlich danken. Gizzi und Babsi, es war ein echter Spaß mit Euch durch das Studium zu spazieren!

Meinen zahlreichen Kollegen der Forschungsgruppe Fröhlich im Laufe der Jahre möchte ich für das perfekte Arbeitsklima und die vielen unvergesslichen Momente danken. Ich werde immer sehr gerne an das Arbeiten in der Forschungsgruppe zurückblicken!

Für die sehr gute wissenschaftliche Zusammenarbeit bei der Forschung und der Erstellung der Diplomarbeit danke ich: Robert Liska, Bernhard Zachhuber, Christoph Wagner, Bernhard Lendl, Markus Holzweber und Herbert Hutter.

Allen weiteren Kollegen am Institut möchte ich für die Zusammenarbeit und Unterstützung danken. Außerdem danke ich allen Institutsangestellten, ohne die ein Laborbetrieb in dieser Form nicht möglich wäre. Insbesondere gilt mein Dank Florian Untersteiner und Sabine Stiedry!

Ein spezielles Dankeschön ergeht auch an Martin Haefele sowie meinen derzeitigen Arbeitgeber DSM Nutritional Products AG. Da ein großer Teil des Studiums berufsbegleitend erfolgte, war die mir ermöglichte Flexibilität ein entscheidender Faktor zum erfolgreichen Abschluss!

Abschließend gilt mein größter Dank meiner Familie ohne deren Unterstützung dieses Studium und diese Arbeit nicht möglich gewesen wären. Alexandra, Emilia, Noah, Papa, Mama, Theresa, Marlene, Marianne, Andrea, Hannes – vielen Dank für das mir liebevoll entgegengebrachte Verständnis!

Liebe Alexandra, vielen Dank für Deine unglaubliche Unterstützung. Ich bin Dir sehr dankbar, dass Du mir dieses Studium ermöglicht hast – Du bist die Beste!

Shanghai, 24.08.2018

Daniel Lumpi

ABSTRACT & KURZFASSUNG

ABSTRACT

A convenient approach for the synthesis of monodisperse oligo(ethylene glycols) (OEGs) up to 12 sub-units is described. A novel cleavage protocol replacing laborious hydrogenolysis is introduced to achieve a fast, inexpensive and widely applicable procedure.

FTIR spectroscopy using a fibre optic sensor was applied to monitor the formation of sensitive key intermediates, resulting in optimized reaction times. By applying this in-line technique, the possibility of real-time analysis under inert conditions was impressively demonstrated.

In addition, a series of polystyrene-oligo(oxyethylene) graft copolymers containing the developed monodisperse OEGs (n = 2 − 12) was synthesized. A strong correlation between the linker (OEG) length and the line widths in the ^{13}C gel-phase NMR spectra was proven, with the grafted chain of 8 OEG sub-units giving comparable results in terms of reactivity and gel-phase NMR monitoring to commercially available TentaGel although offering significantly increased loading capacities. Multistep on-resin reaction sequences were performed to prove the applicability of the resins in solid-phase organic synthesis.

KURZFASSUNG

Die Synthese von Oligo(ethylenglykolen) (OEGs) bis zu 12 Untereinheiten wird beschrieben. Das neu entwickelte Abspaltungsprotokoll der Schutzgruppe, als Ersatz zur Hydrierung, führt zu einem effizienten, preisgünstigen und breit anwendbaren Herstellverfahren.

FTIR Spektroskopie, unter Anwendung eines faseroptischen Sensors, wurde zur Verfolgung sensitiver Zwischenstufen eingesetzt, was zu einer deutlichen Optimierung der Reaktionszeiten führte. Diese in-line Technik ermöglichte dabei die Echtzeitanalyse unter inerten Reaktionsbedingungen.

Zusätzlich erfolgte die Synthese einer Serie von Polystyrol-Oligo(ethylenglykol) Copolymeren, welche die entwickelten monodispersen OEGs (n = 2 − 12) enthalten. Eine starke Korrelation zwischen der Länge des Linker (OEG) und der Linienbreite im ^{13}C Gelphasen-NMR Spektrum wurde bestätigt. Dabei führte die Verwendung einer Kettenlänge von 8 OEG Untereinheiten, trotz signifikant erhöhter Beladung, zu vergleichbaren Resultaten bezüglich Reaktivität und Gelphasen NMR Analyse wie kommerziell erhältliche Tentagel-Harze. Mit Hilfe von Mehrschritt-Reaktionssequenzen konnte die Anwendbarkeit der Harze im Bereich der Festphasensynthese demonstriert werden.

TABLE OF CONTENTS

1. INTRODUCTION

1.1. Monodisperse OEGs in biomedical engineering

Oligomers of ethylene glycol (OEGs) have a wide range of applications in many fields of science and industry. They can be applied as synthons for crown ether-type derivatives,[1] non-ionic surfactants,[2] templates for the synthesis of porous inorganic materials,[3] and more recently, functional mono-layers were used to develop biocompatible material.[4-6] In the field of biomedical engineering "hydrogels" are applied due to their unique properties;[7] a more detailed introduction to biomedical applications is given below (chapter 1.1.1.). Particularly PEG fabricated hydrogels have proven advantageous since bulk properties can be tailored through adjustments to the molecular weight and concentration of the PEG subunits.[8] Another application field of OEGs is bioconjugation of proteins, in order to increase the water solubility, which serves as one of the most effective drug delivery systems.[9-11] As a matter of fact, the physical and chemical properties of these modified materials often depend significantly on the number of repetition units of the OEG tether.

The same principles apply for the design of OEG/PEG-grafted polystyrene resins in the field of solid phase organic synthesis (SPOS). The physical and chemical properties, but moreover the properties for on-resin analyses (e.g. gelphase ^{13}C NMR),[12,13] of the resins strongly correlate to the OEG/PEG-linker length applied.[14] The improved characteristics with regard to a "solution-like" environment at high numbers of repetitive ethylene glycol units negatively impact the loading capacity of the resin. Hence, access to monodisperse OEGs enables the optimized design of OEG/PEG-grafted polystyrene resins for SPOS applications.[13]

1.1.1. Hydrogels

Hydrogels have become very popular in biomedical engineering due to their unique properties such as high water content, softness, flexibility and biocompatibility.[7]

Characteristics of hydrogels:[15,16]

- Three-dimensional crosslinking polymer chains
  (through physical, ionic or covalent interactions)
- Not dissolvable in water
- Ability to absorb and retain water
  (dispersed throughout the structure)

The close resemblance of hydrogels to living tissue offers many opportunities for applications in biomedical areas such as contact lenses, hygiene products, drug delivery systems, wound dressing and tissue engineering scaffolds (details on tissue engineering are given below).[7] A comprehensive review on biomedical applications of hydrogels is available by E. Calo and V. V. Khutoryanskiy.[7]

Hydrogels in tissue engineering[17,18]

The natural extracellular matrix (ECM) represents a complex and dynamic environment in human tissue, which is in bidirectional interaction with the embedded cells providing stimuli for e.g. cell proliferation and differentiation. However, these complex interactions are not yet fully understood. Hence, current investigations focus on mimicking key characteristics of the ECM to study cell responses on different chemical, mechanical and topological cues. As different tissues rely on different physical properties and chemical composition of the ECM, there are a number of considerations for the rational design of artificial cell environments.

Hydrogels, being structurally similar to ECM, exhibit a high water content, shape resistivity (but are still deformable) and favorable mechanical properties such as stiffness (comparable to many biological tissues).[19] Therefore, hydrogels represent one of the most promising materials for tissue engineering. In addition their capability of forming 3D cell suspensions, supporting sufficient nutrient diffusion, resulted in successful synthetic hydrogel constructs such as skin[20], tendon[21] and cartilage substitutes[22].

The general approach in tissue engineering is to seed cells into prefabricated scaffolds (that support oxygen diffusion). However, the control of cell density and cell distribution is difficult applying the seeding approach.[23] Therefore, new approaches have recently been developed. Utilizing hydrogel precursors, which can be cross-linked *via* biocompatible mechanisms, potentially allows for the formation of these networks in vivo (in the presence of cells and tissue); thus, encapsulation is realized as part of the fabrication process.[17]

1.1.2. Solid phase organic synthesis

The growing demand in biomedical research is to obtain natural product derived or natural product inspired small molecules to understand biological processes. The access to small molecules as chemical modulators and dissectors of signaling pathways is particularly matter of interest. However, finding chemical probes fulfilling these criteria is a challenging task. Applying aforementioned probes for better understanding of biological processes (normal vs. disease related), the chemical entities could provide valuable starting points for probe discovery research. Inspired by bioactive natural products, the demand to access natural product analogs and natural product-like compounds with the goals of charting the natural product chemical territory has also grown.[24]

High-throughput synthesis methods, such as solid phase organic synthesis (SPOS), have been fundamental in generating complex natural architectures, and in a few cases, their applications are emerging in probe discovery research.[24] Automated synthesis as well as advanced small molecule combinatorial chemistry led to dramatic growth of the use of SPOS resins.[25]

Key advantageous aspects of SPOS:[14]

- Simple separation of target molecules or intermediates bound to solid phase from soluble components in the reaction mixture and the solvent (no evaporation required)
- High reactant concentrations or equivalents in the reaction solution promote the degree of reaction completion
- Simple repetitive work-up procedures allow for integration and automation of SPOS

Further aspects of SPOS:[14]

- 2 additional chemical steps (attachment to and cleavage from solid phase) added to the synthetic route
- Kinetics of solid phase reactions are controlled by diffusion / accessibility of the reactants on the resin and therefore tend to be slower than solution phase reactions
- High excess of reactants can be a limiting factor from a synthesis design perspective
- Reaction monitoring (on-resin analysis) remains a challenging task[12]

1.2. ATR-IR in-line reaction monitoring[26]

This chapter introduces the ATR-IR in-line reaction monitoring technique, which was applied during this thesis to monitor and optimize reaction times for the deprotonation of mono-protected glycols under inert conditions. This literature summary has been previously published as a book chapter[26] and in part in the PhD thesis of D. Lumpi[27].

1.2.1. Introduction

The use of reaction monitoring to determine operation parameters in organic synthesis and pharmaceutical chemistry still commonly relies on off-line approaches. However, application of on-line or in particular in-line methodologies provides highly valuable data with respect to process optimization and scale-up.[28,29] This statement is especially true for time resolved spectroscopic *in-situ* techniques, which allow to gain insights into key intermediate formation or structures, and therefore also provide valuable information for mechanistic considerations.[30,31]

One of the major advantages of in-line techniques (both *in-situ* and real-time) over off-line approaches is that the investigation occurs inside the reaction system, thus eliminating sample alterations prior to analysis. These alterations during probing, including the loss of inertness or changes of reaction conditions, may result in erroneous readings; especially when directly compared to the (batch) process. This dramatically affects investigations at low temperatures. Both sampling and standard bypass approaches do not ensure constant thermal conditions in the course of analysis, which potentially leads to incorrect results. For obtaining real-time information on chemical composition of samples in gas, liquid or solid phase, mid-infrared (IR) spectroscopy proved to be highly versatile, especially when performed utilizing the attenuated total reflectance (ATR) technique.[31-34]

This chapter focuses on in-line monitoring of both highly sensitive and reactive organic key intermediates (reagents) by mid-IR fibre probes based on the ATR technique (Figure 1.2.1.). At first a concise overview on mid-IR spectroscopy is given, which outlines advantages of IR fibre optics as well as ATR technologies and provides insights on fibres suitable for mid-IR fibre applications. The second part is intended to introduce fibre-optic probes available and typical characteristics, referring to literature about chemical and physical properties of modern IR fibre materials, showcasing potential areas of application also briefly commenting on alternative spectroscopic methods.

Figure 1.2.1. Mid-IR fibre and ATR probe (left) and IR probe focused on the ATR element (right).

1.2.2. Monitoring by mid-infrared spectroscopy

Spectroscopy in the mid-infrared of a spectral range from approximately 4000 cm^{-1} to 400 cm^{-1} (2.5 µm to 25 µm) emerged as an effective tool for both qualitative and quantitative analysis. Within this range most of the fundamental molecular vibrations, the first overtones and combination frequencies occur. Such, typically relatively sharp, absorption bands generally possess high absorption coefficients. These desirable spectroscopic properties facilitate an identification of molecules by its specific spectral "fingerprint", but also comprise valuable structural information (e.g. functional groups, substitution patterns, etc.).[35] The distinctive absorption bands associated with individual molecules enables to analyze individual components in even complex mixtures by either evaluating isolated bands or by applying modern chemometric methods (e.g. PCA), which process the entire spectral information. Consequently, mid-IR spectroscopy represents a widely applicable tool for investigations of dynamic processes (e.g. chemical reactions, phase transitions, sedimentations, etc.). Moreover, information about interactions of the analyst with the surrounding media can be acquired because vibrational modes tend to be affected by the molecule's environment.[36]

Therefore, in many perspectives, mid-IR spectroscopy provides clearly more information than spectroscopy in other regions of the spectrum, such as the visible or the near-infrared range.[36]

1.2.3. Mid-infrared optical fibre probes

Modern-technology fibre optics offers important and versatile tools in spectroscopy. In the field of vibrational spectrometry fibre optics had a great influence on near-IR and Raman spectroscopy. The development of mid-IR transparent fibres (discussed in chaper 1.2.5.) in the last decades had a significant impact on IR methods.[37] The fibre application makes it possible to overturn the established method of analyzing samples within the typically stationary IR spectrometer by enabling the direct placement of the fibre-optic probe inside the reaction system of interest.[35]

The technologies of mid-IR spectroscopy providing highly relevant physico-chemical information, and the flexibility of fibre-optic probes offering new possibilities of application to measure samples in gas, liquid and solid phase, result in a breakthrough in molecular spectroscopy. Nowadays, spectroscopy utilizing IR fibre probes is routinely used in research laboratories, process development facilities and industrial quality control. This routine application can be explained by the fact that data, often not available by other methods, can be conveniently acquired.[35]

Additionally, ATR based mid-IR fibre optic probes represent an entirely non-invasive technique, which has recently been shown to be a promising tool e.g. for biotechnological applications[38] and, even more impressively, for obtaining spectroscopic information *in vivo*[39].

In principle, the sensor constructions rely on five basic sensing schemes: transmission, reflection, grazing angle reflection, attenuated total reflection (ATR), and a variant on the ATR effect known as the fibre evanescent wave sensor (FEWS).[35]

1.2.4. Attenuated total reflection

The majority of reported mid-IR fibre probes rely on the well-established attenuated total reflection (ATR) technique, revealing many advantages in the general applicability over e.g. absorption measurements in short pathway flow cells. In the ATR method only a thin film (a few micrometers) at the proximity of the ATR element is subject to the measurement. The thickness of the analyzed film is defined by the penetration depth of the evanescent field (Figure 1.2.2.).
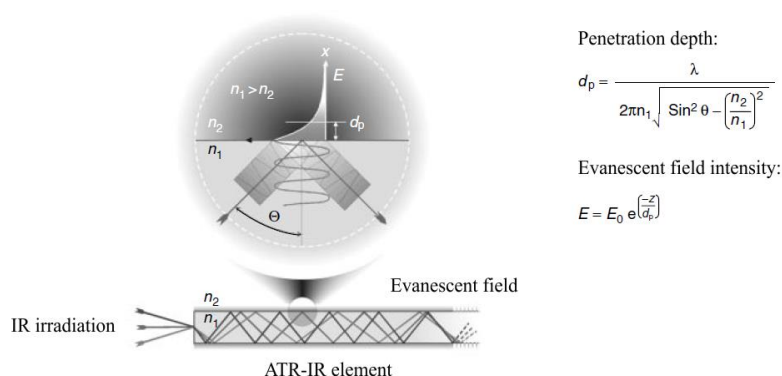

Penetration depth:

$$d_p = \frac{\lambda}{2\pi n_1 \sqrt{\mathrm{Sin}^2\,\theta - \left(\frac{n_2}{n_1}\right)^2}}$$

Evanescent field intensity:

$$E = E_0\, e^{\left(\frac{-z}{d_p}\right)}$$

Figure 1.2.2. Principle of total reflection of an infrared beam at the boundary of the ATR element to a medium with lower refractive index $n_2 < n_1$ (n_1, n_2, refractive indices; θ, angle of incidence; E, exponentially decaying evanescent field; d_p, penetration depth; λ, wavelength of incident radiation); Figure reproduced from Mizaikoff and Lendl.[40]

The interactions of the incident and the internally reflected electromagnetic waves generate an exponentially decaying evanescent field, which penetrates the adjacent medium to a certain depth. The depth of penetration depends on the irradiation wavelength, the incident angle and the refractive indices of both the ATR element and the contact medium. The equations describing this behavior are given in Figure 1.2.2.[40]

1.2.5. Infrared transparent fibres

This chapter serves as brief insight into the most important, for the main part commercially available, IR fibre optics. Detailed reviews on IR fibres are given in literature by J.A. Harrington[41] and with special focus on mid-IR applications by Lendl and Mizaikoff[37].

The basic requirements for mid-IR fibres include physical properties such as transparency over the spectral range requested for the intended investigations, robustness (mechanically), stability (thermally and chemically) as well as adequate flexibility.[37] The characteristic of the optical transparency is typically evaluated by focusing on relevant loss mechanisms. The most important losses include intrinsic and extrinsic losses, Fresnel losses and bending losses (Sanghera & Aggarwal, 1998, as cited in Lendl and Mizaikoff[37]). Available mid-IR fibre optics available meet these challenges to different extents.

First developments on non-silica based IR transparent fibres from chalcogenide glasses, mainly arsenic sulphide, were published in 1965, exhibiting losses higher than 10 dB/m (Kapany & Simms, 1965, as cited in Harrington[41]). Due to an elevated demand for IR fibres in short-haul applications increased research efforts were reported from the mid-1970.[41] Up to date, both optical and mechanical characteristics of IR fibres cannot compete with silica fibres being not applicable in the IR region due to a transmission only up to approximately 2.5 µm. Losses in the range of a few decibels per meter still limit these to short-haul applications. Nevertheless, modern mid-IR fibres for short-haul have already enabled a broad variety of developments in spectroscopy and important usage in practical (e.g. medicinical) applications (Minnich[31], and references therein).

A logical categorization of the most important IR fibres can be drawn out as follows: glass, crystalline and hollow waveguides. Table 1.2.1. outlines this categorization also providing further subdivision based on materials and structures.[41]

Table 1.2.1. Categories of the most important of IR fibres;

Data reproduced from Harrington[41].

Main category	Sub category	Examples
Glass	Heavy metal fluoride (HMFG) Germante Chalcogenide	ZrF_4-BaF_2-LaF_3-AlF_3-NAF (ZBLAN) GeO_2-PbO AsS_3 and AsGeTeSe
Crystal	Polycrystalline (PC) Single crystal (SC)	AgBrCl Sapphire
Hollow waveguide	Metal/dielectric film Refractive index <1	Hollow glass waveguide Hollow sapphire at 10.6 µm

A graphical comparison of attenuation losses of the most relevant mid-IR fibres is given in Figure 1.2.3. Among these, polycrystalline silver halide fibres have been shown to be a promising candidate for mid-IR (ATR) fibre probes, especially for measurements at wavelength > 10 µm. The combination of the flexible structure and IR transmission of these fibres ensures a convenient analytical approach.
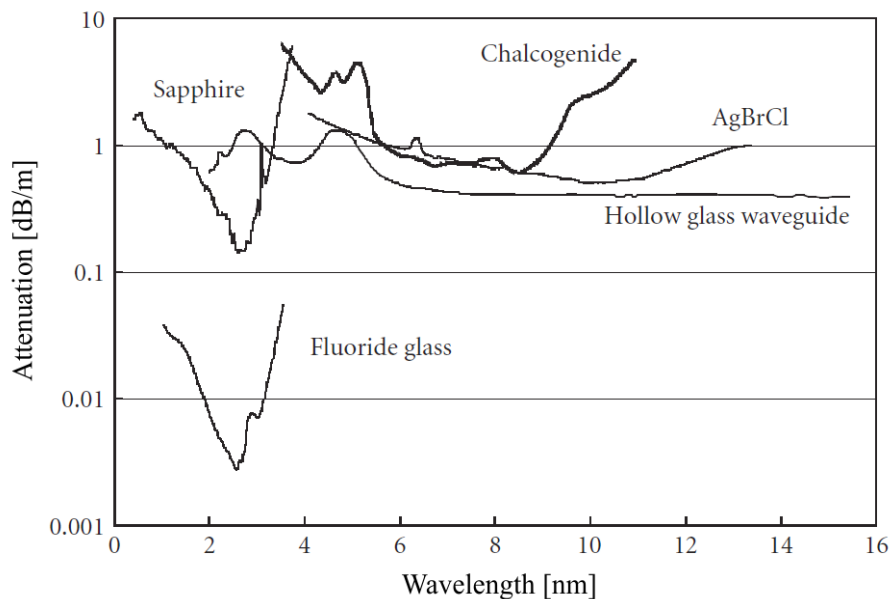
Figure 1.2.3. Composite loss spectra for some common IR fibre optics: ZBLAN fluoride glass, SC sapphire, chalcogenide glass, PC AgBrCl, and hollow glass waveguide; Plot reproduced from Harrington[41].

1.2.6. Alternative spectroscopic methods for reaction monitoring

Besides IR spectroscopy, RINMR (rapid injection nuclear magnetic resonance) experiments also received considerable attention in the field of spectroscopic investigations of highly reactive species, especially under cryogenic conditions. The RINMR methodology, often based on the developments of McGarrity[42], Ogle and Loosli was successfully applied by several research groups to investigate reactive intermediates also at low temperatures and short time scales. Other than conventional NMR studies the rapid injection design relies on a piston-driven syringe injection assembly above the vessel inside the bore of the spectrometer magnet. This setup simultaneously provides turbulent mixing in the sample. In first studies McGarrity et al. could establish that butyllithium in THF exists in equilibrium of the tetramer and the dimer complex with the proportion of dimer increasing as the temperature is decreased.[43] Moreover, kinetic examination proved that the dimeric butyllithium is more reactive toward the applied electrophiles than the tetramer by a factor of 10.[44] Improved designs of RINMR systems implementing features such as multiple reactant and faster rapid injection were developed in the last decade.

Concluding, RINMR is a powerful tool to monitor reactive intermediates, directly providing highly relevant structural data. However, the experimental complexity of this technique, in contrast to ATR-IR fibre probe applications, certainly limits its versatility.

1.3. Objective

The first and primary goal of this diploma thesis is the development of a synthetic protocol to obtain monodisperse oligo(ethylene glycols) (OEGs) complying with the following requirements:

- Selective (avoidance or simple and efficient removal of by-products)
- Efficient (optimized reaction parameters and times)
- Low cost (low cost reactants and high atom efficiency)
- Broadly applicable (avoidance of special equipment and hazardous reaction conditions)
- Scalable (efficient work-up procedures)

Preliminary research in the group of J. Fröhlich by C. Braunshier and C. Hametner revealed that procedures fulfilling all aforementioned targets have not been available in literature. Hence, the diverse applications of OEGs in many fields of science (chemistry, engineering, biology, etc.) make the research relevant for a broad community.

The scope for the range of accessible monodisperse OEGs by the synthetic route in this diploma thesis is limited to n = 6, 8, 10 and 12 (see Figure 1.3.1.). However, a building block sequence set-up enabling access to larger OEG chains (n > 12) further expands the versatility of the protocol.
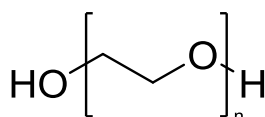
Figure 1.3.1. Molecular structure of OEGs.

The focus is mainly given by the intended application of the developed OEGs in the field of solid phase organic synthesis (SPOS). Preliminary research on novel resins for SPOS in our research group revealed the dependence between OEG/PEG-"linker" length and line-width in gel-phase ^{13}C NMR spectra,[12] which is a crucial factor for on-resin analysis (further details are given in chapter 2.3.1.). Hence, the developed OEG based poly(styrene-oxyethylene) graft copolymers (PS-PEG) could be optimized regarding loading capacity and spectral quality (non-destructive analysis).[13]

In addition to the improved availability of monodisperse OEGs, which represents the foundation for a convenient access to the novel PS-PEG resins, the second goal of this thesis is to prove the performance and reliability of these resins. Hence, a comprehensive collection of application examples for the PS-PEG resins is a matter of interest.

2. GENERAL PART

2.1. Synthetic approach

Potential retrosynthetic disconnections towards monodisperse OEGs are shown for OEG (n = 6) in Figure 2.1.1. All approaches are limited to nucleophilic substitution reactions (leaving group and protective group introductions) due to objectives given by experimental and practical requirements (efficient work-up, low cost, broad applicability, etc. – also see chapter 1.3.).
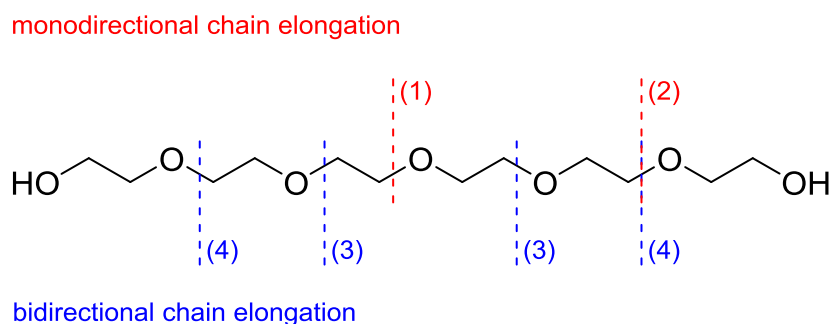

Figure 2.1.1. Retrosynthetic disconnections for monodisperse OEG (n = 6).

Within the scope of target compounds of this thesis (n = 6, 8, 10, 12) several options of chain elongation have been evaluated as follows:

- Both options of monodirectional chain elongation require for specific substrates for all desired target compounds (synergetic effects limited).
  (1) Monoprotected (protective group) and/or monoactivated (leaving group) substrate for n = 3, 4, 5 and 6 for respective target compounds n = 6, 8, 10 and 12.
  (2) Monoprotected (protective group) and/or monoactivated (leaving group) substrate for n = 1, 5, 7, 9 and 11 for respective target compounds n = 6, 8, 10 and 12.

- Both options for bidirectional chain elongation offer access to all target compounds with only four specific starting materials (high synergetic effect).
  (3) + (4) Monoprotected (protective group) as well as biactivated (leaving group) substrate for n = 2 and 4 affords all desired target compounds n = 6, 8, 10 and 12.
  In addition, this strategy can be readily extended to larger n values by biactivation (leaving group) of the respective target compounds (example: n = 8 yields n = 14 and n = 18 straight forward by this strategy).

Therefore, both bidirectional disconnection 3 and 4 were chosen for further literature screening.

To the best of our knowledge, the most promising synthetic approach, applying bidirectional chain elongation, was published by Keegstra et al. (Scheme 2.1.1.).[45] Taking this sequence as a starting point, we intended to both optimize and/or substitute key steps to shorten reaction times from periods as long as several days to more acceptable values. Optimizing the sequence results in an easy to handle, fast and low-cost synthetic procedure for well-defined OEGs.


1a-b: k=2,4   **2a-b**: m=2,4   **3a-d**: n=6,8,10,12   **4a-d**: n=6,8,10,12
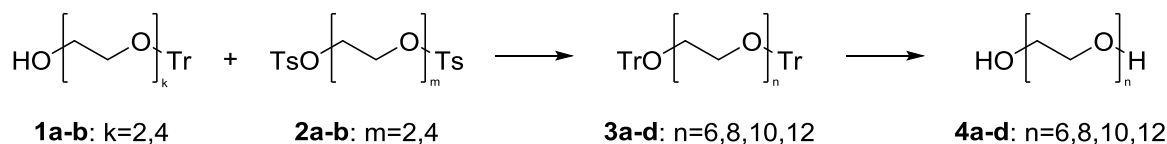
Scheme 2.1.1. Synthetic route according to Keegstra et al.[45]

The literature search was supported by experimental attempts to optimize the sustainability of the synthetic sequence (e.g. atom efficiency by replacing protective groups) in the J. Fröhlich research group under supervision of C. Braunshier and C. Hametner. However, the molecular set-up of the reaction turned out to be suitable in terms of reactivity (e.g. stability of protective groups) but an optimization of reaction parameters and conditions remains a matter of interest. The details of the optimizations are summarized for each reaction step separately in chapters 2.2.1. – 2.2.3.

2.1.1. Deprotonation reaction

*The synthesis is carried out as follows: Under inert atmosphere, a 4-neck round bottom flask equipped with mechanical stirrer, reflux condenser, thermometer as well as dropping funnel and the ATR-IR probe inlet is charged with sodium hydride (NaH) and dry THF. To the well stirred suspension is added the mono-trityl protected glycol **1** at ambient temperature.*

Both trityl protective groups and NaH as base proved to be appropriate choices with regard to stability and reactivity. The first step of the reaction shown in Scheme 2.1.2. (deprotonation of mono-trityl protected glycols **1a-b**) is reported to take at least 18 h to reach completion.[45]

1a-b: k=2,4   **2a-b**: m=2,4   **3a-d**: n=6,8,10,12
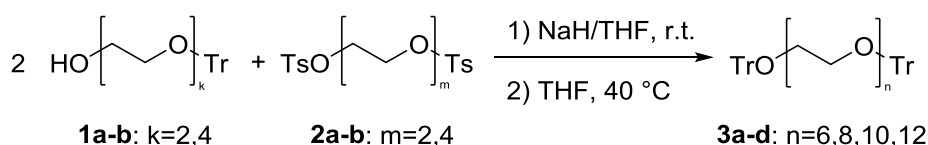
Scheme 2.1.2. Synthesis of Glycols **3a-d**; Monitoring via ATR-IR-sensor spectroscopy.

To verify this, it was necessary to monitor the conversion in an inert, anhydrous reaction medium. Encouraged by recent studies,[31,46,47] a mid-IR fibre optic probe was chosen for fast in-line monitoring

of the chemical reaction under investigation. The ATR fibre system consisted of the FT-IR spectrometer Bruker Matrix F® in connection with an ATR fibre probe (A.R.T. Photonics, Berlin; Ø 12 mm) and a MCT (mercury cadmium telluride) detector (Belov Technology, Co., Inc.). The probe was directly inserted through the ground neck of the reaction vessel and comprised two 1 m silver halide fibres (Ø 1 mm) connecting to a conical two bounce diamond ATR element housed in a rod of hastelloy. Using this set-up (see Figure 2.1.2.) it was possible to follow the reactions to be studied in real-time covering a spectral range from 600 to 2000 wavenumbers.
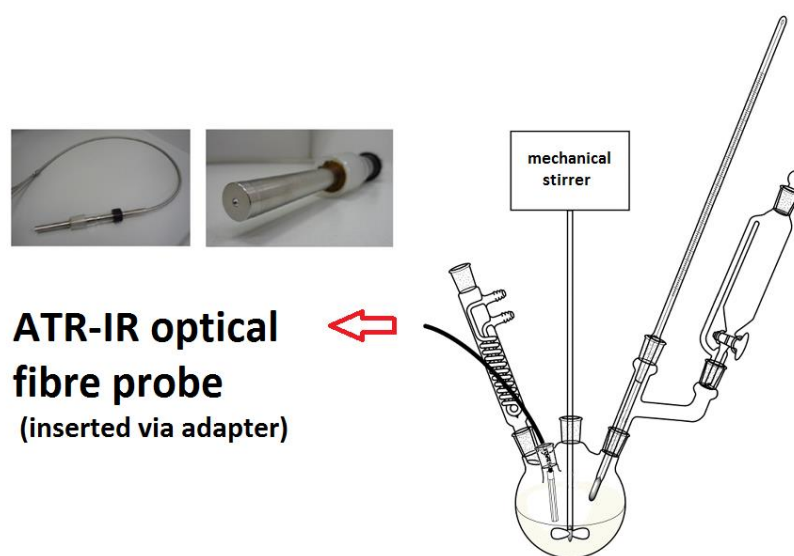
Figure 2.1.2. Experimental set-up for the deprotonation reaction.

The major advantage of in-line *vs.* at-line ATR-IR-spectroscopy is that monitoring takes place inside the reaction system, thus eliminating steps such as work-up of samples prior to analysis, which avoids the risk of contamination or loss of inertness. In our work, we focus on the deprotonation of the mono-protected glycols **1a-b**. The progress of these reactions can either be determined by tracking changes in absorbance values at selected wavenumbers or applying modern chemometric methods, which process the entire spectral information. Among these multivariate curve resolution, alternating least squares (MCR-ALS) needs to be mentioned.[48] This technique decomposes the recorded data set into smaller matrices containing information on the spectra and the concentration profiles of each component involved in the reaction. A recently available user-friendly interface for Matlab facilitates this type of data analysis. All IR measurements were conducted in collaboration with the B. Lendl research group supported mainly by B. Zachhuber and C. Wagner.

Indeed, measurements indicated a rapid conversion of glycols **1a-b** to the corresponding alkoxides; 2D and 3D plots for the deprotonation reaction of **1b** are depicted in Figure 2.1.3.
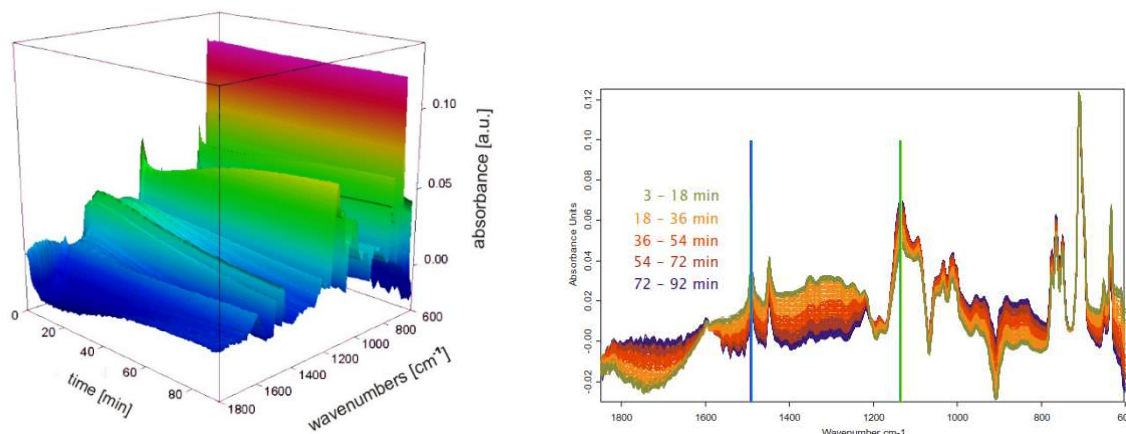
Figure 2.1.3. ATR-IR in-line monitoring of deprotonation reaction of **1b**; 3D-plot (left) and 2D-plot (right).

Absorbance values at characteristic wavenumbers for the substrate and the product are plotted *vs.* reaction time in Figure 2.1.4. (representative for **1b**). The blue curve derives from substance **1b**, the green graph originates from deprotonated **1b**. Monitoring here did not employ the more complex MCR-algorithm, but just non-overlapped single band monitoring. The graph clearly shows that after 90 min no significant changes of absorption values can be observed, thus being an indicator for the end of the reaction.
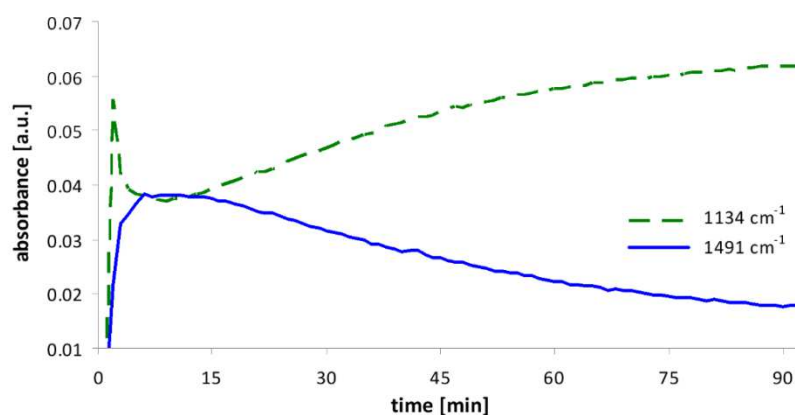
Figure 2.1.4. ATR-IR in-line monitoring for the deprotonation of monoprotected glycol **1b**;
Distortions for t ≤ 10 min are attributed to equilibration effects (temperature and concentration).

In fact, we could prove that this step is completed after a reaction time of 90 min for glycol **1b** and 210 min for **1a** respectively. The longer reaction times for **1a** are attributed to electronic effects and dissolution processes involved for the solid material. The additional reaction time of 30 min for both substrates **1a** and **1b** was chosen to ensure full conversion (homogeneity issues, etc.). The respective yields of the entire reaction, including the subsequent nucleophilic addition, are given in chapter 2.1.2.

Further data analyses, considering the entire spectral information, were carried out by B. Zachhuber. The calculations were performed applying the MCR-ALS (further information on the MCR-ALS method is given in the supporting information of D. Lumpi et al.[49]); the results are depicted in Figure 2.1.5. and consistently indicate a completion of the reaction after 90 min.
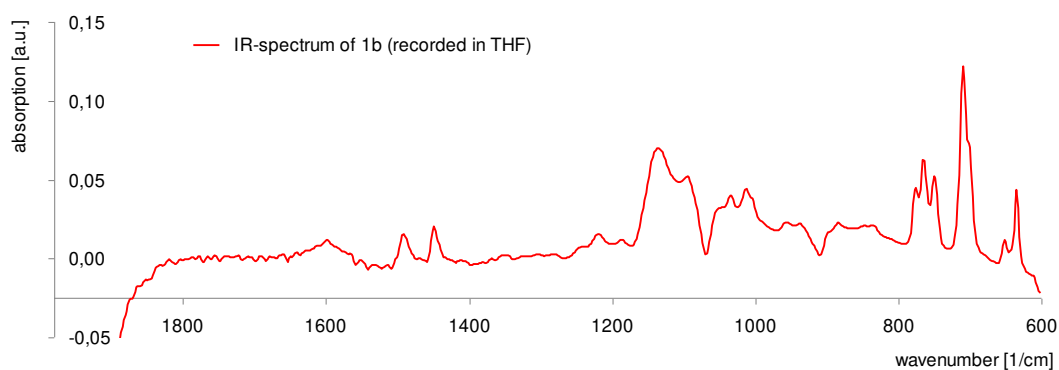
(a)
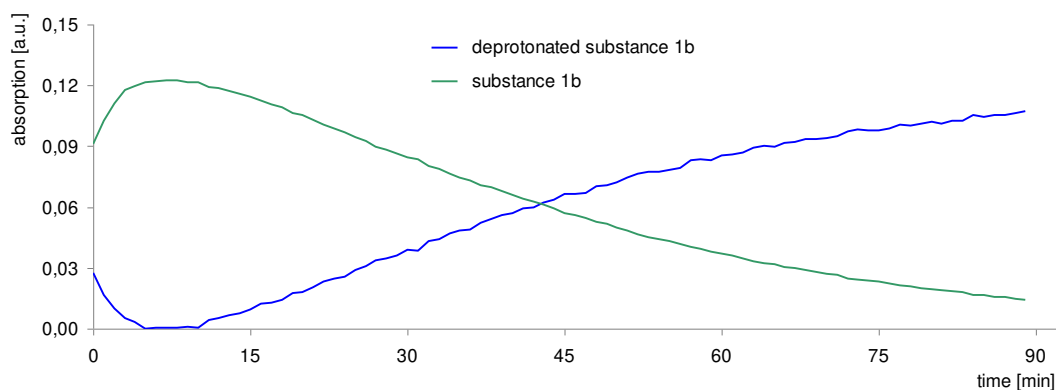
(b)
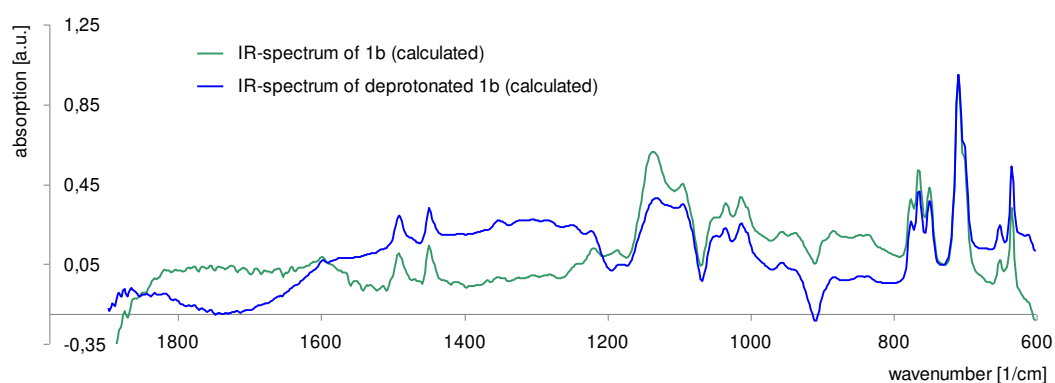
(c)

Figure 2.1.5. MCR-ALS calculations of the deprotonation of trityl-protected **1b**; (a) calculated absorption profiles, (b) spectra calculations, (c) pure substance **1b** spectrum.

2.1.2. Nucleophilic Addition

*The synthesis is carried out as follows: After completion of the deprotonation reaction according to IR-monitoring, the mixture is cooled to 0 °C and a solution of di-tosylated glycols **2** in dry THF is added. The temperature is adjusted to 40 °C and the suspension stirred until full conversion (indicated by thin layer chromatograpy). The work-up is accomplished by extraction and solvent evaporation to yield the pure di-tritylated compounds **3**.*

According to the original procedure, the nucleophilic reaction of the alkoxide with the tosylated glycols **2a-b** (see Scheme 2.1.2. in chapter 2.1.1.) has to be performed at ambient temperature. Refluxing the reaction mixture in THF as solvent to increase conversion rates leads to products, which were dark in color and contaminated by inseparable impurities (undefined formation of higher homologues). However, optimization studies showed that performing the reaction at 40 °C shortens the time from 96 h to 58-80 h avoiding the formation of unwanted by-products (yields and reaction times are summarized in Table 2.1.1.).

Table 2.1.1. Reaction times and yields for the preparation of **3a-d**.

Entry	Glycol 1	Tosylate 2	Time [h][a]	Product 3	Yield [g][b]	Yield [%][b]
1	**1a**	**2a**	4/84	**3a**	18.8	98
2	**1a**	**2b**	4/84	**3b**	165.4	97
3	**1b**	**2a**	2/60	**3c**	23.2	98
4	**1b**	**2b**	2/60	**3d**	24.6	95

[a] Times given refer to deprotonation and overall reaction time, respectively
[b] Isolated yields

The reaction conversion was monitored by thin layer chromatography (TLC). ATR-IR in-line monitoring, although already installed in the experimental set-up, did not yield conclusive results. This fact can be explained as follows: (1) temperature changes and dilution due to the addition of additional solvent; (2) the long-term stability of the applied optic set-up was limited to a few hours due to instabilities of the sensor positioning. Both factors lead to significant effects on the spectral baseline and therefore to external effects (signal shifts) more significant than the changes caused by

reaction conversion. The optical set-up is illustrated in Figure 2.1.6.; it is also worth mentioning that more long-term stable and compact optical set-ups are commercially available.
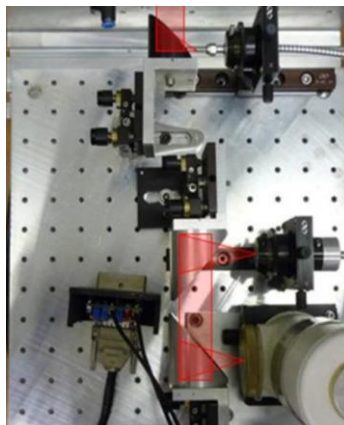

Figure 2.1.6. Representative optical set-up of ATR-IR monitoring system.

Important prerequisites to ensure the desired outcome of the reaction:

- Stick to the given reaction times to ensure full conversion
- Follow the given temperature profiles to avoid decomposition
- Exact compliance with given reaction equivalents to avoid impurities caused by reactants (see Figure 2.1.7.)

Deviations from the key points above potentially lead to impurities difficult to separate from the main product resulting in tedious work-up procedures (e.g. liquid chromatography).
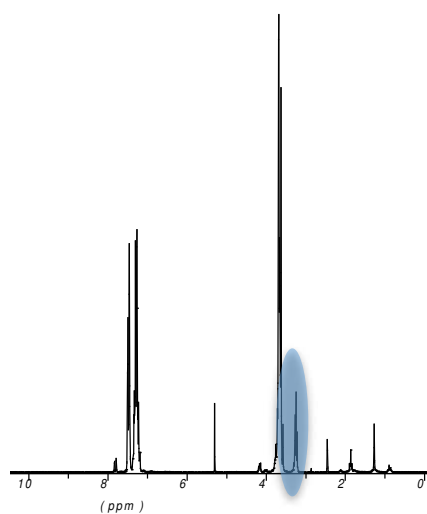
Figure 2.1.7. ^{1}H NMR spectra of nucleophilic addition reaction;
Spectrum of raw product indicating incomplete conversion or wrong equivalent adjustment,
area marked in blue specific for reactant **1a**, spectrum reproduced from Waldner[50].

2.1.3. Deprotection reaction

The synthesis is carried out as follows: The di-tritylated glycols 3 and AcOH (80 %) are stirred for 2 h at 40 °C. Then the mixture is cooled to ambient temperature, poured on ice water and the precipitate filtered off over a glass sinter funnel. After concentration, the filtrate is again poured on ice water and filtered through the existing filter bed. After the solvent evaporation the pure product is obtained.

To obtain the desired oligo(ethylene glycols) **4a-d**, the protecting groups have to be cleaved off. Virtually all published procedures use hydrogenolysis under high-pressure conditions in the presence of palladium for several days to achieve this final transformation. Aside from long reaction time, this procedure suffers from some more disadvantages. The most serious one is the need for equipment allowing to perform gas reactions under high pressure, which might be a limiting factor. Furthermore, the reaction was never quantitative in our hands, always leaving small amounts of protected glycols in the product. Finally, the use of halogenated organic solvents, e.g. dichloromethane and transition metal catalysts might become troublesome, if the final product is intended to be used in the field of pharmaceutics or biology, especially when the procedure is performed on industrial scale.

Our approach was to substitute this deprotection step against a safe, fast and inexpensive procedure. To the best of our knowledge, the well known acidic cleavage of trityl groups was not reported for this substance class until now (see Scheme 2.1.3.). This is quite surprising, as we could show that the usage of aqueous acetic acid leads to pure products **4a-d** in nearly quantitative yields avoiding any tedious workup or implementation of chromatographic methods.

H_2,Pd/C, DCM, r.t., 2-4 days

TrO[O]$_n$Tr   HO[O]$_n$H

3a-d: n=6,8,10,12   80% AcOH, 40 °C, 2 h   **4a-d**: n=6,8,10,12
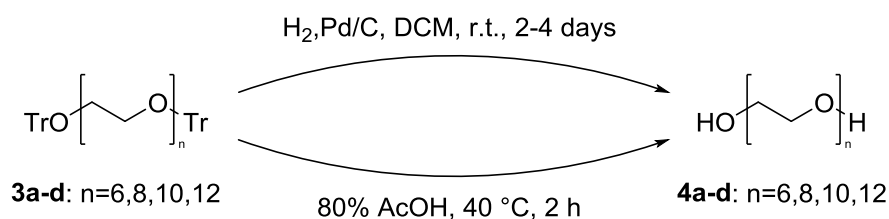
Scheme 2.1.3. Synthesis of glycols **4a-d**; Hydrogenolysis vs. acidic cleavage.

In preliminary experiments the reaction optimization was conducted. The maximum acceptable reaction temperature was determined to be 40 °C; higher reaction temperatures lead to the formation of specific by-products. To obtain the molecular structure of the formed by-product an additional experiment performing the deprotection reaction for **3b** with an excess of AcOH (80 %) at boiling temperature was carried out by B. Waldner.[50] The results clearly indicate the formation of the di-acetate (see spectrum of raw product in Figure 2.1.8.).
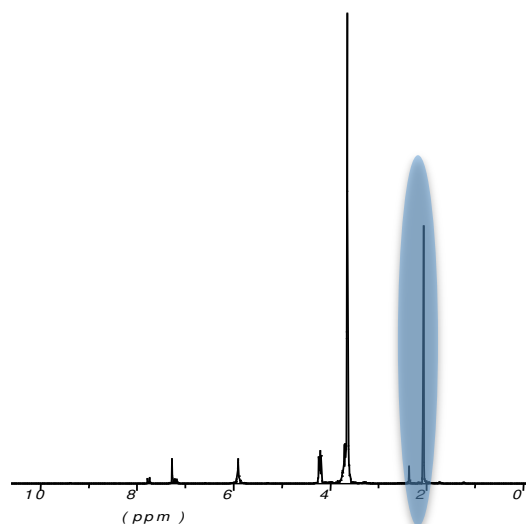
Figure 2.1.8. ^{1}H NMR spectra of raw di-acetate of **4b**, area marked in blue specific for acetate groups; Spectrum reproduced from Waldner[50].

In case of unwanted formation of the di-acetate (overheating of reaction mixture, etc.), the deprotection of the acetate groups *via* methanolate catalysed transesterification was proven for one example. Applying sodium methoxide (NaOMe) in dry MeOH yielded the desired glycol in almost quantitative yield; the detailed experimental procedure is available in the report of D. Lumpi[51].

The reaction times at a reaction temperature of 40 °C (AcOH, 80 %) were first probed by HPLC (high performance liquid chromatography). Preliminary small-scale trials for the deprotection of **3d** indicate a reaction time of roughly 60 min; HPLC spectra are depicted in Figure 2.1.9.
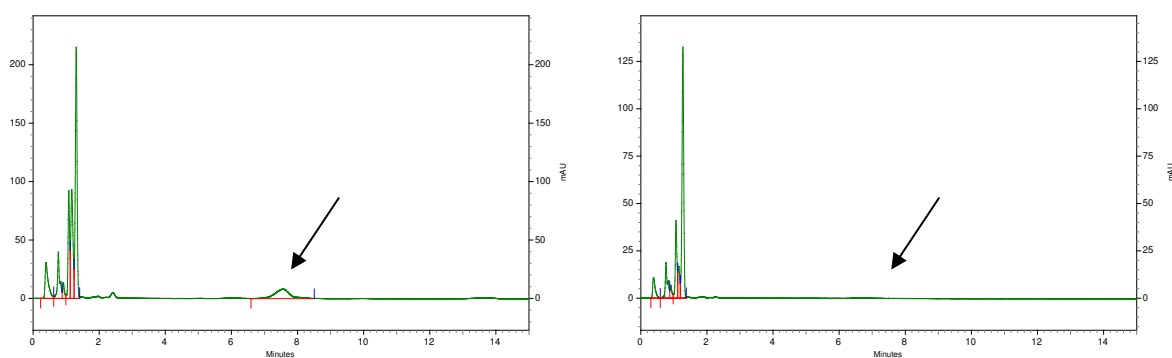
Figure 2.1.9. HPLC spectra of the deprotection reaction; Reaction time = 30 min (left); Reaction time = 60 min (right); Retention time of substrate **3d** = 7.55 min.

Based on this first indication ATR-IR monitoring was chosen to further determine the reaction time on experimental scale. All IR measurements were conducted in collaboration with the B. Lendl research group supported mainly by B. Zachhuber and C. Wagner. The acquired IR data, representatively depicted for substrate **3c**, are illustrated in Figure 2.1.10.
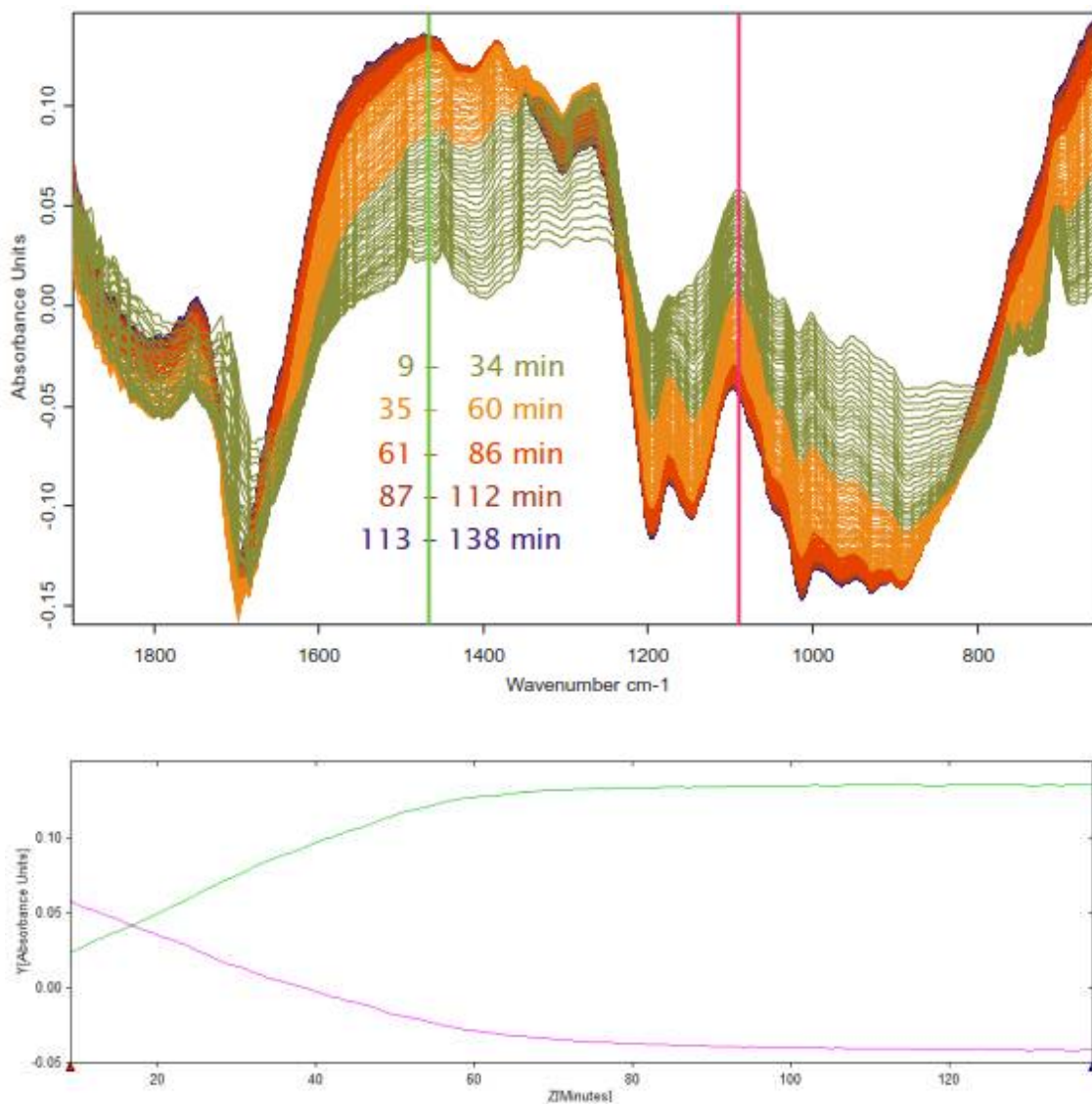

Figure 2.1.10. ATR-IR in-line monitoring of deprotection reaction of **3c**; 2D-plot (top); Concentration profile (bottom); Substrate = pink @ 1094 cm^{-1}, product = green @ 1470 cm^{-1}).

The data indicates a reaction time of 90 min to reach full conversion on experimental scale; this value was confirmed for all substrates either by IR or HPLC measurements. Hence, the reaction time was defined to 120 min; the additional reaction time of 30 min for all substrates was chosen to ensure full conversion (homogeneity issues, etc.). The results are given in Table 2.1.2.

Table 2.1.2. Yields for the preparation of **4a-d**.

Entry	Tritylate 3	Product 4	Yield [g][a]	Yield [%][a]
1	**3a**	**4a**	5.5	98
2	2 **3b**	**4b**	53.2	96
3	3 **3c**	**4c**	9.0	98
4	4 **3d**	**4d**	10.8	99
[a]Isolated yields; reaction conditions: AcOH (80 %), 40 °C, 2 h				

Comparing this new protocol to hydrogenolysis, the advantages are clearly visible: dramatically shortened reaction times (2 h *vs*. 4 days), easier workup and higher product quality (purity determined by ^{1}H NMR; compared to products synthesized in our lab according to literature[45]).

Moreover, nearly theoretical amounts of triphenylmethanol (pure according to combustion analysis) is isolated during work-up, which can be efficiently transformed to tritylchloride[52] enhancing the atom efficiency of the entire synthetic route.

2.2. Application example

As referenced in the introduction, solid phase organic synthesis (SPOS) plays a significant role in many fields of chemistry and engineering (pharmaceutical chemistry, biomedical engineering, etc.). The research presented in the chapter "application example" specifically demonstrates the applicability of the developed monodisperse OEGs (chapter 2.1.) in the field of SPOS.

2.2.1. Context of contribution

Poly(styrene-oxyethylene) graft copolymer (PS-PEG) resins for solid phase organic synthesis (SPOS) provide good swelling in a variety of solvents from medium to high polarity compared to non-grafted polymer resins.[53] PS-PEG resins are designed by grafting ethylene oxide to the PS backbone creating long flexible polydisperse chains, which leads to a "solution-like" environment for the attached moieties. Therefore, also high quality gelphase ^{13}C NMR spectra, an important non-destructive on-resin analysis, can be achieved.[25,54,55] The main drawback of PS-PEG resins is the low loading capacity of the resins (e.g. TentaGel; about 0.3 mmol/g) compared to a PS resin (Merrifield; 1.0-1.5 mmol/g).[13]

The aim of previous research[13] in the J. Fröhlich research group was the development of new resins bearing shorter monodisperse OEG/PEG-"linkers" (n = 2-12 units) compared to commercially available TentaGel (n = ~ 68 units). The reduction in OEG/PEG-"linker" length enables increased loading capacity and improved spectral quality (gelphase ^{13}C NMR) by a decrease of OEG/PEG content of the resin.

The synthetic approach is illustrated in Scheme 2.2.1.; further information is available in literature.[13]
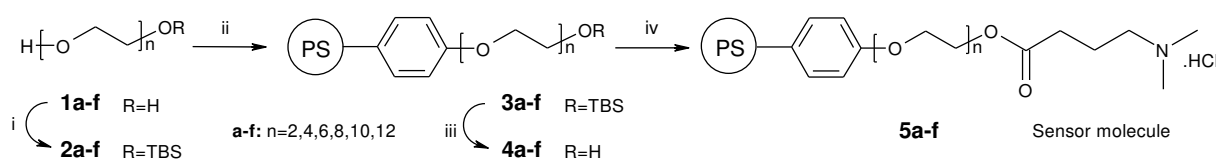
Scheme 2.2.1. Synthetic approach in the research of C. Braunshier et al.;
Scheme reproduced from C. Braunshier et al.[13]

The target resins **4a-f** were loaded with a sensor molecule (see Scheme 2.2.1.) and subjected to gelphase ^{13}C NMR spectroscopy. Both an increase of sensor signal intensity as well as a reduced PEG signal was found for decreasing OEG/PEG-"linker" length. To quantify the spectral quality the average half-height line width of all non-quaternary carbon peaks of the immobilized sensor molecule was

determined (see Figure 2.2.1.). In fact, improving the solvation and mobility of the attached sensor with increasing OEG/PEG-"linker" length, the line width decreases. However, a significant effect on the line-with, and therefore the spectral quality, was only determined up to 8 OEG/PEG units.[13]
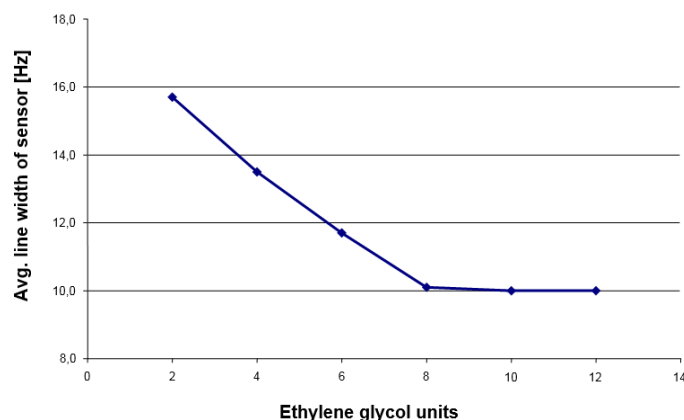

Figure 2.2.1. Effect of OEG group length on the average half height line width of the sensor molecule; Graph reproduced from C. Braunshier et al.[13]

Hence, it has been demonstrated that the introduction of monodisperse OEGs enables the preparation of SPOS resins with and increased loading capacity (0.9 mmol/g for n = 8 (**5d**) vs. 0.3 mmol/g for TentaGel) still revealing virtually the same spectral quality (half-height line width gelphase ^{13}C NMR).[13]

The development of a solid synthetic procedure towards monodisperse OEGs, as outlined in the first part of this thesis, sets the basis for the accessibility of the new resins. In the second section of this thesis, the effectivity and reliability of the developed PS-PEG resins is to be proven in a comprehensive selection of practical application examples.

2.2.2. Statement of contribution

The synthetic and analytical methodology was developed by CB, CH and JF. DL performed parts (mainly hydantoin route and starting resin synthesis) of the synthetic experiments under supervision of CB, CH and JF. Solid phase NMR was performed by DL, CB, EH and CH. Infrared spectroscopy was performed by CB and DL. Microscopic images were recorded by DL supported by M. Holzweber and H. Hutter. The manuscript was drafted by DL, CB and EH; all authors contributed to corrections and discussions of the manuscript prior to submission.

None of the content has been previously published or utilized in Master or PhD related theses by DL.

DL = Daniel Lumpi / CB = Christian Braunshier / EH = Ernst Horkel /
CH = Christian Hametner / JF = Johannes Fröhlich

2.2.3. Original work[56]

The original manuscript published in the journal Combinatorial Science ("Synthesis and Application of Monodisperse Oligo(Oxyethylene)-Grafted Polystyrene Resins for Solid-Phase Organic Synthesis"; DOI: 10.1021/co500028h) is reprinted on the subsequent pages.

ACS Combinatorial Science

Synthesis and Application of Monodisperse Oligo(Oxyethylene)-Grafted Polystyrene Resins for Solid-Phase Organic Synthesis

Daniel Lumpi, Christian Braunshier,* Ernst Horkel, Christian Hametner, and Johannes Fröhlich

Institute of Applied Synthetic Chemistry, Vienna University of Technology, Getreidemarkt 9/163, 1060 Vienna, Austria

S *Supporting Information*

ABSTRACT: In a preliminary investigation by our group, we found that poly(styrene-oxyethylene) graft copolymers (PS-PEG), for example, TentaGel resins, are advantageous for gel-phase ^{13}C NMR spectroscopy. Because of the solution-like environment provided by the PS-PEG resins, good spectral quality of the attached moiety can be achieved, which is useful for nondestructive on-resin analysis. The general drawbacks of such resins are low loading capacities and the intense signal in the spectra resulting from the PEG linker (>50 units). Here, we describe the characterization of solvent-dependent swelling and reaction kinetics on a new type of resin for solid-phase organic synthesis (SPOS) that allows an accurate monitoring by gel-phase NMR without the above disadvantages. A series of polystyrene-oligo-(oxyethylene) graft copolymers containing monodisperse PEG units ($n = 2-12$) was synthesized. A strong correlation between the linker (PEG) length and the line widths in the ^{13}C gel-phase spectra was observed, with a grafted PEG chain of 8 units giving similar results in terms of reactivity and gel-phase NMR monitoring to TentaGel resin. Multistep on-resin reaction sequences were performed to prove the applicability of the resins in solid-phase organic synthesis.

KEYWORDS: *PS-PEG resin, SPOS, gel-phase NMR spectroscopy, nondestructive on-resin analysis, on-resin reaction monitoring*
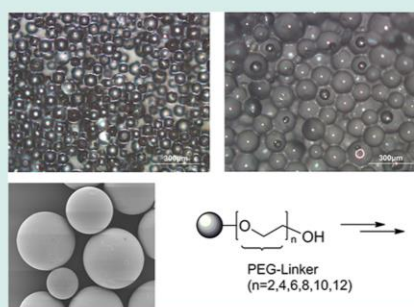
■ INTRODUCTION

For the synthesis of substance libraries, the use of combinatorial chemistry techniques is nowadays state of the art. As a result of the advantage of simplifying synthesis and product isolation, polymer-supported approaches are widely applied, and therefore suitable for potential automation. Recent developments in organic synthesis have established the applicability as a catalyst carrier (e.g., cross-coupling chemistry) enabling practicable recycling of expensive compounds.[1–4]

As a matter of fact, solid-phase organic synthesis (SPOS) plays a major role in combinatorial chemistry.[5,6] The success of any SPOS strategy strongly depends on the properties of the applied resin. Cross-linked polystyrene resins (PS) were initially used, with the disadvantage of limited swelling properties in polar solvents, like methanol or water. To obtain beads with a more universal swelling behavior, PS-based resins have been modified with poly(ethylene glycol) (PEG) chains as spacer (PS–PEG) or cross-linking units.

The PS–PEG supports (TentaGel), first reported by Bayer and Rapp,[7] show good swelling properties in a variety of solvents from medium to high polarity. Furthermore, the resins provide high quality ^{13}C gel-phase NMR spectra, a convenient technique for nondestructive on-resin analysis.[8–16] The copolymers are produced by grafting ethylene oxide to the PS backbone, creating long flexible polydisperse chains (the commercial resins TentaGel and ArgoGel bear about 60–70 PEG units) to provide a "solution-like" environment for attached moieties. The main drawback of such resins is the

low degree of loading capacity (about 0.2–0.3 mmol/g), compared to classical PS resin (e.g., Merrifield, 1–1.5 mmol/g), and an intense signal in the gel-phase spectra resulting from the long oxyethylene units.[13] Moreover, the effect of variable linker chain length on the efficiency of immobilized catalyst systems has previously been demonstrated.[17]

Our strategy relies on substituting the long PEG chains for shorter monodisperse oligo(oxyethylene) tethers ($n = 2-12$ units) with the goal of increasing the loading and minimizing the PEG signal in the gel-phase spectra. In our previous publication, the design and synthetic access of these PS–PEG resins has been presented,[18] conducting a systematic investigation focusing on the effects of the PEG group length on the quality of gel-phase ^{13}C NMR spectra. As a result, an optimum PEG chain length in terms of NMR properties and loading capacity has been determined. The objective of this manuscript is to demonstrate the applicability of the PS–PEG resins in SPOS compared to commercially available resins.

The contribution is divided into two subunits. First, an extension of the investigation toward an efficient synthetic route toward PS–PEG resins is described, including an advanced analytical characterization (IR, gel-phase NMR, combustion analysis, microscopy) of the obtained solid supports. Second, examples of successful application in diverse

multistep reaction sequences are outlined (Wang-linker synthesis, palladium-catalyzed cross coupling, hydantoin synthesis). The performance of the developed resins is compared to commercially available supports (Wang resin, Reactagel, TentaGel). Hence, this study reveals the advantageous properties in terms of efficiency and reaction monitoring, as well as the broad synthetic applicability of the designed resins in the field of SPOS.

■ RESULTS AND DISCUSSION

Scheme 1 shows an overview of the synthesis of the resins **4a–f**. Application examples are presented in Scheme 2 and subsequently discussed in detail.

Scheme 1. Synthesis of the PS−PEG Resins 4a−f and Attachment of Sensor Molecule[a]
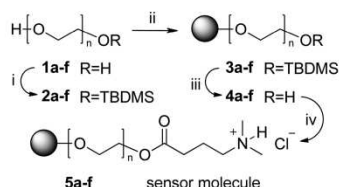
[a]Reaction conditions: (i) pyridine/imidazole, TBDMS-Cl, DCM, 0 °C → rt, 24 h; (ii) DEAD, PS-phenol resin, $P(C_6H_5)_3$, DCM/THF = 1/1, rt, overnight; (iii) TBAF, THF, rt, overnight; (iv) 4-(dimethylamino)-butanoic acid, hydrochloride, 1-hydroxybenzotriazole, DMAP, DIC, DCM/DMF = 9/1, rt, 2 d.

Synthesis of the PS−PEG Resin (4a−f). Starting from accessible reagents, the intention of our strategy was the design

of a modular synthetic route based on monodisperse oligo(ethylene glycols) and polymer-bound phenol, leading to tailor-made resins for SPOS. Finally, we present a convenient three-step synthesis: monoprotection of glycols, attachment to solid-phase and deprotection. This synthetic approach as well as the implications of the linker length for the ^{13}C gel-phase NMR spectroscopy have previously been reported by our group.[18] However, the full experimental details and a characterization of the resins are given in this manuscript.

Glycols **1a−c** ($n = 2, 4, 6$) are commercially available. Higher homologues have been synthesized according to a recently published procedure.[19] As shown in Scheme 1, the initial step in the resin synthesis was the monoprotection of glycols **1a−f** ($n = 2, 4, 6, 8, 10, 12$) by conversion with *tert*-butyldimethylsilyl chloride (TBDMS-Cl).[20] This protective group has been proved to show the best performance in terms of stability and cleavage behavior. By comparison, in the next reaction step (Mitsunobu reaction), trimethylsilyl was not suitable for reasons of stability. Furthermore, the synthetic approach toward mono-TMS-protected oligo(oxyethylene glycols) is inconvenient (formation of azeotropic mixtures[21]). The triphenylmethyl group was appropriate for Mitsunobu conditions, but deprotection on solid-phase could not be accomplished.

As a second step, protected glycols **2a−f** were attached to polymer-bound phenol by applying Mitsunobu reactions.[22] As a result of this strategy, an aryl-alkyl linkage was formed, instead of a benzylic ether PS-graft linkage (e.g., TentaGel), which is known to be unstable in strongly acidic conditions.

Finally, for the deprotection, resins **3a−f** were swollen in THF and treated with a solution of TBAF in THF to give monodisperse PEG-grafted resins **4a−f** in quantitative yield as

Scheme 2. Application Examples 1−3[a]
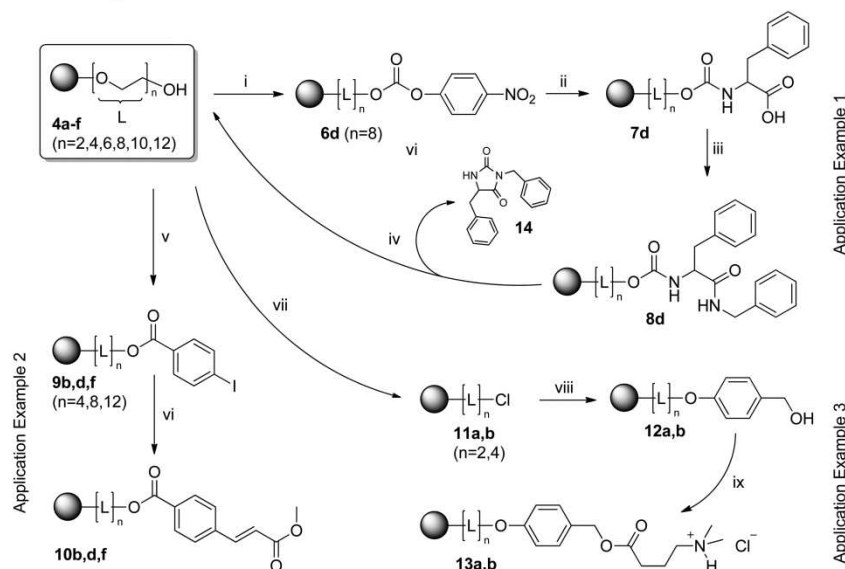
[a]Reaction conditions: (i) 4-nitrophenyl-chloroformate, Et$_3$N, rt, 60 h; (ii) L-phenylalanine, BSA, DMAP, DMF, rt, 48 h; (iii) 1-hydroxybenzotriazole, DIC, benzylamine, DMF, rt, overnight; (iv) 1,1,3,3-tetramethylguanidine, MeOH, reflux, 24 h; (v) 4-iodobenzoic acid, 1-hydroxybenzotriazole, DMAP, DIC, DCM/DMF = 9/1, rt, overnight; (vi) methylmethacrylate, P(C$_6$H$_5$)$_3$, tetra-*n*-butylammoniumchloride, Pd(OAc)$_2$, DMF/H$_2$O/NEt$_3$, 40 °C, overnight; (vii) SOCl$_2$, toluene, 75 °C, overnight; (viii) 4-hydroxybenzyl alcohol, NaH, DMF, 75 °C, overnight, (ix) 4-(dimethylamino)butanoic acid, hydrochloride, 1-hydroxybenzotriazole, DMAP, DIC, DCM/DMF = 9/1, r.t., 2 d.
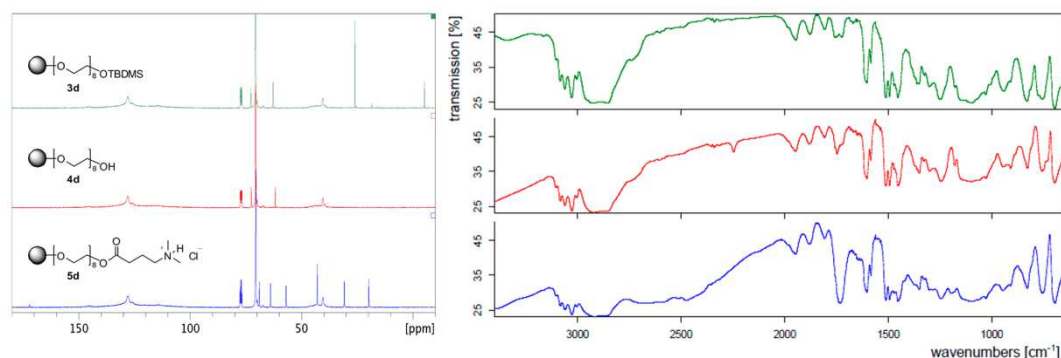
368

dx.doi.org/10.1021/co500028h | ACS Comb. Sci. 2014, 16, 367−374

Figure 1. Reaction monitoring on solid-phase of resins **3d–5d** via ^{13}C gel-phase NMR and FT-IR spectroscopy. For a detailed view of the NMR spectra see associated content.

determined by ^{13}C gel-phase NMR spectroscopy (Figure 1). For a systematic investigation of the effect of the PEG group length on the quality of gel-phase ^{13}C NMR spectra, a sensor molecule (4-(dimethylamino)-butanoic acid, hydrochloride) was attached and resulted in resins **5a–f**.[18] The sensor molecule was attached to the resins' hydroxyl groups using a carbodiimide-based coupling method.[23]

Figure 1 shows the reaction monitoring of each synthetic step on solid-phase (**3d–5d**), applying two different analytical techniques (FT-IR and ^{13}C gel-phase NMR spectroscopy). Allowing a precise determination of the reaction progress, NMR spectroscopy has proved to be superior. For instance, the deprotection of **3d** can be clearly monitored via the signals from the TBDMS-group (3 signals in the region <30 ppm). The formation of NMR signals, particularly in the region of 15−35 ppm, allows to examine the attachment of the sensor molecule toward **5d**. By comparison, a significant difference in the FT-IR spectra is the C=O peak in the range of 1700 cm^{-1} corresponding to the ester in substance **5d**.

As shown in preliminary research, swelling properties, loading (Table 1) and gel-phase NMR characteristics have

been demonstrated to be excellent.[18] As a result, resin **4d** with eight ethylene glycol units has shown the best performance in terms of loading capacity combined with spectral quality. The surface morphology and spherical behavior of the developed resins was investigated by polarized optical microscopy and scanning electron microscopy (SEM). The images demonstrate homogeneous and spherical properties of the beads; in addition, the good swelling properties in chloroform are clearly visible (Figure 2).

Application Examples of Monodisperse PS−PEG Resin. In the next step, we intended to demonstrate the applicability of the presented resins to SPOS. Complex multistep syntheses require a solid support that performs in both polar and nonpolar solvents. This was the major selection criterion of our on-resin sequence examples. To evaluate the resin performance, we induced the identical reaction sequences on commercially available resins (Wang, TentaGel).

In application example 1, the developed resin **4d** (PEG 8 spacer) was compared to a commercially available resin (TentaGel) in a multistep synthesis involving various reactants, solvents and conditions. For this purpose, a published synthetic route toward hydantoin **14** was chosen.[24]

Figure 3 shows the corresponding ^{13}C gel-phase NMR spectra. Because polar solvents are involved in the sequence, TentaGel, which shows a chemically comparable spacer structure, was used as a reference resin. The synthesis was performed by starting from identical amounts of the respective resin leading to 14 mg (TentaGel) and 44 mg (resin **4d**) substance **14**. This result, a more than 3-fold amount of isolated hydantoin **14**, impressively reveals the effect of higher loading of the resin due to a shorter spacer unit. Thus, a substantially lower amount of resin **4d** is needed to obtain an intended quantity of a target substance. After the reaction, the recovered

Table 1. Swelling Volume [mL/g] of Selected Resins at 25 °C in Different Solvents (Data Extracted from Preliminary Research)[18]

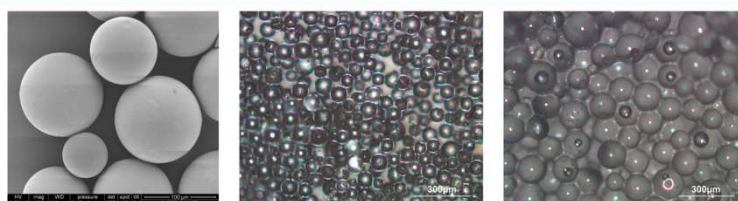| entry	resin	loading [mmol/g]	MeOH	DMF	THF	DCM
1	Merrifield	1.5	0.7	4.3	7.5	7.3
2	**4b** ($n = 4$)	1.1	1.5	6.8	8.5	7.8
3	**4d** ($n = 8$)	0.9	2.1	6.7	7.1	8.0
4	**4f** ($n = 12$)	0.7	2.1	6.0	7.3	8.6
5	TentaGel	0.3	2.7	4.1	4.2	5.7

Figure 2. Microscopy images of resin **4d**. SEM image (left); polarized optical microscopy image of **4d**, dry (middle) and swollen in chloroform (right).
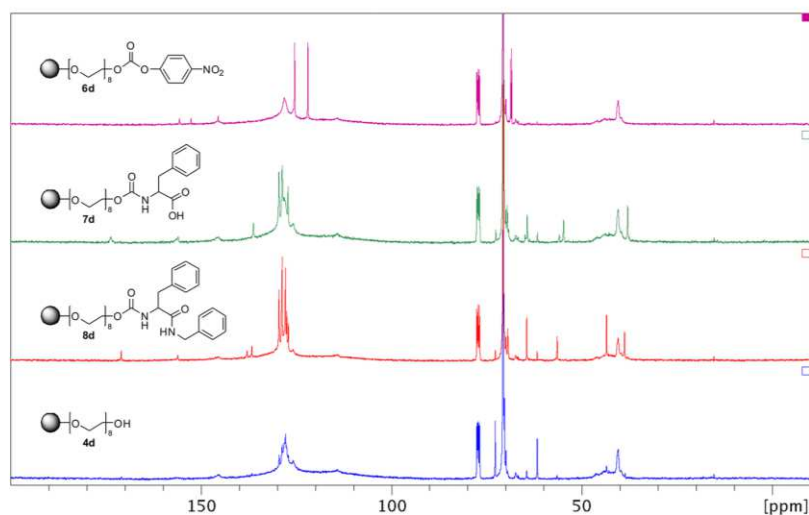
ACS Combinatorial Science   Research Article

Figure 3. On-resin reaction monitoring of the hydantoin route (application example 1).

beads feature ^{13}C gel-phase NMR spectra comparable to the starting material, which is an important factor for resin recycling. Both higher loading and the possibility of recycling are essential for efficient industrial scale syntheses.

Application example 2 points out the applicability in heterogenic catalytic systems (Heck coupling[25]). After conversion of resin **4b,d,f** with 4-iodobenzoic acid, the palladium catalyzed cross-coupling step (methacrylate as coupling reagent) was performed. The evaluation of the ^{13}C gel-phase NMR spectra showed an increased conversion by applying extended length of the PEG tether, which is supported by the swelling behavior (low conversion for **9b** ($n = 4$), good result for **9d** ($n = 8$), quantitative conversion for **9f** ($n = 12$)). In comparison with the result obtained from TentaGel, cross coupling of resin **9f** yielded the same performance (similar reaction progress as determined by gel-phase NMR spectroscopy), with the advantage of higher loading and improved on-resin analysis.

In application example 3 (Scheme 2), an end-group modification to a Wang-Linker system[26] (conversion using thionyl chloride and 4-hydroxybenzyl alcohol) was performed to achieve resin **12a–b**. The goal was to investigate the stability of our PEG linker in harsh reaction conditions (thionyl chloride) and to allow a comparison with commercially available Wang and TentaGel resins. The attachment of the Wang linker enables the application of the developed PS–PEG resins in the field of peptide synthesis as a result of mild cleavage conditions for the target peptides. Subsequently, the attachment of a sensor molecule (4-(dimethylamino)butanoic acid, hydrochloride) to obtain resin **13a–b** enabled the comparison of the characteristics of gel-phase NMR spectroscopy of **13a–b** with commercially available beads (the functionalization of the reference beads with the sensor has been previously described[13]). To characterize each spectrum by a single value, an average half-height line width of all nonquaternary carbon peaks of the immobilized sensor molecule was determined. Small values correspond to high-quality spectra, resulting in a better line shape. The values for the commercially available resins are 28.4 Hz for Wang and 7.3 Hz for TentaGel.[13] By comparison, the half-hight line widths of

resins **13a** and **13b** were determined as 24.4 and 19.2 Hz, respectively, which is a clear improvement relative to Wang.

The above-mentioned sensor was chosen for the present work due to its high polarity, which makes it a very demanding sensor for attachment and gel-phase NMR. The polarity of the sensor is a key criterion for the achievable quality of the gel-phase spectrum on a given resin. Highly polar sensor molecules (like the (4-(dimethylamino)butanoic acid, hydrochloride) can only be measured in good quality if bound to a solid-phase via a suitable PEG linker: no signals were obtained for these molecules on Merrifield resin.[13] The acid was bound to the hydroxyl groups of the resins as described before (carbodiimide method); quantitative conversions for each step could be observed.

■ **CONCLUSION**

In conclusion, we have shown that polystyrene resins grafted with short, monodisperse PEG units ($n = 2–12$) can easily be synthesized in a modular synthetic route from polymer-bound phenol by Mitsunobu coupling. The resulting solid supports offer advantageous properties for gel-phase NMR spectroscopy and are excellent resins for SPOS. In order to prove the applicability, three reaction sequences on solid-phase have been performed (Wang-linker synthesis, palladium catalyzed cross coupling, hydantoin synthesis). Compared to commercially available PS–PEG resins, our support offers equal swelling properties in polar and apolar solvents, better on-resin analytic properties and significantly higher loading, thus being a suitable choice for industrial application. This approach to tailor-made resins enables the adjustment of the resin properties by a proper linker selection depending on the respective field of application.

■ **EXPERIMENTAL PROCEDURES**

All reactions were conducted under an atmosphere of argon in oven-dried glassware with magnetic stirring. Unless otherwise stated, reagents were purchased from commercial sources and purified in the usual manner. DEAD (diethyl azodicarboxylate), 4-(dimethylamino)butanoic acid, hydrochloride, hexa(ethylene glycol) and TBDMS-Cl (*tert*-butylchlorodimethylsilane) were

purchased from Aldrich and used without prior purification. Di(ethylene glycol) **1a** and tetra(ethylene glycol) **1b** were obtained from Merck and used as purchased. Oligo(ethylene glycols) **1c–f**[19] (n = 6, 8, 10, 12) and mono-TBDMS protected glycols **2a–c**[20] were prepared in analogy to literature.

The resins used were as follows: polymer-bound phenol (1.7 mmol/g, 1% divinylbenzene, 100–200 mesh) was purchased from Aldrich; TentaGel resin (0.3 mmol/g, 1% divinylbenzene, 80–100 μm), and Reactagel-OH resin (0.7 mmol/g, 1% divinylbenzene, 100–200 mesh) were purchased from Advanced ChemTech. All resins were dried prior to usage.

Anhydrous DMF was purchased from Acros. Tetrahydrofuran was dried over and distilled from sodium/benzophenone ketyl. Dichloromethane was dried over and distilled from CaH$_2$. Technical grade solvents were distilled prior to usage. Analytical TLC was performed on Merck silica gel 60 F254 plates. Chromatographic separations at preparative scale were carried out on silica gel (Merck silica gel 60, 40–63 um).

Nuclear magnetic resonance (NMR) spectra were obtained using a Bruker DPX-200 or Avance DRX-400 Fourier transform spectrometer operating at the following frequencies: DPX-200:200.1 MHz (^{1}H) and 50.3 MHz (^{13}C); DRX-400:400.1 MHz (^{1}H) and 100.6 MHz (^{13}C). All ^{13}C gel-phase spectra were performed at the Avance DRX-400 spectrometer. Chemical shifts are reported in delta (δ) units, parts per million (ppm) downfield from tetramethylsilane using solvent residual signals for calibration. Coupling constants are reported in Hertz (Hz); multiplicity of signals is indicated by using following abbreviations: s = singlet, d = doublet, t = triplet, q = quartet, b = broad. Multiplicities of ^{13}C signals were obtained by measuring JMOD spectra. Significant peaks corresponding to compounds attached to solid-phase are indicated in the NMR code. IR spectra were recorded on a BioRad FTS 135 FT-IR spectrometer from KBr pellets or using the ATR technique. Elemental analyses were carried out at the Microanalytical Laboratory, University of Vienna.

Synthesis of TBDMS-Protected Glycols. *General Procedure.* A solution of glycol **1a–f** in anhydrous DCM was cooled to 0 °C and the base (imidazole or anhydrous pyridine) was added slowly. The solution was stirred for 5 min before a solution of TBDMS-Cl in anhydrous DCM was added dropwise. The reaction mixture was stirred at 0 °C for 1 h, and after it was warmed to room temperature, it was stirred for an additional 24 h. Water was added to the formed suspension, and after phase separation, the organic layer was consecutively washed with 10% aqueous HCl, saturated NaHCO$_3$ solution and brine. After it was dried over MgSO$_4$, the solvent was distilled off under reduced pressure to give the crude product, which was subjected to column chromatography for further purification leading to monoprotected glycols **2a–f**.

2,2,3,3-Tetramethyl-4,7,10,13,16,19,22,25-octaoxa-3-sila-heptacosane-27-ol **2d**. According to the general procedure, octa(ethylene glycol) (19.20 g, 51.8 mmol, 1.7 eqiv.), imidazole (2.13 g, 31.3 eqiv., 1.0 eqiv.), TBDMS-Cl (4.69 g, 31.1 mmol, 1.0 eqiv.), and ~70 mL of anhydrous DCM were used. Column chromatography: 400 g of silica gel, gradient elution using hexanes/ethyl acetate = 1/5 → ethyl acetate → ethyl acetate/MeOH = 4/1. The title compound **2d** was obtained as slightly yellow oil (6.92 g, 46%). ^{1}H NMR (200 MHz, CDCl$_3$): δ = 3.80–3.45 (m, 32H), 2.80 (bs, 1H), 0.87 (s, 9H), 0.04 (s, 6H) ppm. ^{13}C NMR (50 MHz, CDCl$_3$): δ = 72.6 (t), 72.5 (t), 70.7 (t), 70.6 (t), 70.5 (t), 70.3 (t), 62.7 (t), 61.7 (t), 25.9 (q), 18.3

(s), −5.3 (q) ppm. Anal. Calcd for C$_{22}$H$_{48}$O$_9$Si: C, 54.52; H, 9.98. Found: C, 54.48; H, 9.72; N, <0.05.

2,2,3,3-Tetramethyl-4,7,10,13,16,19,22,25,28,31-decaoxa-3-silatritriacontane-33-ol **2e**. According to the general procedure, deca(ethylene glycol) (5.60 g, 12.2 mmol, 1.0 equiv), imidazole (0.82 g, 12.0 mmol, 1.0 equiv), TBDMS-Cl (1.81 g, 12.0 mmol, 1.0 equiv), and ~100 mL of anhydrous DCM were used. Column chromatography: 200 g of silica gel, gradient elution using CHCl$_3$/MeOH = 25/1 → CHCl$_3$/MeOH = 5/1 → CHCl$_3$/MeOH = 4/1. Compound **2e** was obtained as colorless oil (2.19 g, 32%). ^{1}H NMR (200 MHz, CDCl$_3$): δ = 3.75–3.43 (m, 40H), 1.91 (bs, 1H), 0.83 (s, 9H), 0.00 (s, 6H) ppm. ^{13}C NMR (50 MHz, CDCl$_3$): δ = 72.6 (t), 70.7 (t), 70.5 (t), 70.2 (t), 62.6 (t), 61.6 (t), 25.9 (q), 18.3 (s), −5.3 (q) ppm. Anal. Calcd for C$_{26}$H$_{56}$O$_{11}$Si: C, 54.52; H, 9.85. Found: C, 54.59; H, 9.70; N, <0.05.

2,2,3,3-Tetramethyl-4,7,10,13,16,19,22,25,28,31,34,37-do-decaoxa-3-silanonatriacontane-39-ol **2f**. According to the general procedure, dodeca(ethylene glycol) (9.83 g, 18.0 mmol, 1.2 equiv), anhydrous pyridine (1.50 g, 19.0 mmol, 1.3 equiv), TBDMS-Cl (2.26 g, 15.0 mmol, 1.0 equiv), and ~50 mL of anhydrous DCM were used. Column chromatography: 400 g of silica gel, gradient elution using CHCl$_3$/MeOH = 30/1 → CHCl$_3$/MeOH = 20/1. Pure compound **2f** was obtained as a colorless oil (4.36 g, 44%). ^{1}H NMR (200 MHz, CDCl$_3$): δ = 3.74–3.44 (m, 48H), 2.13 (bs, 1H), 0.83 (s, 9H), 0.00 (s, 6H) ppm. ^{13}C NMR (50 MHz, CDCl$_3$): δ = 72.6 (t), 72.5 (t), 70.7 (t), 70.5 (t), 70.3 (t), 62.7 (t), 61.7 (t), 25.9 (q), 18.3 (s), −5.3 (q) ppm. Anal. Calcd for C$_{30}$H$_{64}$O$_{13}$Si: C, 54.52; H, 9.76; Found: C, 54.10; H, 9.47; N, <0.05.

General Procedure for Mitsunobu Reaction on Solid-Phase. DEAD (5.0 equiv) was added dropwise to a mixture of 1.0 equiv of polymer-bound phenol (100–200 mesh, 1% divinylbenzene, Aldrich, 1.7 mmol/g) in dry DCM/THF = 1/1 (50 mL/g resin) under argon. In the next step, the corresponding monoprotected glycols **2a–f** (5.0 equiv), dissolved in dry THF, and finally triphenylphosphine were added slowly. The reaction mixture was stirred overnight and filtered, and the solid residue was washed 3 times with DCM/THF = 1/1, DCM, isopropanol, DCM, and finally with methanol. The resulting resin **3a–f** was dried to constant weight in vacuo. To complete the conversion, the whole procedure was repeated.

PS-PEG(2)-O-TBDMS **3a**. Starting from 999.8 mg (1.70 mmol) of polymer-bound phenol, we isolated 1.2069 g of yellow resin.

PS-PEG(4)-O-TBDMS **3b**. Starting from 1.1413 g (1.94 mmol) of polymer-bound phenol, we isolated 1.5156 g of yellow resin.

PS-PEG(6)-O-TBDMS **3c**. Starting from 513 mg (0.87 mmol) of polymer-bound phenol, we isolated 733 mg of pink resin.

PS-PEG(8)-O-TBDMS **3d**. Starting from 1.5750 g (2.68 mmol) of polymer-bound phenol, we isolated 2.3409 g of pink resin.

PS-PEG(10)-O-TBDMS **3e**. Starting from 354.5 mg (0.60 mmol) of polymer-bound phenol, we isolated 517.0 mg of pink resin.

PS-PEG(12)-O-TBDMS **3f**. Starting from 584.1 mg (0.99 mmol) of polymer-bound phenol, we isolated 857.6 mg of yellow resin.

General Procedure for the Deprotection of TBDMS Group on Solid-Phase. Resins **3a–f** were suspended in 30 mL/g dry THF under argon. Then 5.0 equiv of 1.0 M

tetrabutylammonium fluoride (TBAF) solution in dry THF were added dropwise. The reaction suspension, forming a brown mixture within 1 h, was stirred overnight at room temperature. Subsequently, the reaction mixture was filtered, and the solid residue was washed 3 times with THF, THF/water, THF, methanol/water, DCM, and finally with methanol. Proper washing is important to get rid of liberated substances. The resulting resin 4a−f was dried to constant weight in vacuo (50 °C).

PS-PEG(2)-OH 4a. Resin 3a (245.6 mg, 0.26 mmol) resulted in yellow resin 4a (217.1 mg, 1.1 mmol/g). Anal. Found: C, 84.10; H, 7.58; N, <0.05. FT-IR (KBr): 3449, 3024, 2913, 2850, 1944, 1872, 1803, 1748, 1601, 1509, 1450, 1354, 1238, 1127, 1054, 1027, 906, 827, 754, 696 cm^{-1}.

PS-PEG(4)-OH 4b. Resin 3b (924.5 mg, 0.89 mmol) resulted in yellow resin 4b (820.4 mg, 1.1 mmol/g). Anal. Found: C, 82.41; H, 7.88; N, <0.05. FT-IR (KBr): 3460, 3025, 2916, 1945, 1876, 1805, 1747, 1602, 1510, 1493, 1452, 1349, 1244, 1108, 1064, 1028, 907, 828, 757, 697 cm^{-1}.

PS-PEG(6)-OH 4c. Resin 3c (318.2 mg, 0.27 mmol) resulted in yellow resin 4c (283.9 mg, 1.0 mmol/g). Anal. Found: C, 80.20; H, 7.90; N, <0.05. FT-IR (KBr): 3449, 3026, 2917, 1945, 1877, 1805, 1744, 1720, 1602, 1509, 1452, 1350, 1244, 1100, 943, 828, 757, 697 cm^{-1}.

PS-PEG(8)-OH 4d. Resin 3d (361.5 mg, 0.25 mmol) resulted in yellow resin 4d (327.0 mg, 0.9 mmol/g). Anal. Found: C, 78.41; H, 7.95; N, <0.05. FT-IR (KBr): 3480, 3026, 2921, 1947, 1878, 1808, 1747, 1602, 1511, 1452, 1349, 1098, 943, 908, 827, 757, 695 cm^{-1}.

PS-PEG(10)-OH 4e. Resin 3e (347.0 mg, 0.19 mmol) resulted in slightly brown resin 4e (343.6 mg, 0.8 mmol/g). Anal. Found: C, 80.32; H, 7.96; N, <0.05. FT-IR (KBr): 3480, 3025, 2915, 1946, 1877, 1805, 1747, 1602, 1509, 1493, 1349, 1243, 1099, 944, 828, 757, 697 cm^{-1}.

PS-PEG(12)-OH 4f. Resin 3f (728.8 mg, 0.44 mmol) resulted in yellow resin 4f (327.0 mg, 0.7 mmol/g). Anal. Found: C, 76.30; H, 8.06; N, <0.05. FT-IR (KBr): 3505, 3026, 2919, 1945, 1874, 1804, 1734, 1602, 1453, 1350, 1289, 1251, 1104, 948, 841, 758, 698 cm^{-1}.

General Procedure for Attachment of Sensor Molecule to Solid Support. Resins 4a−f were suspended in dry DCM/DMF = 9/1 (15 mL/g resin), and then 4-(dimethylamino)butanoic acid, hydrochloride (5.0 equiv), and 1-hydroxybenzotriazole (5.0 equiv) were added in a minimum amount of dry DMF. 4-(*N,N*-Dimethylamino)pyridine (1.0 equiv) in dry DMF and *N,N'*-diisopropylcarbodiimide (5.0 equiv) were added to the mixture and stirred under argon at room temperature for 2 days. The resulting suspension was filtered and the solid residue was washed 3 times with DMF, then with DCM, and finally with methanol. The resin was dried to constant weight in vacuo.

PS-PEG(2)-4-(dimethylamino)butanoic Acid, Hydrochloride 5a. 4a (165.7 mg, 1.01 mmol) resulted in yellow resin 5a (194.0 mg). ^{13}C gel-phase NMR (100 MHz, CDCl$_3$): δ = 172.1 (s, O−C=O), 63.9 (t, CH$_2$−O−C=O), 57.0 (t, CH$_2$−N), 43.0 (q, N−CH$_3$), 30.8 (t, CH$_2$−C=O), 19.8 (t, CH$_2$−CH$_2$−CH$_2$) ppm; assignment of the signals was supported by 2D-NMR experiments.

PS-PEG(4)-4-(dimethylamino)butanoic Acid, Hydrochloride 5b. 4b (302.2 mg, 0.89 mmol) resulted in yellow resin 5b (358.9 mg). ^{13}C gel-phase NMR (100 MHz, CDCl$_3$): δ = 172.1 (s), 63.9 (t), 57.0 (t), 43.1 (q), 30.9 (t), 19.9 (t) ppm.

PS-PEG(6)-4-(dimethylamino)butanoic Acid, Hydrochloride 5c. 4c (140.7 mg, 0.27 mmol) resulted in yellow resin 5c (159.8 mg). ^{13}C gel-phase NMR (100 MHz, CDCl$_3$): δ = 172.2 (s), 63.9 (t), 57.1 (t), 43.1 (q), 30.9 (t), 20.0 (t) ppm.

PS-PEG(8)-4-(dimethylamino)butanoic Acid, Hydrochloride 5d. 4d (193.0 mg, 0.18 mmol) resulted in yellow resin 5d (222.3 mg). ^{13}C gel-phase NMR (100 MHz, CDCl$_3$): δ = 172.0 (s), 63.9 (t), 56.9 (t), 42.9 (q), 30.8 (t), 19.7 (t) ppm.

PS-PEG(10)-4-(dimethylamino)butanoic Acid, Hydrochloride 5e. 4e (198.0 mg, 0.12 mmol) resulted in yellow resin 5e (219.2 mg). ^{13}C gel-phase NMR (100 MHz, CDCl$_3$): δ = 172.2 (s), 63.9 (t), 57.2 (t), 43.1 (q), 30.9 (t), 20.0 (t) ppm.

PS-PEG(12)-4-(dimethylamino)butanoic Acid, Hydrochloride 5f. 4f (228.8 mg, 0.16 mmol) resulted in yellow resin 5f (261.8 mg). ^{13}C gel-phase NMR (100 MHz, CDCl$_3$): δ = 172.2 (s), 63.9 (t), 57.0 (t), 43.1 (q), 30.9 (t), 19.9 (t) ppm.

Application Example 1 (Hydantoin Synthesis). The synthetic steps toward hydantoin 14 were accomplished following published procedures.[24] All synthetic steps are in accordance with the literature, modifications concerning reaction time and reactant amounts are noted.

Activation of the Solid Support. Resin 4d or TentaGel S PHB (0.2 mmol/g), respectively, were activated in the presence of a 10-fold excess of 4-nitrophenyl chloroformate and Et$_3$N (5.0 equiv) at a reaction time of 60 h.

Polymer-Bound 4-Nitrophenylcarbonates. Resin 4d (1.340 g) led to a white resin 6d (1.450 g). ^{13}C gel-phase NMR (100 MHz, CDCl$_3$): δ = 155.4 (s, ArC−O), 152.4 (s, C=O), 145.3 (ArC−NO$_2$), 125.2 (d, ArC−H), 121.7 (d, ArC−H) ppm. TentaGel S PHB resin (1.127 g) resulted in slightly yellow resin 6g (1.180 g). ^{13}C gel-phase NMR (100 MHz, CDCl$_3$): δ = 155.2, 152.1, 145.0, 124.9, 121.5 ppm.

Attachment of the Amino Acid. The respective resins 6d and 6g were treated with a solution of ʟ-phenylalanine (4.0 equiv) in BSA (4.0 equiv) and DMF, followed by the addition of DMAP (2.0 equiv) and stirred for a reaction time of 48 h.

Polymer-Bound N-Carboxy-ʟ-phenylalanin. PS-PEG Resin 6d (1.141 g, 0.52 mmol) led to a white resin 7d (1.155 g). ^{13}C gel-phase NMR (100 MHz, CDCl$_3$): δ = 173.4 (s, O=C−OH), 155.3 (s, C=O), 136.1 (ArC−CH$_2$), 129.3 (d, ArC−H), 128.4 (d, ArC−H), 126.9 (d, ArC−H) ppm. TentaGel resin 6g (350 mg, 0.07 mmol) resulted in yellow resin 7g (341 mg). ^{13}C gel-phase NMR (100 MHz, CDCl$_3$): δ = 172.9, 155.8, 136.2, 129.4, 129.2, 126.4 ppm.

Addition of the Amine. Resins 7d and 7g were suspended in DMF; dissolved 1-hydroxybenzotriazole (4.0 equiv) was added, and subsequently, DIC (4.0 equiv) was transferred to the vessel dropwise. Then, the mixture was stirred for 1 h. Finally, benzylamine (4.0 equiv) was added, and the reaction was allowed to proceed overnight. After the filtration of the resin, the procedure was repeated to ensure full conversion.

Polymer-Bound N-Carboxy-ʟ-phenylalanin-benzylamide. Bead 7d (930 mg, 0.43 mmol) resulted in beige resin 8d (935 mg). ^{13}C gel-phase NMR (100 MHz, CDCl$_3$): δ = 170.7 (s, O=C−NR), 155.9 (s, C=O), 137.6 (ArC−CH$_2$), 136.4 (s, ArC−CH$_2$) ppm. Starting from resin 7g (984 mg, 0.17 mmol) yellow resin 8g (854 mg) was achieved. ^{13}C gel-phase NMR (100 MHz, CDCl$_3$): δ = 170.4, 155.6, 137.5, 136.2 ppm.

Release of the Hydantoin. The cleavage of hydantion 14 was realized by reaction of 1,1,3,3-tetramethylguanidine (2.0 equiv) in MeOH with bead 8d (507 mg) and resin 8g (503 mg), respectively. The reaction was allowed to proceed at reflux (65 °C) for 24 h (to complete the cleavage for 8d the reaction

372

dx.doi.org/10.1021/co500028h | *ACS Comb. Sci.* 2014, 16, 367−374

was repeated at reflux overnight). After work-up, **4d** and TentaGel resin could be recovered showing ^{13}C gel-phase spectra comparable to the starting resin. The filtrates were concentrated in vacuo and purified by column chromatography (4.5 g silica gel, diethyl ether) leading to 44 mg of **14** starting from resin **8d** and 14 mg of hydantoin **14** applying TentaGel-based resin **8g**.

3,5-Bis(phenylmethyl)-2,4-imidazolidinedione 14. **14** was obtained as white solid. ^{1}H NMR (400 MHz, CDCl$_3$): δ = 7.35–6.95 (m, 10H), 5.44 (bs, 1H), 4.62–4.43 (m, 2H), 4.18 (ddd, J = 8.5 Hz, 3.8 Hz, 1.2 Hz, 1H), 3.19 (dd, J = 14.0 Hz, 3.8 Hz, 1H), 2.78 (dd, J = 14.0 Hz, 8.5 Hz, 1H) ppm. ^{13}C NMR (100 MHz, CDCl$_3$): δ = 172.8 (s), 157.0 (s), 135.7 (s), 134.9 (s), 129.3 (d, 2C), 128.8 (d, 2C), 128.6 (d, 2C), 128.2 (d, 2C), 127.7 (d), 127.3 (d), 58.3 (d), 42.0 (t), 37.6 (t) ppm. Anal. Calcd for C$_{17}$H$_{16}$N$_2$O$_2$: C, 72.84; H, 5.75; N, 9.99. Found: C, 72.62; H, 5.48; N, 9.71.

Application Example 2 (Heck-Coupling Route). Loading of the Resins with 4-Iodobenzoic Acid. Resin **4b,d,f** and Reactagel (0.7 mmol/g) were stirred in a mixture DCM/DMF (9/1) for 15 min to ensure sufficient swelling. 4-Iodobenzoic acid (5.0 equiv) and 1-hydroxybenzotriazole (5.0 equiv) dissolved in DMF, as well as DIC (5.0 equiv), were added to the resin. Finally DMAP (1.0 equiv) was transferred to the reaction vessel and the mixture was stirred overnight at room temperature under argon. The work-up of the beads was in accordance with the procedure reported in the literature; because of incomplete loading of resins **9d** and **9f** (determined by ^{13}C gel-phase NMR spectra), the reaction sequence was repeated applying a 0.2-fold amount of all reactants compared to the first loading step.

Polymer-Bound 4-Iodobenzoic Acid. Starting from resin **4b** (610 mg), we could isolate 691 mg of **9b** as a yellowish resin. ^{13}C gel-phase NMR (100 MHz, CDCl$_3$): δ 166.0 (s, O=C–OR), 137.6 (d, ArC–H), 131.1 (d, ArC–H), 129.5 (s, ArC–C=O), 100.8 (s, ArC–I). Resin **4d** (292 mg) led to 330 mg of slightly yellow beads **9d** after a second loading step. ^{13}C gel-phase NMR (100 MHz, CDCl$_3$): δ 165.9, 137.6, 131.1, 129.5, 100.8. **4f** (210 mg) overall resulted in 244 mg of white resin **9f**. ^{13}C gel-phase NMR (100 MHz, CDCl$_3$): δ = 165.9, 137.6, 131.1, 129.5, 100.7 ppm. Starting from Reactagel (1.138 g), we could obtain 1.175 mg of white resin **9g**. ^{13}C gel-phase NMR (100 MHz, CDCl$_3$): δ = 165.8, 137.5, 131.0, 129.4, 100.7 ppm.

Heck-Coupling Reactions. The different resins (**9b,d,f** and loaded Reactagel **9g**) were swollen in a mixture of DMF/H$_2$O/NEt$_3$ over a period of 15 min. Subsequently, methyl methacrylate (2.0 equiv), triphenylphosphine (0.4 equiv), tetra-*n*-butylammonium chloride (0.4 equiv) and finally palladium(II)acetate (0.2 equiv) were added. The reaction was carried out overnight at 40 °C under argon atmosphere; the isolation of the beads was carried out according to literature.[25] The black/gray color of the resin is attributed to residual palladium remaining adsorbed on the beads.

Polymer-Bound Phenylmethylmethcrylate. Resin **9b** (291 mg) leads to black resin **10b** (264 mg). ^{13}C gel-phase NMR (100 MHz, CDCl$_3$): δ = 166.8 (s, O=C–OCHH$_3$), 165.9 (s, O=C–OR), 143.4 (d, H–C=C), 138.5 (s, ArC–C=C), 120.1 (d, H–C=C), 51.8 (q, CH$_3$) ppm. ^{13}C gel-phase NMR spectra indicated incomplete conversion, which is attributed to the low swelling ability in polar-solvent mixtures of the resin bearing a short PEG spacer unit. Starting from **9d** (196 mg), we could obtain 198 mg of **10d** as a black solid. ^{13}C gel-phase NMR (100 MHz, CDCl$_3$): δ = 166.8, 165.9, 143.3, 138.5,

120.1, 51.8 ppm. Beads **9f** (187 mg) resulted in 191 mg of gray resin **10f**. ^{13}C gel-phase NMR (100 MHz, CDCl$_3$): δ = 166.9, 165.8, 143.4, 138.6, 120.1, 51.8 ppm. Starting from Reactagel-based **9g** (291 mg), we could isolate 272 mg of **10g** as back beads. ^{13}C gel-phase NMR (100 MHz, CDCl$_3$): δ = 166.7, 165.6, 143.2, 138.4, 120.0, 51.7 ppm.

Application Example 3 (Wang Linker Attachment). General Procedure for the Chlorination of PS–PEG Resins. Beads **4a–b** were suspended in anhydrous toluene. Thionyl chloride (7.0 equiv) was added, and the reaction mixture was stirred overnight at 75 °C. After it was cooled to 55 °C, the resin was filtered and washed with warm toluene (5×) and methanol (3×). The polymer-bound poly(ethylene glycol) derivatives **11a–b** were dried to constant weight in vacuo.

Chlorinated PS-PEG-Bound Linker. Resin **4a** (1.648 g) in 20 mL anhydrous toluene yielded in 0.787 g white resin **11a**. ^{13}C gel-phase NMR (100 MHz, CDCl$_3$): δ = 71.5 (t), 69.9 (t), 67.4 (t), 42.7 (t, *C*-Cl) ppm. PS-PEG beads **4b** (0.904 g, 1.36 mmol) in 20 mL of anhydrous toluene resulted in 0.873 g of white resin **11b**. ^{13}C gel-phase NMR (100 MHz, CDCl$_3$): δ = 71.3 (t), 70.8 (t), 69.8 (t), 67.2 (t), 42.7 (t) ppm.

Addition of the Wang Linker. General Procedure. Sodium hydride (5.0 equiv) was added to a solution of 4-hydroxybenzyl alcohol (5.0 equiv) in anhydrous DMF. After it was stirred for 30 min at room temperature, resins **11a–b** were added to the reaction mixture. The suspension was heated to 75 °C and stirred overnight at this temperature. The resin was filtered off and washed twice with each of the following solvents: DMF, DMF/H$_2$O, THF/H$_2$O, MeOH/H$_2$O, MeOH, alternating DCM, and MeOH. The isolated resin was dried to constant weight in vacuo overnight.

PS-PEG-Bound Wang Linker. Resin **11a** (0.516 g, 0.538 mmol) in 25 mL of anhydrous DMF resulted in 0.549 g of brown resin **12a**. ^{13}C gel-phase NMR (100 MHz, CDCl$_3$): δ = 128.5 (d, ArC–H), 114.6 (d, ArC–H), 69.9 (t), 67.4 (t, CH$_2$–O–Ar), 64.8 (t, CH$_2$–OH) ppm. Starting from **11b** (0.574 g, 0.599 mmol) in 25 mL of anhydrous DMF, we could isolated 0.621 g of brown resin **12b**. ^{13}C gel-phase NMR (100 MHz, CDCl$_3$): δ = 128.5 (d), 114.6 (d), 70.6 (t), 69.6 (t), 67.3 (t), 64.7 (t) ppm.

Attachment of Sensor Molecule to the Wang Linker. The reaction was carried out analogous to the general procedure of the sensor attachment, except for stirring the reaction mixture overnight.

PS-PEG-Bound Sensor 4-(Dimethylamino)butanoic Acid, Hydrochloride. Beads **12a** (0.196 g, 0.193 mmol) in 7 mL of solvent yielded 0.217 g of brown polymer **13a**. ^{13}C gel-phase NMR (100 MHz, CDCl$_3$): δ = 172.1 (s, O–C=O), 57.2 (t, CH$_2$–N), 43.3 (q, N–CH$_3$), 31.1 (t, CH2–C=O), 20.2 (t, CH$_2$–CH$_2$–CH$_2$) ppm. Starting from **12b** (0.209 g, 0.191 mmol) in 7 mL of solvent, we isolated 0.240 g of brown resin **13b**. ^{13}C gel-phase NMR (100 MHz, CDCl$_3$): δ = 172.0 (s), 57.0 (t), 43.1 (q), 30.9 (t), 20.0 (t) ppm.

■ ASSOCIATED CONTENT

Ⓢ Supporting Information

Gel-phase ^{13}C NMR characterization of target PS–PEG resins (**3a–f**, **4a–f**), gel-phase ^{13}C NMR spectra of compounds **4a–f**, **5a–f** and the application example 2 (Heck coupling, compounds **9b,d,f** and **10b,d,f**, Reactagel), and IR spectra of compounds **4a–f**. This material is available free of charge via the Internet at http://pubs.acs.org.

ACS Combinatorial Science

■ AUTHOR INFORMATION

Corresponding Author
*E-mail: christian@braunshier.at. Phone: 0043 650 4531979.
Fax: 0043 1 58801 15499.

Notes
The authors declare no competing financial interest.

■ REFERENCES

(1) Kirschning, A.; Monenschein, H.; Wittenberg, R. Functionalized polymers-emerging versatile tools for solution-phase chemistry and automated parallel synthesis. *Angew. Chem., Int. Ed.* **2001**, *40* (4), 650−679.

(2) Cossy, J.; Arseniyadis, S.; Meyer, C.; Grubbs, R. H. *Metathesis in Natural Product Synthesis: Strategies, Substrates and Catalysts*. Wiley: Weinheim, Germany, 2011; pp 349−372.

(3) Brehm, E.; Breinbauer, R. Investigation of the origin and synthetic application of the pseudodilution effect for Pd-catalyzed macrocyclisations in concentrated solutions with immobilized catalysts. *Org. Biomol. Chem.* **2013**, *11* (29), 4750−4756.

(4) Basu, B.; Paul, S. Solid-phase organic synthesis and catalysis: Some recent strategies using alumina, silica, and polyionic resins. *J. Catal.* **2013**, *2013*, 20.

(5) Toy, P. H.; Lam, Y. *Solid-Phase Organic Synthesis: Concepts, Strategies, and Applications*; Wiley: Hoboken, NJ, 2012.

(6) Andrushko, V.; Andrushko, N. *Stereoselective Synthesis of Drugs and Natural Products*; Wiley: Hoboken, NJ, 2013.

(7) Bayer, E.; Hemmasi, B.; Albert, K.; Rapp, W.; Dengler, M. In *Peptides, Structure and Function*, 8th American Peptide Symphosium, Rockford, IL, 1983; Hruby, V. J., Rich, D. H., Eds.; Pierce Chemical Company: Rockford, IL, 1983; pp 87−90.

(8) Sternlicht, H.; Kenyon, G. L.; Packer, E. L.; Sinclair, J. Carbon-13 nuclear magnetic resonance studies of heterogeneous systems. Amino acids bound to cationic exchange resins. *J. Am. Chem. Soc.* **1971**, *93* (1), 199−208.

(9) Giralt, E.; Rizo, J.; Pedroso, E. Application of gel-phase carbon-13 NMR to monitor solid phase peptide synthesis. *Tetrahedron* **1984**, *40* (20), 4141−4152.

(10) Yan, B. Monitoring the progress and the yield of solid-phase organic reactions directly on resin supports. *Acc. Chem. Res.* **1998**, *31* (10), 621−630.

(11) Vaino, A. R.; Janda, K. D. Solid-phase organic synthesis: A critical understanding of the resin. *J. Comb. Chem.* **2000**, *2* (6), 579−596.

(12) Dal Cin, M.; Davalli, S.; Marchioro, C.; Passarini, M.; Perini, O.; Provera, S.; Zaramella, A. Analytical methods for the monitoring of solid phase organic synthesis. *Farmaco* **2002**, *57* (6), 497−510.

(13) Braunshier, C.; Hametner, C. Gel-phase ^{13}C NMR spectroscopy of selected solid phase systems. *QSAR Comb. Sci.* **2007**, *26* (8), 908−918.

(14) Greenland, B. W.; Liu, S.; Cavalli, G.; Alpay, E.; Steinke, J. H. G. Synthesis of beaded poly(vinyl ether) solid supports with unique solvent compatibility. *Polymer* **2010**, *51* (14), 2984−2992.

(15) Espinosa, J. F. High resolution magic angle spinning NMR applied to the analysis of organic compounds bound to solid supports. *Curr. Top. Med. Chem.* **2011**, *11* (1), 74−92.

(16) Siyad, M. A.; Kumar, G. S. V. Poly(ethylene glycol) grafted polystyrene dendrimer resins: Novel class of supports for solid phase peptide synthesis. *Polymer* **2012**, *53* (19), 4076−4090.

(17) Cozzi, F. Immobilization of organic catalysts. When, why, and how. *Adv. Synth. Catal.* **2006**, *348* (12 + 13), 1367−1390.

(18) Braunshier, C.; Hametner, C.; Froehlich, J.; Schnoeller, J.; Hutter, H. Novel monodisperse PEG-grafted polystyrene resins: Synthesis and application in gel-phase ^{13}C NMR spectroscopy. *Tetrahedron Lett.* **2008**, *49* (50), 7103−7105.

(19) Lumpi, D.; Braunshier, C.; Hametner, C.; Horkel, E.; Zachhuber, B.; Lendl, B.; Froehlich, J. Convenient multigram synthesis of monodisperse oligo(ethylene glycols): Effective reaction monitoring by infrared spectroscopy using an attenuated total reflection fibre optic probe. *Tetrahedron Lett.* **2009**, *50* (47), 6469−6471.

(20) Ishizone, T.; Han, S.; Okuyama, S.; Nakahama, S. Synthesis of water-soluble polymethacrylates by living anionic polymerization of trialkylsilyl-protected oligo(ethylene glycol) methacrylates. *Macromolecules* **2003**, *36* (1), 42−49.

(21) Sprung, M. M.; Nelson, L. S. Trimethylsilyl derivatives of polyols. *J. Org. Chem.* **1955**, *20*, 1750−1756.

(22) Rano, T. A.; Chapman, K. T. Solid phase synthesis of aryl ethers via the Mitsunobu reaction. *Tetrahedron Lett.* **1995**, *36* (22), 3789−3792.

(23) Bennett, W. D.; Christensen, J., Eds. *Advanced ChemTech Handbook of Combinatorial & Solid Phase Organic Chemistry*; Advanced ChemTech: Louisville, KY, 1998.

(24) Kita, R.; Svec, F.; Frechet, J. M. J. Hydrophilic polymer supports for solid-phase synthesis: Preparation of poly(ethylene glycol) methacrylate polymer beads using "classical" suspension polymerization in aqueous medium and their application in the solid-phase synthesis of hydantoins. *J. Comb. Chem.* **2001**, *3* (6), 564−571.

(25) Hiroshige, M.; Hauske, J. R.; Zhou, P. Formation of C−C bond in solid phase synthesis using the Heck reaction. *Tetrahedron Lett.* **1995**, *36* (26), 4567−4570.

(26) Gooding, O. W.; Baudart, S.; Deegan, T. L.; Heisler, K.; Labadie, J. W.; Newcomb, W. S.; Porco, J. A., Jr.; Van, E. P. On the development of new poly(styrene-oxyethylene) graft copolymer resin supports for solid-phase organic synthesis. *J. Comb. Chem.* **1999**, *1* (1), 113−122.

3. EXPERIMENTAL PART

General methods

All reactions containing water or air sensitive reagents were performed in oven-dried glassware under inert atmosphere (argon). Reagents were purchased from commercial sources and used without further purification. Anhydrous THF and DCM were obtained by filtration through drying columns. Analytical thin-layer chromatography (TLC) was performed on aluminium-backed plates, pre-coated with silica (Merck silica gel 60 F254). Visualization of the developed chromatogram was performed by UV absorbance (254 nm) and/or colourisation with PMA/CAN dip reagent (10 g phosphomolybdic acid hydrate, 1 g cerium(IV)ammonium nitrate, 20 g conc. sulphuric acid) and subsequent heating.

NMR spectra were recorded at 200 MHz for ^{1}H and 50 MHz for ^{13}C. Data for ^{1}H NMR are reported as follows: chemical shift in parts per million from TMS with the solvent as an internal reference (CDCl$_3$ δ = 7.26 ppm, DMSO-d$_6$ δ = 2.50 ppm), multiplicity (s = singlet, bs = broad singlet, d = doublet, t = triplet and m = multiplet), coupling constant in Hz and integration. ^{13}C NMR spectra are reported in ppm from TMS using the central peak of the solvent as reference (CDCl$_3$ δ = 77.00 ppm, DMSO-d$_6$ δ = 39.52 ppm); multiplicity with respect to proton (deduced from APT experiments, s = quaternary C, d = CH, t = CH$_2$, q = CH$_3$).

For off-line spectra recording a Fourier transform infrared spectrometer equipped with a broad band MCT detector was used. Spectra were recorded on a single bounce diamond ATR unit placed in the sample compartment of the FTIR spectrometer.

In-line IR monitoring was performed using a mid-IR fibre optic probe from ART Photonics attached to a FTIR spectrometer. The probe was directly inserted through the ground neck of the reaction vessel and comprised two 1 m silver halide fibres (i.d. 1 mm) connecting to a conical diamond ATR element housed in a rod of hastelloy. Using this set-up it was possible to follow the reactions to be studied in real-time covering a spectral range from 600 to 2000 wavenumbers.

Preparation of mono-trityl-protected glycols (1) and di-tosylated glycols (2)

7,7,7-Triphenyl-3,6-dioxaheptanol **(1a)**, 13,13,13-triphenyl-3,6,9,12-tetraoxatridecanol **(1b)**, 1,5-Bis-(tosyloxy)-3-oxapentane **(2a)** and 1,11-Bis(tosyloxy)-3,6,9-trioxaundecane **(2b)** were prepared according to literature.[57] Purities were verified by NMR spectroscopy.

Preparation of di-tritylated glycols 3

General procedure

The detailed synthetic procedure for the preparation of di-tritylated glycols **3** is given in this general procedure exemplarily for compound **3b** (largest experimental scale in this series of compounds). The synthetic procedures for compounds **3a**, **3c** and **3d** refer to this general procedure and mention specific details or deviations from the general procedure in the respective section.

Synthesis of 1,1,1,27,27,27-hexaphenyl-2,5,8,11,14,17, 20,23,26-nonaoxaheptacosane 3b

1a: k=2   **2b**: m=4   **3b**: n=8
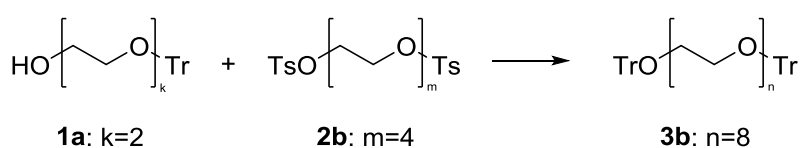
Under argon atmosphere, a 4-neck round bottom flask equipped with mechanical stirrer, reflux condenser, thermometer as well as dropping funnel and the ATR-IR probe inlet was charged with sodium hydride (12.00 g, 500 mmol, 2.5 equiv.) and dry THF (500 mL). To the well stirred suspension was added a solution of mono-trityl protected glycol **1a** (139.38 g, 400 mmol, 2.0 equiv.) in dry THF (500 mL) at ambient temperature. After completion of the reaction according to IR-monitoring (4 h), the mixture was cooled to 0 °C and a solution of di-tosylated glycol **2b** (100.52 g, 200 mmol, 1.0 equiv.) in dry THF (500 mL) was added. The temperature was adjusted to 40 °C and the suspension was stirred for 80 h. For work-up, the reaction mixture was poured onto ice water (1200 mL) / chloroform (800 mL). The phases were separated and the aqueous phase was extracted with chloroform (500 mL). The combined organic layers were washed with brine (500 mL) and dried over sodium sulfate. After removing the solvent under reduced pressure, the title compound was obtained.

Yield: 165.36 g (97 %) clear, slightly orange, viscous oil

Spectral data (copies of ^{1}H-NMR, ^{13}C-APT-NMR and ATR-IR spectra) and combustion analysis for 3b
^{1}H NMR (200 MHz, DMSO-d$_6$) δ = 7.48–7.15 (m, 30 H), 3.67–3.39 (m, 28 H), 3.06 (t, J = 4.8 Hz, 4 H).
^{13}C APT NMR (50 MHz, DMSO-d$_6$) δ = 143.8 (s), 128.2 (d), 127.8 (d), 126.9 (d), 85.9 (t), 70.1 (t), 69.9 (t), 69.85 (t), 69.82 (t), 69.77 (t), 69.7 (t), 63.0 (t).
$C_{54}H_{62}O_9$ (855.09): calcd. C 75.85, H 7.31; found C 76.15, H 7.15, N <0.05.
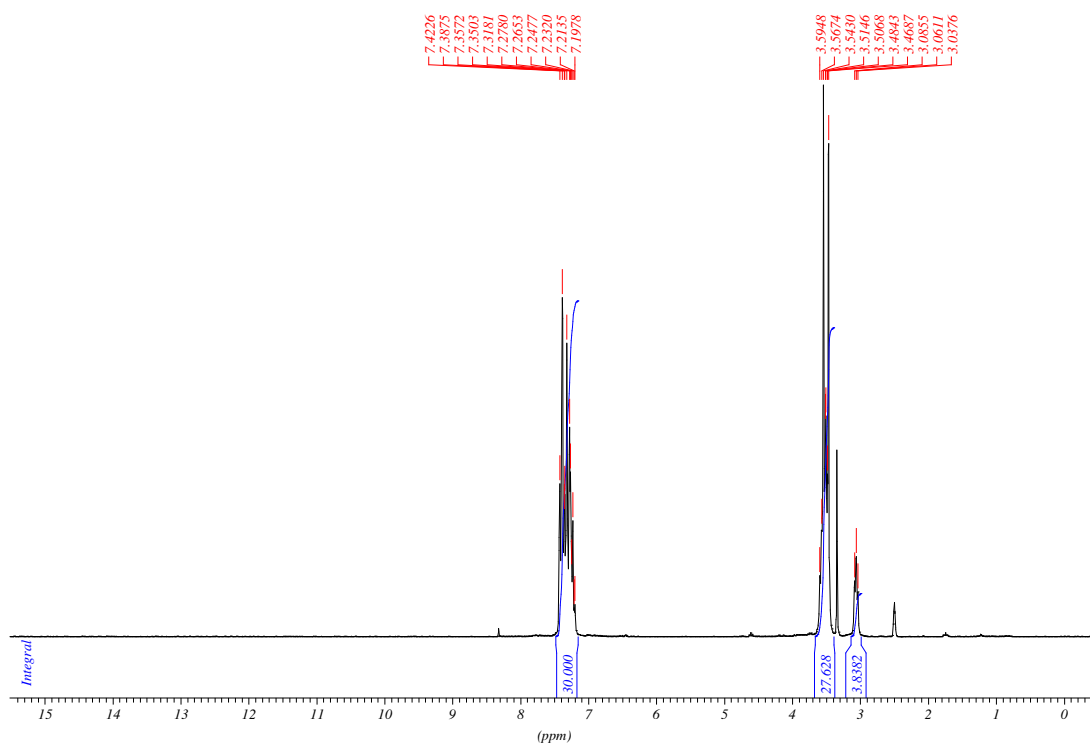
Spectrum 3.1. ^{1}H NMR (200 MHz, DMSO-d$_6$) of substance **3b**.
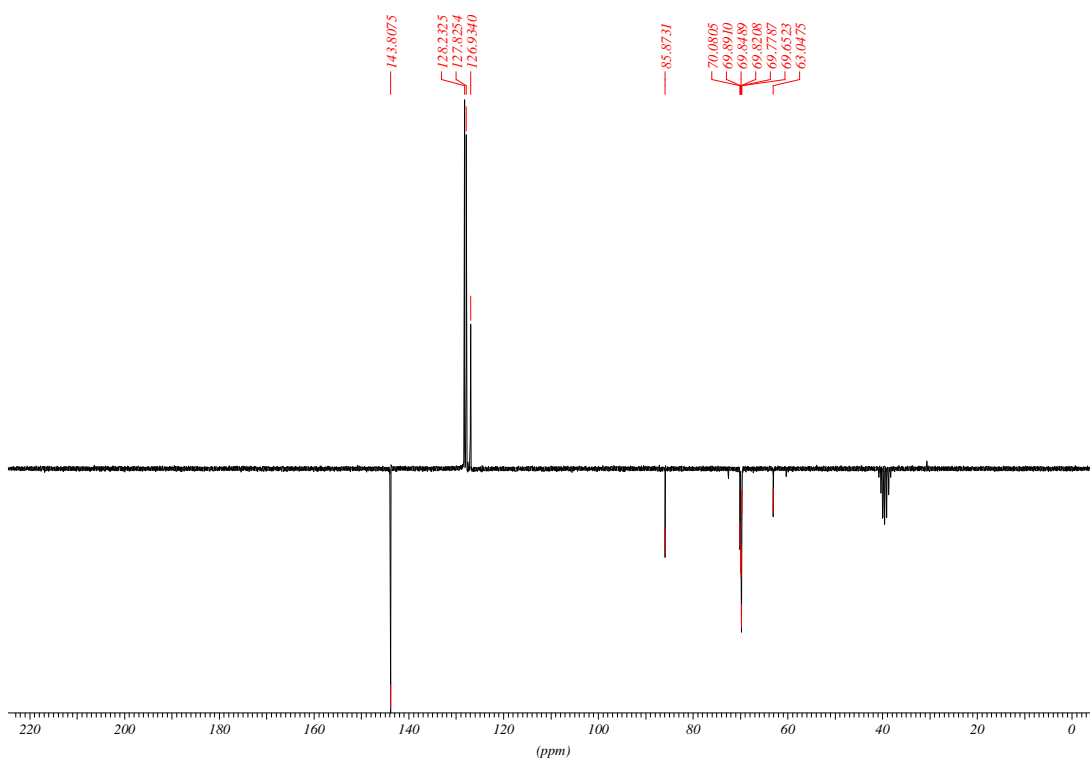
Spectrum 3.2. ^{13}C APT NMR (50 MHz, DMSO-d$_6$) of substance **3b**.
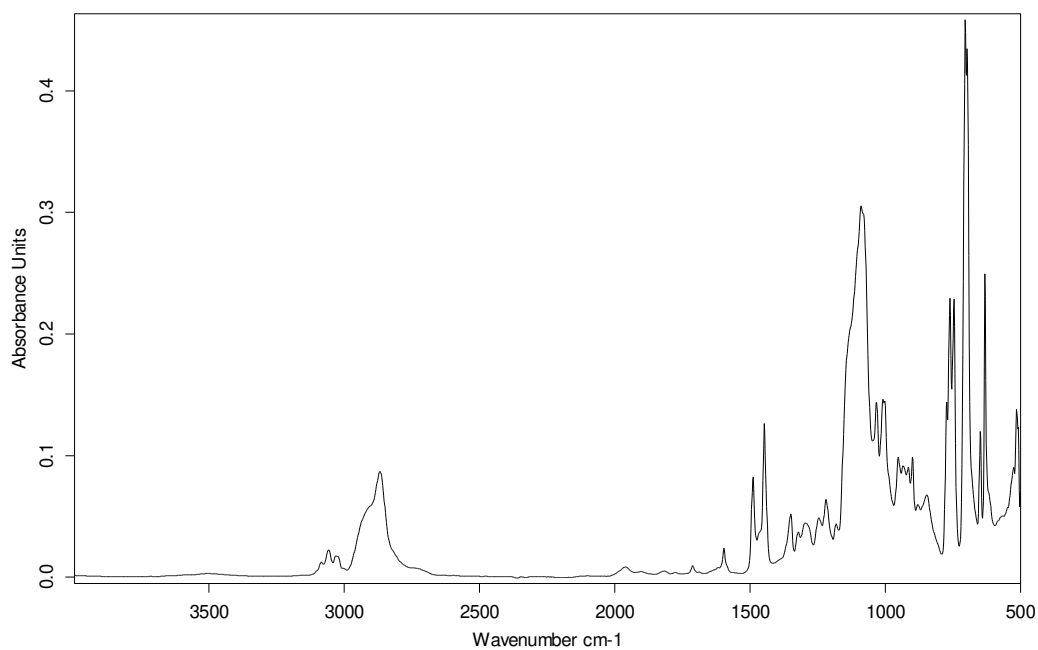
Spectrum 3.3. IR spectrum (ATR) of substance **3b**.

*Synthesis of 1,1,1,21,21,21-hexaphenyl-2,5,8,11,14,17,20-heptaoxaheneicosane **3a***


1a: k=2   **2a**: m=2   **3a**: n=6
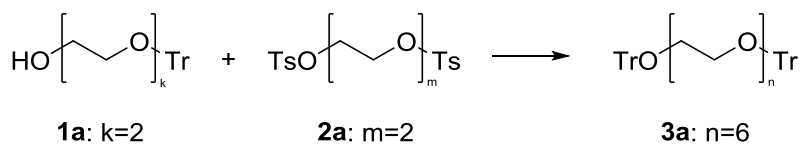
Compound **3a** was prepared following the procedure for substance **3b**, described in the general procedure using **2a** (10.36 g, 25 mmol, 1 eq.), **1a** (17.42 g, 50 mmol, 2 eq.) and NaH (1.50 g, 63 mmol, 2.5 eq.) in dry THF (180 mL). The deprotonation was carried out for 4 h at 25 °C and the substitution was stirred for 80 h at 40 °C under inert atmosphere. The work-up was according to the general procedure extracting the aqueous phase 4-times with $CHCl_3$.

Yield: 18.75 g (98 %) clear, slightly yellow, viscous oil

*Spectral data (copies of ^{1}H-NMR, ^{13}C-APT-NMR and ATR-IR spectra) for **3a***

^{1}H NMR (200 MHz, DMSO-d_6) δ 7.42 – 7.23 (m, 30H), 3.59 – 3.51 (m, 20H), 3.06 (t, J = 4.8 Hz, 4H).

^{13}C APT NMR (50 MHz, DMSO-d_6) δ 143.8 (s), 128.2 (d), 127.8 (d), 126.9 (d), 85.9 (t), 69.8 (t), 63.1 (t).
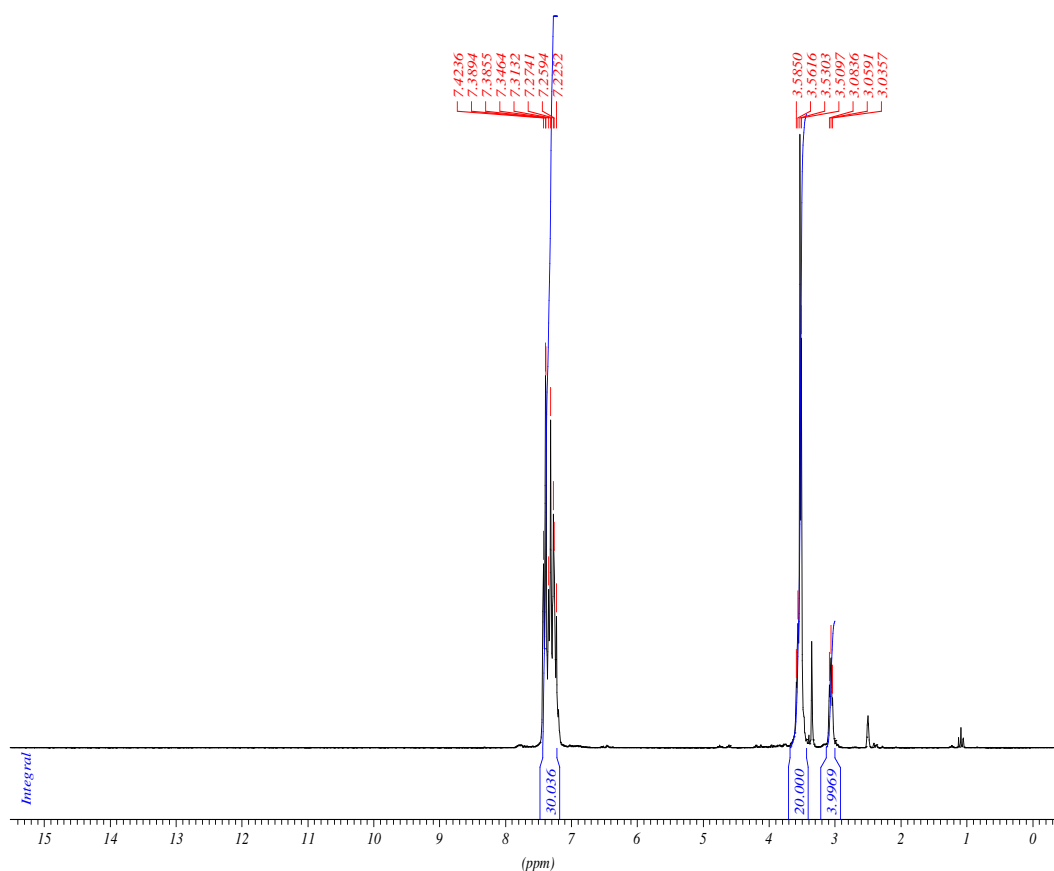
Spectrum 3.4. ^{1}H NMR (200 MHz, DMSO-d_6) of substance **3a**.
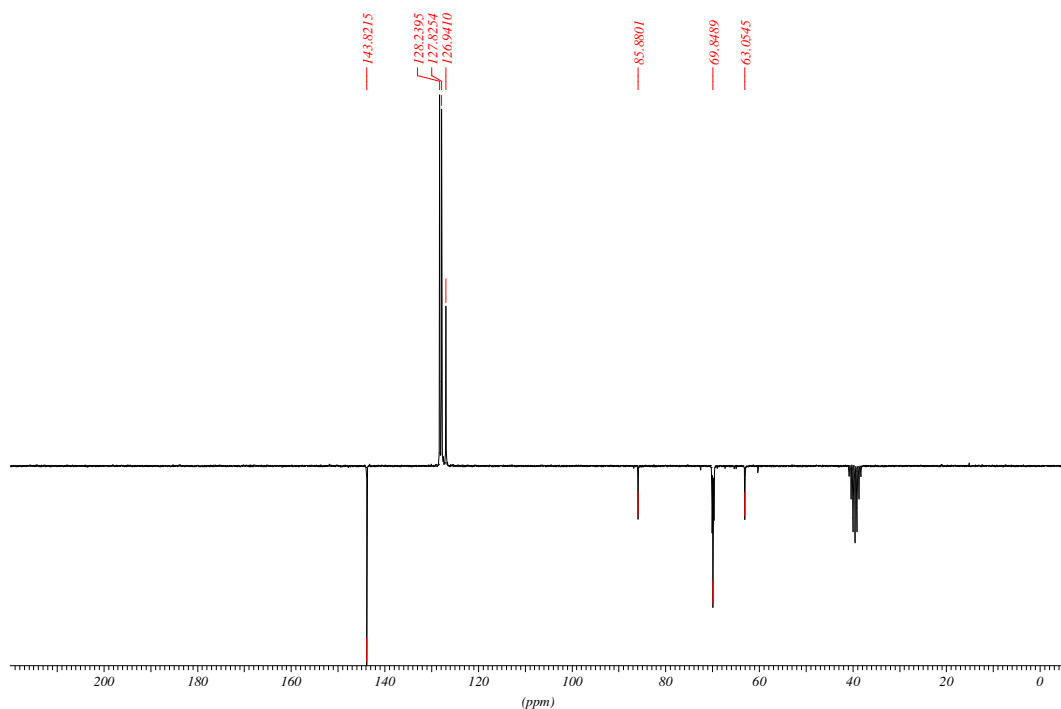
Spectrum 3.5. ^{13}C APT NMR (50 MHz, DMSO-d$_6$) of substance **3a**.
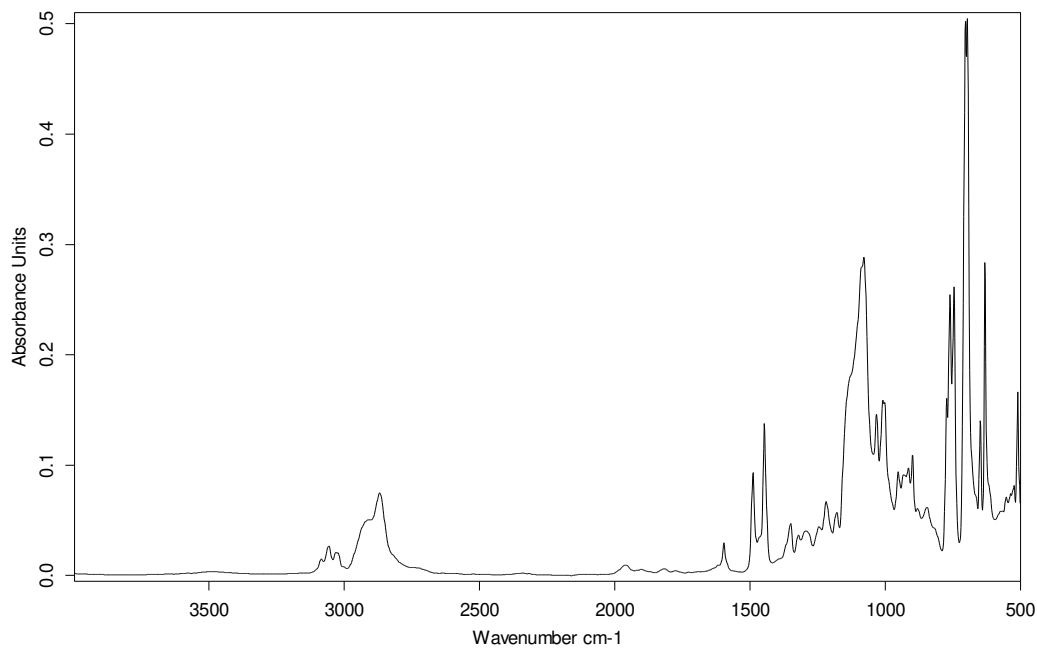
Spectrum 3.6. IR spectrum (ATR) of substance **3a**.

Synthesis of 1,1,1,33,33,33-hexaphenyl-2,5,8,11,14,17,20,23,26,29,32-

undecaoxatritriacontane **3c**

1b: k=4   **2a**: m=2   **3c**: n=10
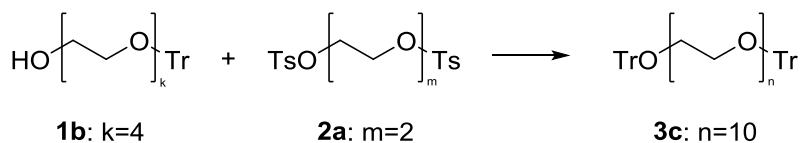
Compound **3c** was prepared following the procedure for substance **3b**, described in the general procedure using **2a** (10.36 g, 25 mmol, 1 eq.), **1b** (21.83 g, 50 mmol, 2 eq.) and NaH (1.50 g, 63 mmol, 2.5 eq.) in dry THF (200 mL). The deprotonation was carried out for 2 h at 25 °C and the substitution was stirred for 58 h at 40 °C under inert atmosphere. The work-up was according to the general procedure extracting the aqueous phase 4-times with CHCl$_3$.

Yield: 23.16 g (98 %) clear, slightly yellow, viscous oil

Spectral data (copies of ^{1}H-NMR, ^{13}C-APT-NMR and ATR-IR spectra) for **3c**

^{1}H NMR (200 MHz, DMSO-d$_6$) δ 7.42 – 7.24 (m, 30H), 3.55 – 3.47 (m, 36H), 3.06 (t, J = 4.6 Hz, 4H).

^{13}C APT NMR (50 MHz, DMSO-d$_6$) δ 143.8 (s), 128.2 (d), 127.8 (d), 126.9 (d), 85.9 (t), 69.8 (t), 63.1 (t).
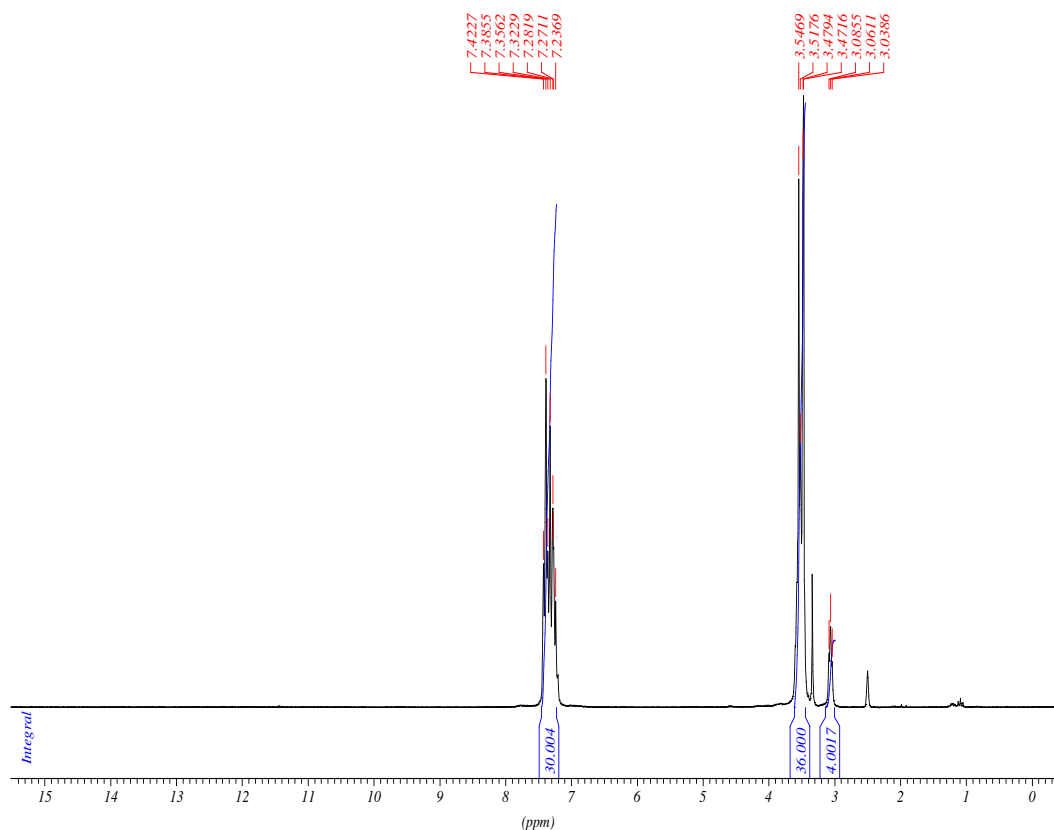
Spectrum 3.7. ^{1}H NMR (200 MHz, DMSO-d$_6$) of substance **3c**.
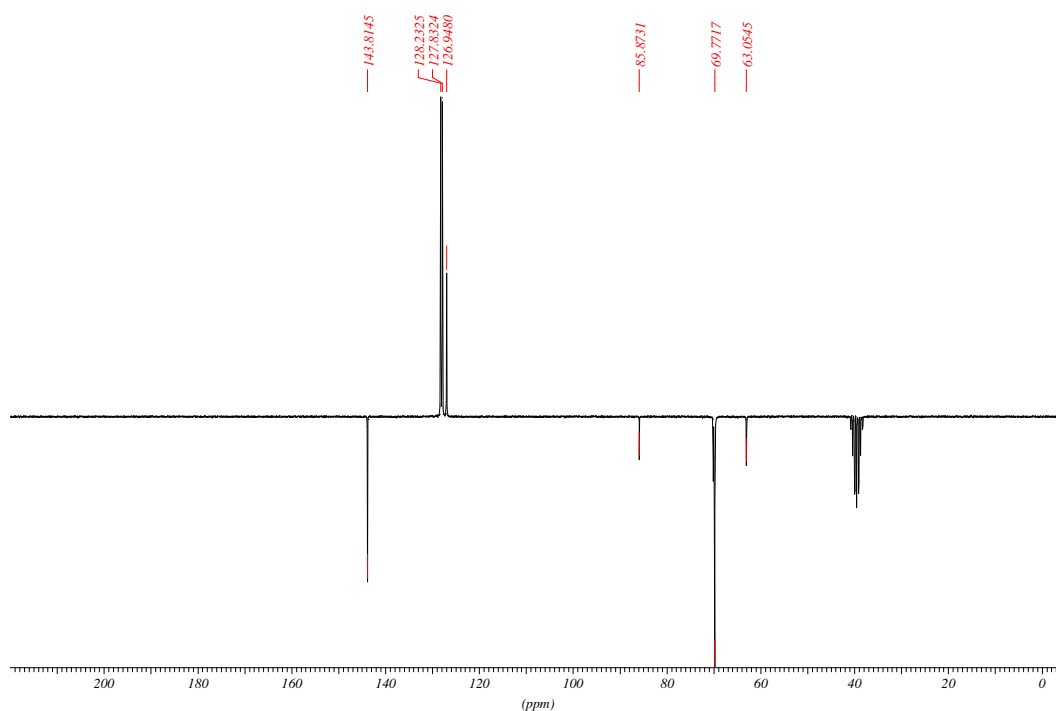
Spectrum 3.8. ^{13}C APT NMR (50 MHz, DMSO-d$_6$) of substance **3c**.
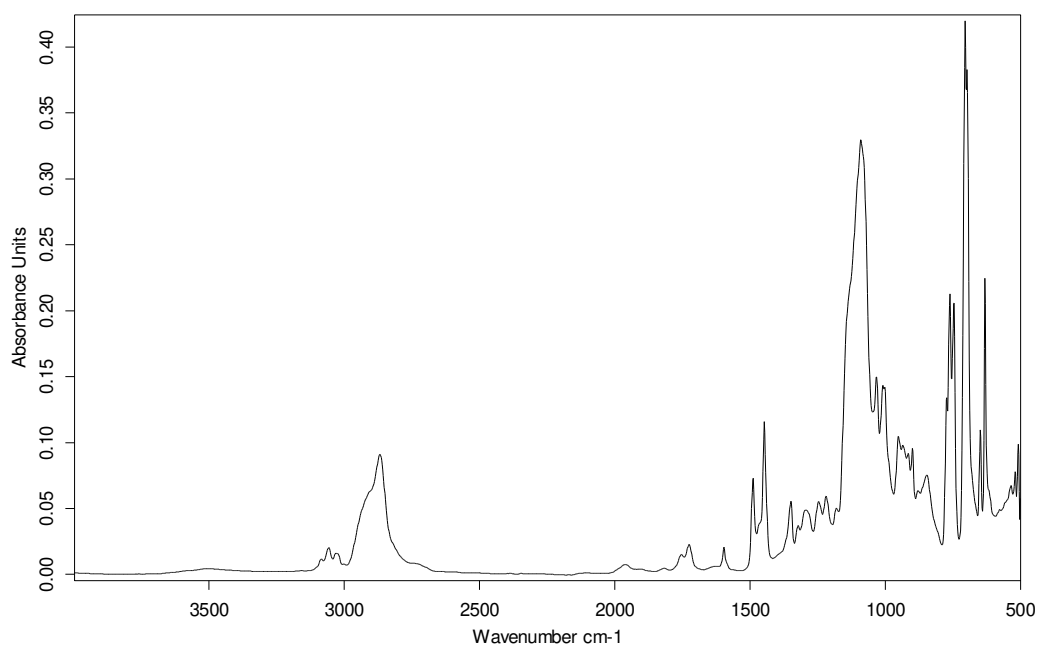
Spectrum 3.9. IR spectrum (ATR) of substance **3c**.

Synthesis of 1,1,1,39,39,39-hexaphenyl-2,5,8,11,14,17,20,23,26,29,32,35,38-tridecaoxanona-triacontane 3d


1b: k=4   **2b**: m=4   **3d**: n=12
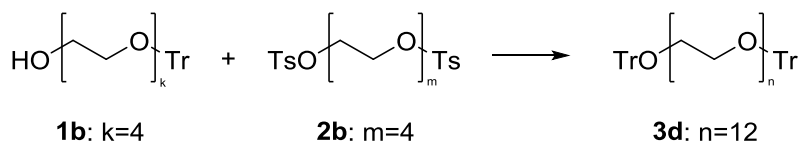
Compound **3d** was prepared following the procedure for substance **3b**, described in the general procedure using **2b** (12.57 g, 25 mmol, 1 eq.), **1b** (21.83 g, 50 mmol, 2 eq.) and NaH (1.50 g, 63 mmol, 2.5 eq.) in dry THF (200 mL). The deprotonation was carried out for 2 h at 25 °C and the substitution was stirred for 58 h at 40 °C under inert atmosphere. The work-up was according to the general procedure extracting the aqueous phase 3-times with $CHCl_3$.

Yield: 24.55 g (95 %) clear, slightly orange, viscous oil

Spectral data (copies of ^{1}H-NMR, ^{13}C-APT-NMR and ATR-IR spectra) for 3d

^{1}H NMR (200 MHz, DMSO-d_6) δ 7.43 – 7.24 (m, 30H), 3.60 – 3.48 (m, 44H), 3.06 (t, J = 4.8 Hz, 4H).

^{13}C APT NMR (50 MHz, DMSO-d_6) δ 143.8 (s), 128.2 (d), 127.8 (d), 127.0 (d), 85.9 (t), 69.8 (t), 63.1 (t).
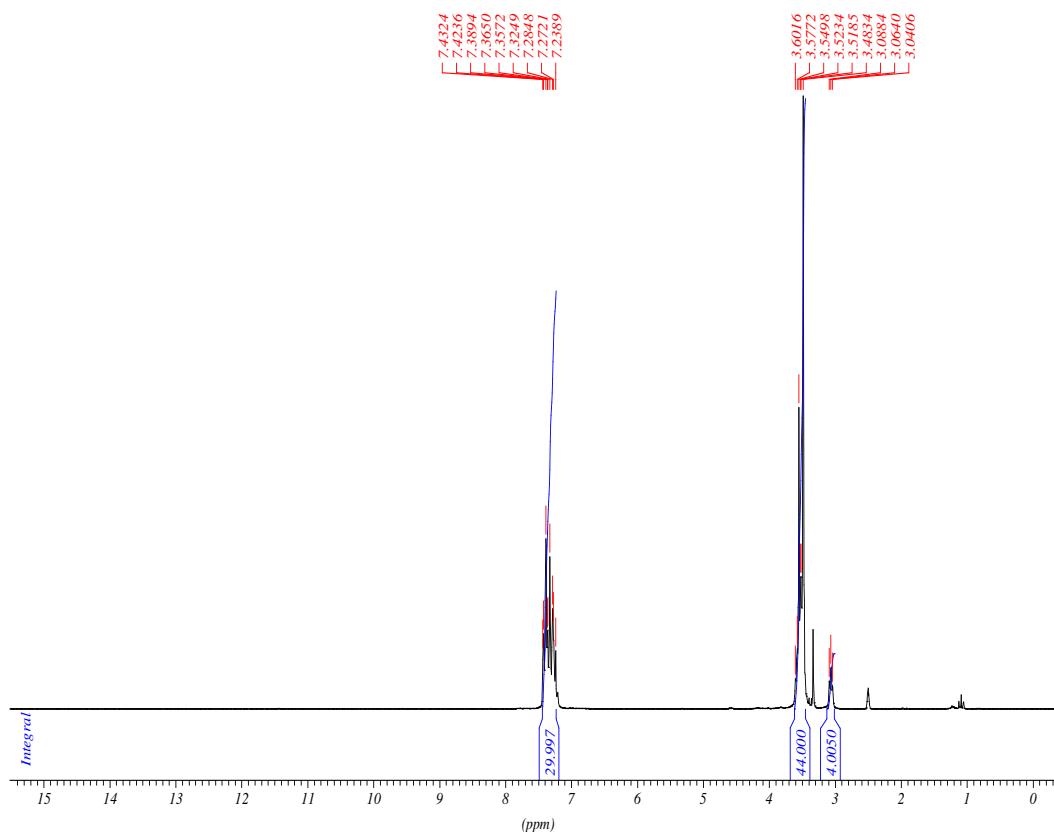
Spectrum 3.10. ^{1}H NMR (200 MHz, DMSO-d_6) of substance **3d**.
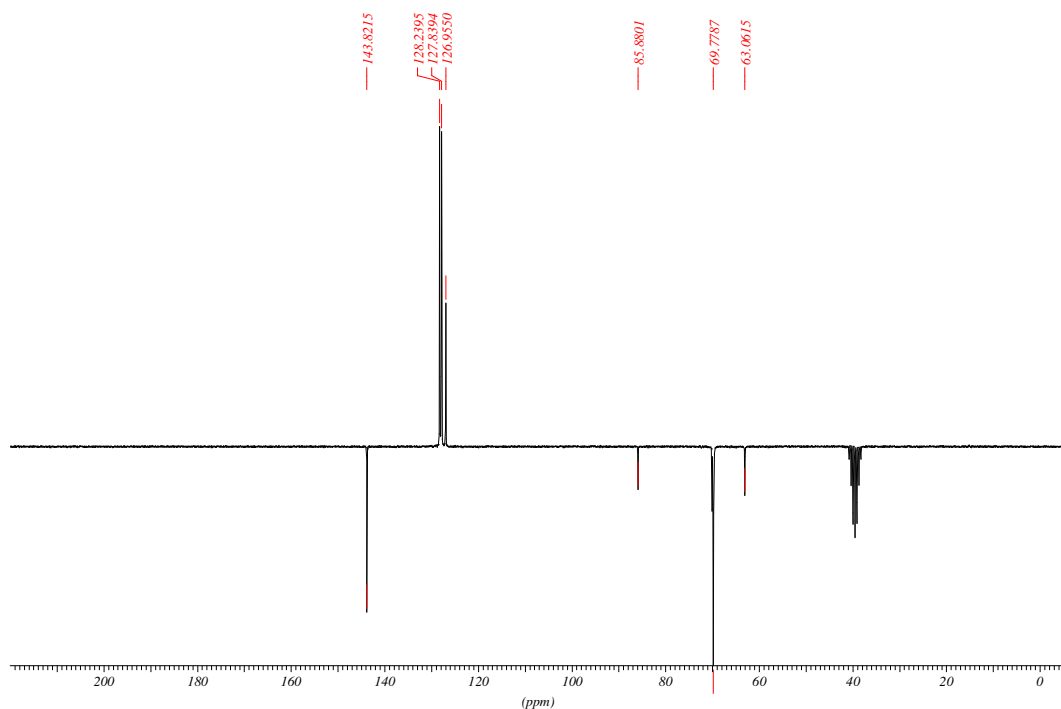
Spectrum 3.11. ^{13}C APT NMR (50 MHz, DMSO-d$_6$) of substance **3d**.
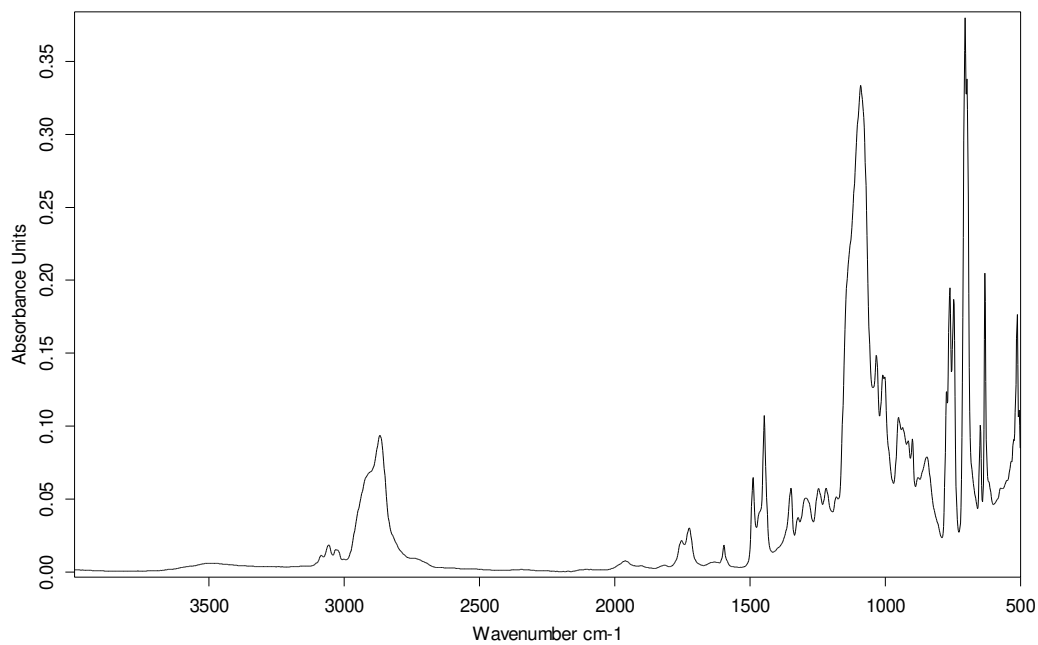
Spectrum 3.12. IR spectrum (ATR) of substance **3d**.

Preparation of target glycols 4

General procedure

The detailed synthetic procedure for the preparation of di-tritylated glycols **4** is given in this general procedure exemplarily for compound **4b** (largest experimental scale in this series of compounds). The synthetic procedures for compounds **4a**, **4c** and **4d** refer to this general procedure and mention specific details or deviations from the general procedure in the respective section.

*Synthesis of 3,6,9,12,15,18,21-heptaoxatricosane-1,23-diol **4b***
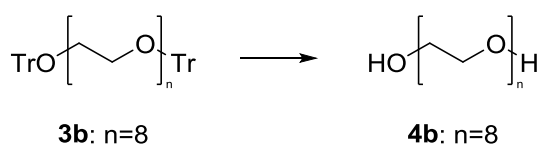
3b: n=8   **4b**: n=8

Compound **3b** (128.26 g, 150 mmol) was stirred with 80 % acetic acid (1200 mL) at 40 °C. After 2 h the reaction was completed according to HPLC analysis. The mixture was allowed to cool to ambient temperature and poured onto ice water (600 mL). The precipitate was filtered off over a glass sinter funnel. The filtrate was concentrated under reduced pressure leaving a cloudy oil. The crude product was mixed with cold water (500 mL) and the suspension was again filtered over the same glass sinter funnel, still containing the bed of triphenylmethanol formed during the first filtration. The filter cake was washed with cold water, giving 77.02 g (99 %) of pure triphenyl methanol after drying at 40 °C / 15 mbar. The solvent of the filtrate was removed under reduced pressure (0.05 mbar) to afford the title compound.

Yield: 53.20 g (96 %) clear, slightly orange oil

*Spectral data (copies of ^{1}H-NMR, ^{13}C-APT-NMR and ATR-IR spectra) and combustion analysis for **4b***

^{1}H NMR (200 MHz, CDCl$_3$) δ = 3.62–3.38 (m, 32 H), 3.30 (bs, 2 H).

^{13}C NMR (50 MHz, CDCl$_3$) δ = 72.2, 70.15, 70.10, 69.9, 61.1.

C$_{16}$H$_{34}$O$_9$ (370.44): calcd. C 51.88, H 9.25; found C 51.81, H 9.34, N <0.05.
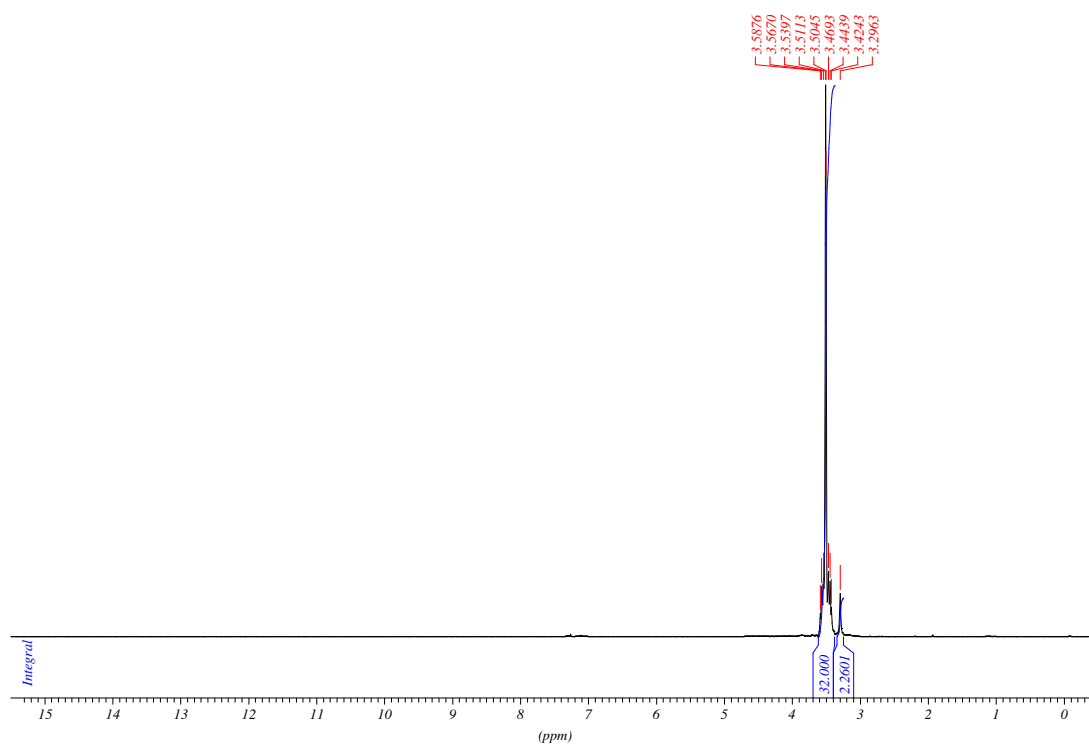
Spectrum 3.13. ^{1}H NMR (200 MHz, CDCl$_3$) of substance **4b**.
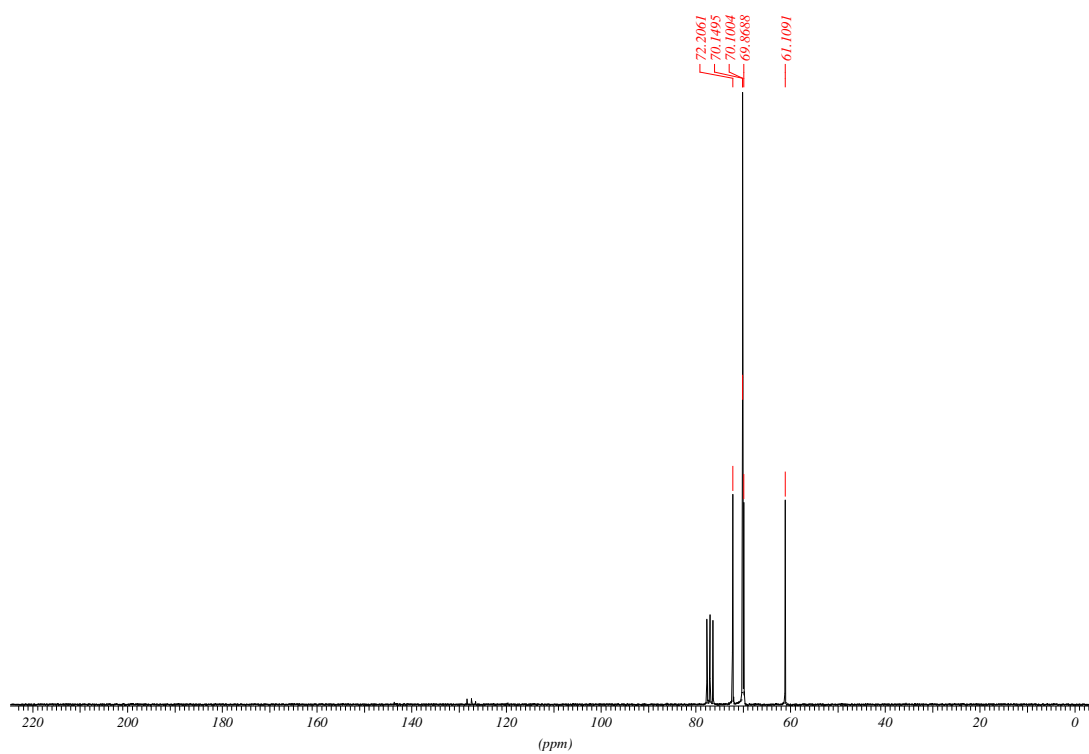
Spectrum 3.14. ^{13}C APT NMR (50 MHz, CDCl$_3$) of substance **4b**.
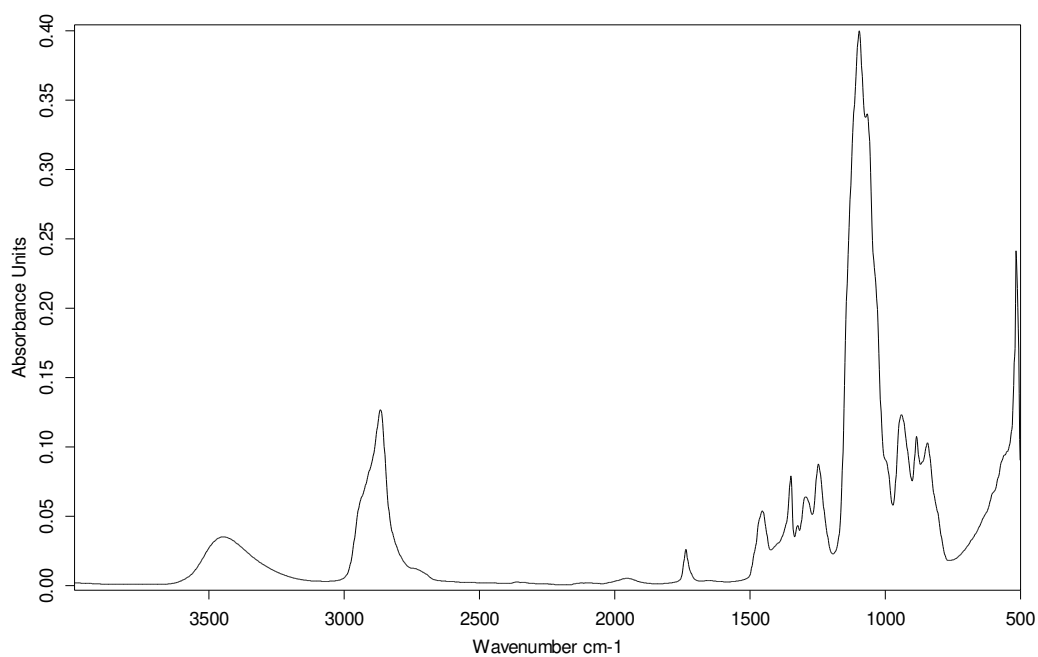
Spectrum 3.15. IR spectrum (ATR) of substance **4b**.

*Synthesis of 3,6,9,12,15-pentaoxaheptadecane-1,17-diol **4a***
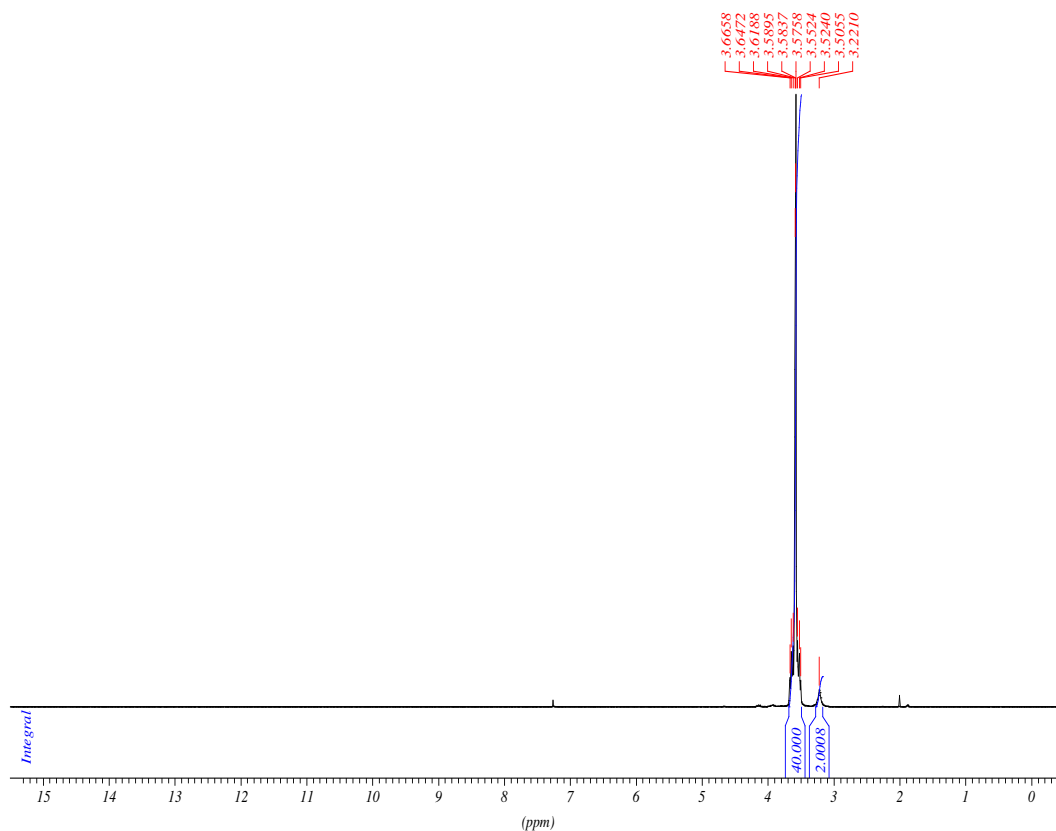

3a: n=6   **4a**: n=6
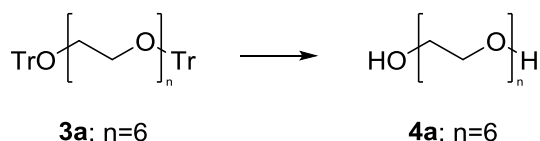
Compound **4a** was prepared according to the procedure for substance **4b**, described in the general procedure stirring **3a** (15.34 g, 20 mmol, 1 eq.) and aqueous acetic acid solution (80 %, 160 mL) for exactly 2 h at 40 °C. Following the general procedure for the work-up 10.21 g (98 %) of pure triphenylmethanol were obtained as a side product.

Yield: 5.51 g (98 %) clear, slightly yellow, viscous oil

*Spectral data (copies of ^{1}H-NMR, ^{13}C-NMR and ATR-IR spectra) for **4a***

^{1}H NMR (200 MHz, CDCl$_3$) δ 3.67 – 3.51 (m, 24H), 3.33 (bs, 2H).

^{13}C NMR (50 MHz, CDCl$_3$) δ 72.4, 70.4, 70.3, 70.3, 70.1, 61.4.
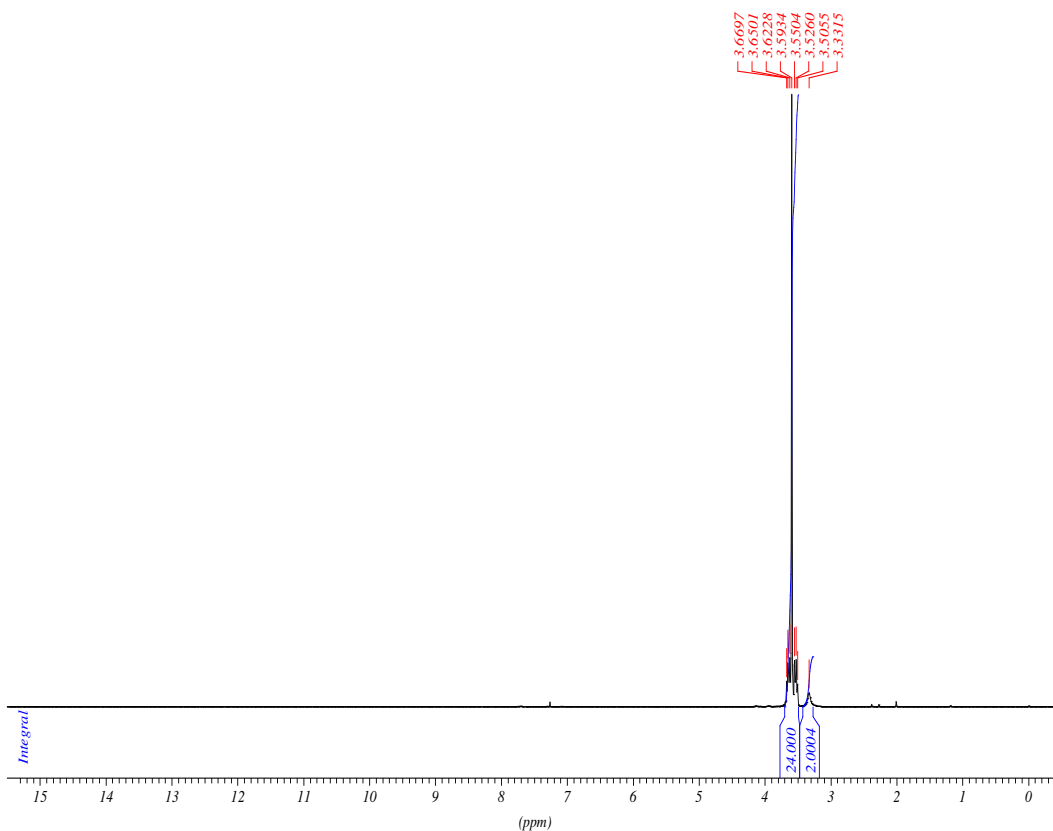
Spectrum 3.16. ^{1}H NMR (200 MHz, CDCl$_3$) of substance **4a**.
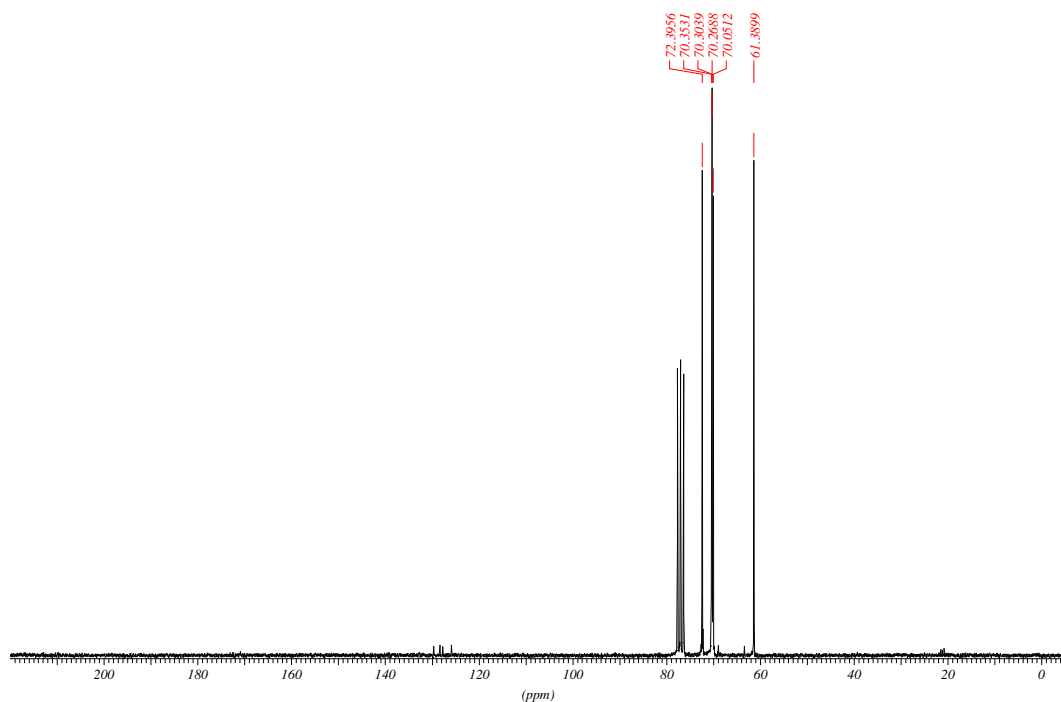
Spectrum 3.17. ^{13}C APT NMR (50 MHz, CDCl$_3$) of substance **4a**.
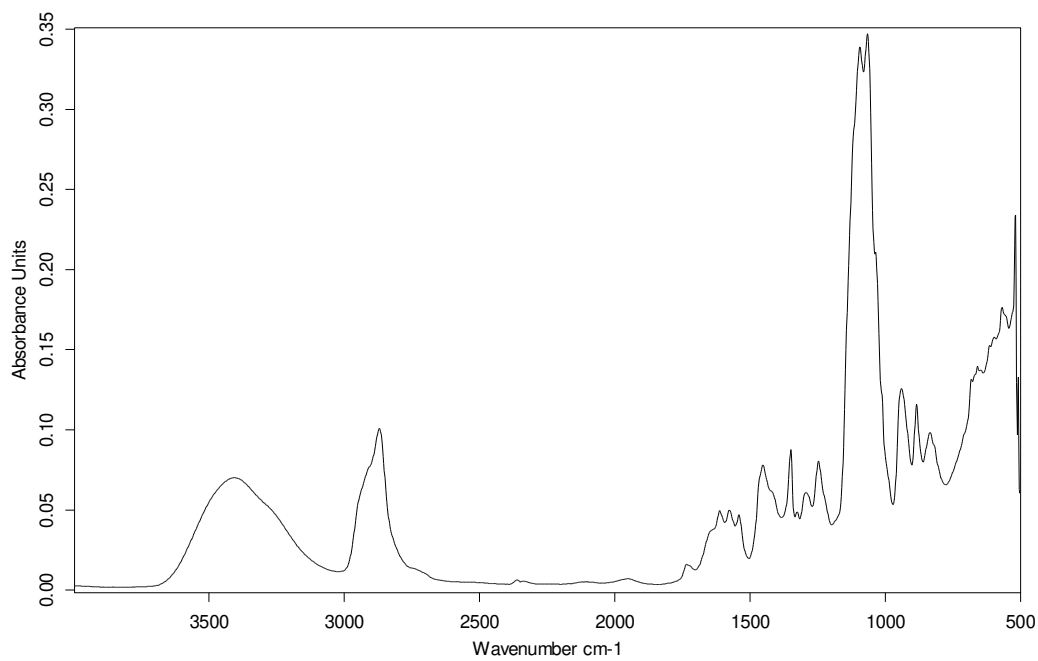
Spectrum 3.18. IR spectrum (ATR) of substance **4a**.

Synthesis of 3,6,9,12,15,18,21,24,27-nonaoxanonacosan-1,29-diol 4c

3c: n=10   **4c**: n=10
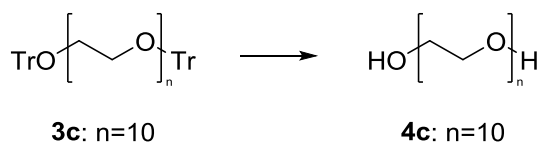
Compound **4c** was prepared according to the procedure for substance **4b**, described in the general procedure stirring **3c** (18.86 g, 20 mmol, 1 eq.) and aqueous acetic acid solution (80 %, 160 mL) for exactly 2 h at 40 °C. Following the general procedure for the work-up 10.32 g (99 %) of pure triphenylmethanol were obtained as a side product.

Yield: 9.03 g (98 %) clear, slightly yellow oil

Spectral data (copies of ^{1}H-NMR, ^{13}C-NMR and ATR-IR spectra) for 4c

^{1}H NMR (200 MHz, CDCl$_3$) δ 3.67 – 3.51 (m, 40H), 3.22 (bs, 2H).

^{13}C NMR (50 MHz, CDCl$_3$) δ 72.4, 70.3, 70.1, 61.4.

Spectrum 3.19. ^{1}H NMR (200 MHz, CDCl$_3$) of substance **4c**.
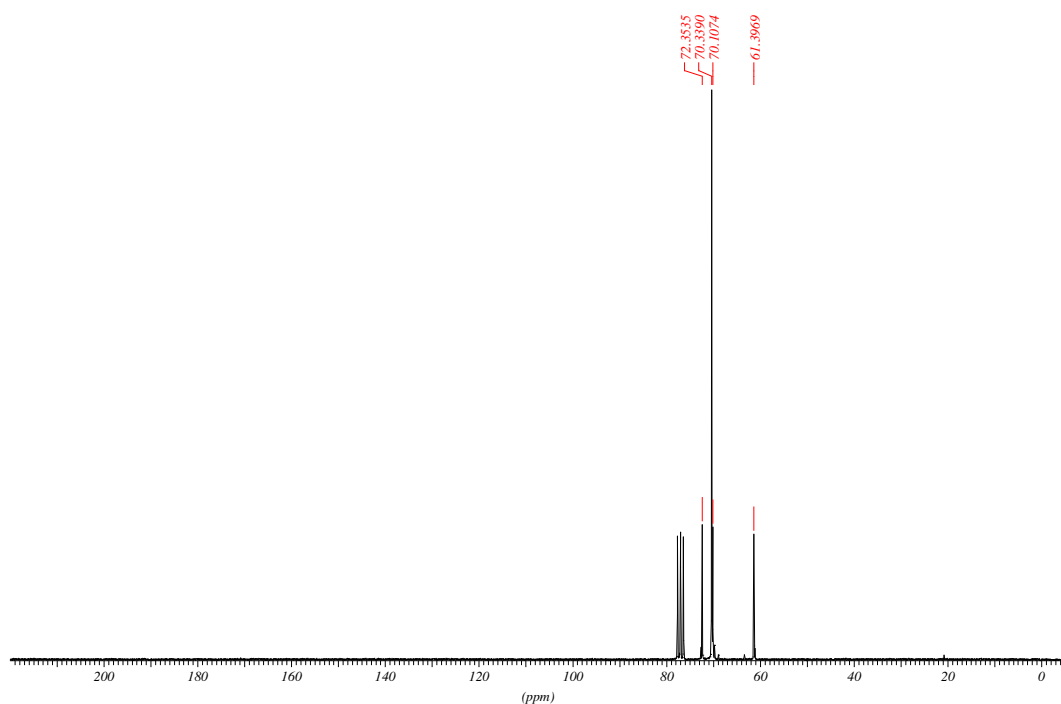
Spectrum 3.20. ^{13}C APT NMR (50 MHz, CDCl$_3$) of substance **4c**.
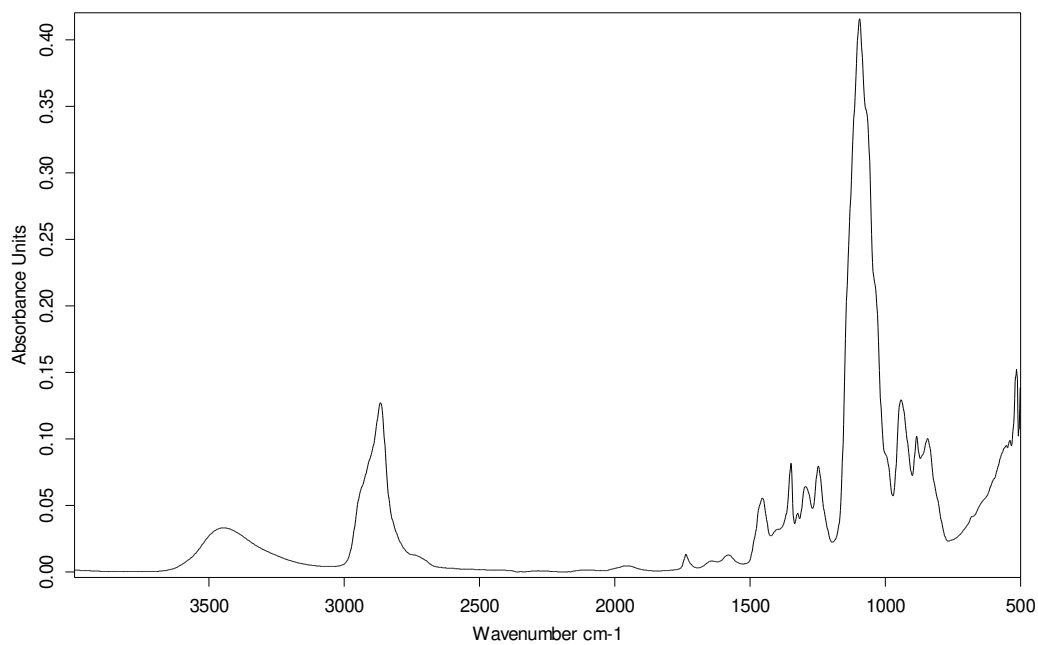
Spectrum 3.21. IR spectrum (ATR) of substance **4c**.

Synthesis of 3,6,9,12,15,18,21,24,27,30,33-undecaoxapentatriacontane-1,35-diol **4d**

3d: n=12   **4d**: n=12
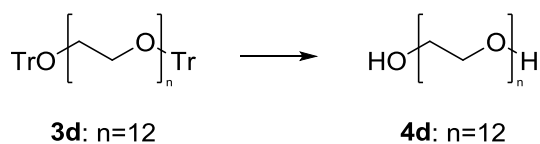
Compound **4d** was prepared according to the procedure for substance **4b**, described in the general procedure stirring **3d** (20.63 g, 20 mmol, 1 eq.) and aqueous acetic acid solution (80 %, 180 mL) for exactly 2 h at 40 °C. Following the general procedure for the work-up 10.13 g (97 %) of pure triphenylmethanol were obtained as a side product.

Yield: 10.78 g (99 %) clear, slightly orange oil

Spectral data (copies of ^{1}H-NMR, ^{13}C-NMR and ATR-IR spectra) for **4d**

^{1}H NMR (200 MHz, CDCl$_3$) δ 3.63 – 3.47 (m, 48H), 3.21 (bs, 2H).

^{13}C NMR (50 MHz, CDCl$_3$) δ 72.2, 70.2, 70.0, 61.2.
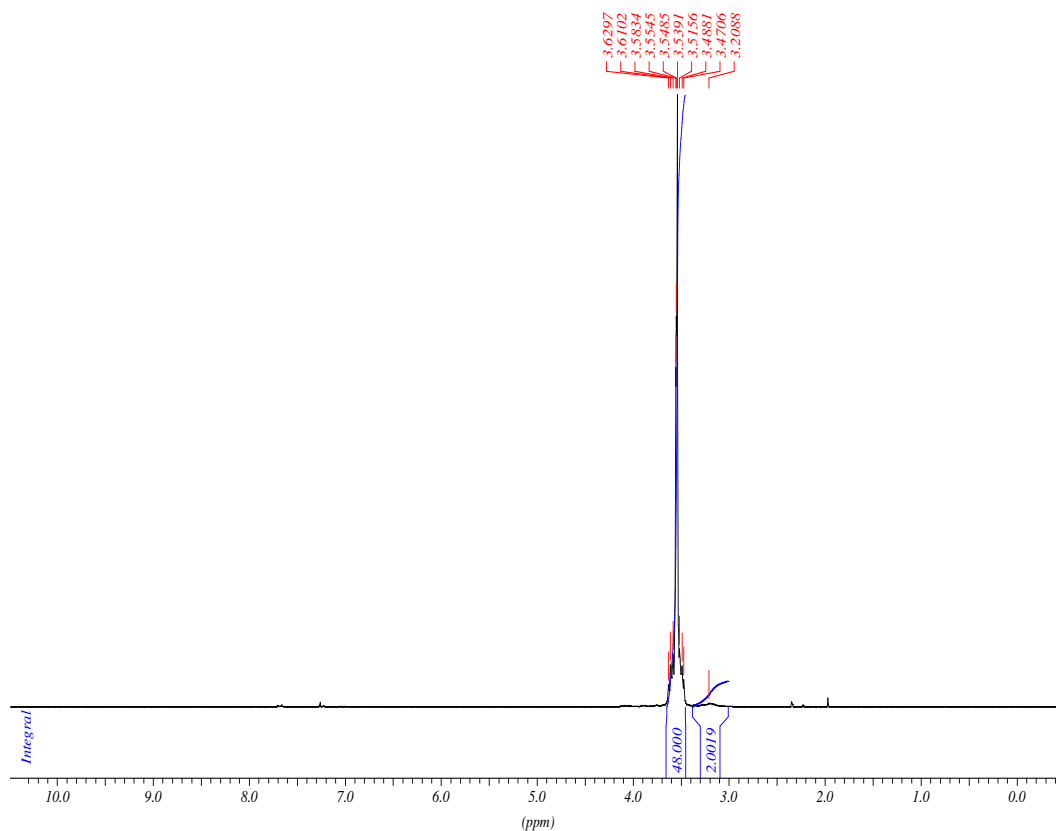
Spectrum 3.22. ^{1}H NMR (200 MHz, CDCl$_3$) of substance **4d**.
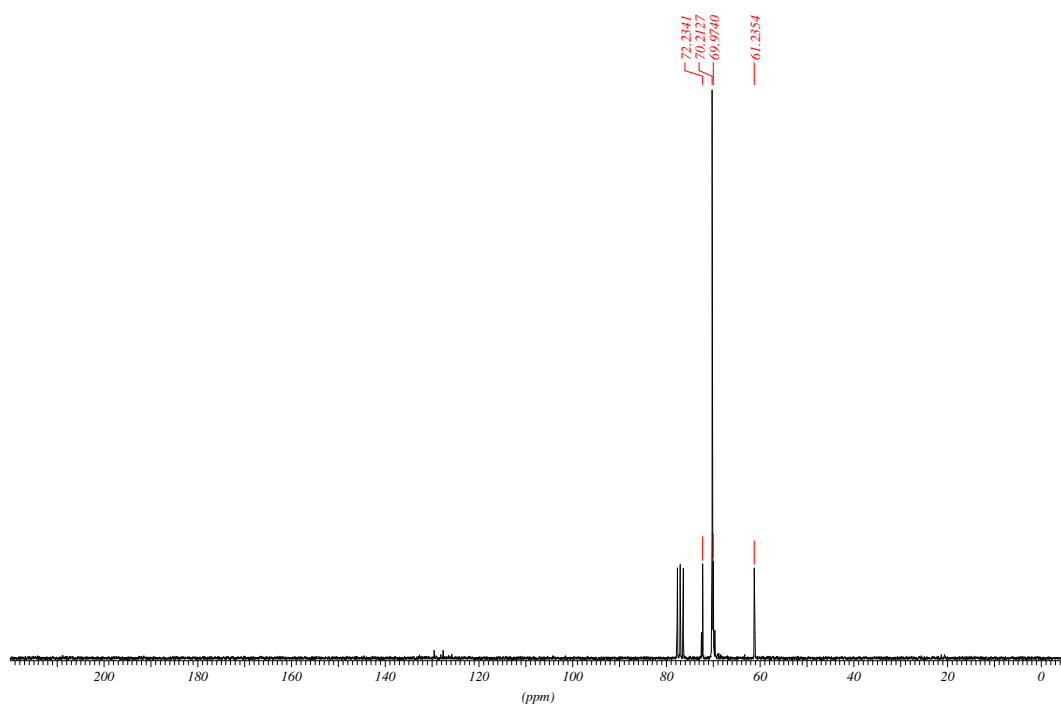
Spectrum 3.23. ^{13}C APT NMR (50 MHz, CDCl$_3$) of substance **4d**.
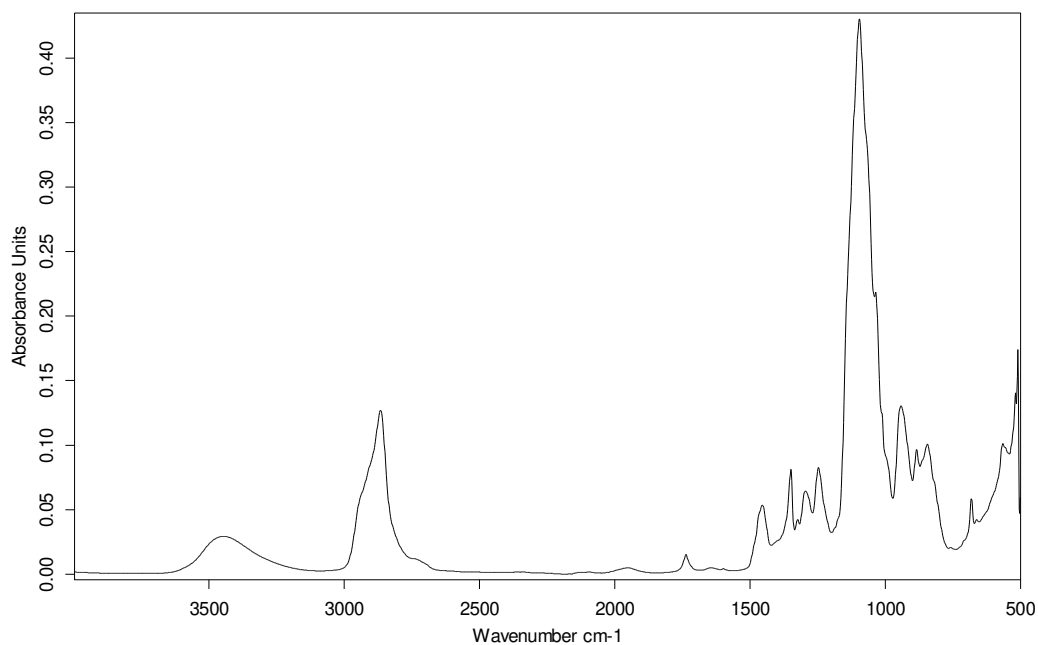
Spectrum 3.24. IR spectrum (ATR) of substance **4d**.

4. SUMMARY & OUTLOOK

In summary, we have reported on an optimized protocol for the synthesis of monodisperse poly(ethylene glycols) up to 12 sub-units. In contrast to other approaches described in literature, neither special equipment for high pressure hydrogenolysis nor any chromatographic purification is needed for the key steps of the sequence, making it attractive for especially large scale or even industrial applications.

In-line ATR-IR spectroscopy was shown to be a powerful analytical tool for the effective monitoring of reactive intermediates. Due to the non-invasive nature, this promising technology might arise as a future solution to examine reactions or highly reactive intermediates under inert condition. The scope or potential applications are widespread.

Based on this methodology, the applications of in-line ATR IR spectroscopy towards lithiation reactions was proven in our group, revealing the ability to monitor reaction intermediates in the halogen dance reaction.[58] The scope towards complex reaction media, including biological matrices such as blood plasma, is currently under investigation.[59] Matter of interest are advanced kinetic investigations on bioorthogonal ligations, strain-promoted alkyne azide cycloaddition (SPAAC), relevant in the fields of biological chemistry and biomedical research.

In the second part of this thesis, polystyrene resins grafted with short, monodisperse OEG sub-units (n=2-12), accessed via a modular synthetic route from polymer-bound phenol by Mitsunobu coupling, have been presented. The resulting solid supports offer advantageous properties for gel-phase NMR spectroscopy and are excellent resins for solid phase organic synthesis. To prove the applicability, three reaction sequences on solid phase have been performed (Wang-linker synthesis, palladium catalyzed cross coupling, hydantoin synthesis). Compared to commercially available PS-PEG resins, our support offers equal swelling properties in polar and apolar solvents, better on-resin analytic properties and significantly higher loading, thus being promising choices for combinatorial science. The presented approach towards tailor made resins enables to adjust the resin properties by proper linker selection depending on the respective field of application.

Concluding, the improved synthetic protocol towards monodisperse OEGs (e.g. hydrogel application), the broadened scope of the in-line ATR-IR-sensor spectroscopy (e.g. monitoring in biological media) as well as the established solid phase organic synthesis resins, based on the developed OEGs, (e.g. marker synthesis), reveal the value of this thesis for biomedical engineering.

5. APPENDIX

- *Manuscript Tetrahedron Letters (original work)*

- *Supporting information Combinatorial Science (original work)*

Convenient multigram synthesis of monodisperse oligo(ethylene glycols): effective reaction monitoring by infrared spectroscopy using an attenuated total reflection fibre optic probe [☆]

Daniel Lumpi [a], Christian Braunshier [a,*], Christian Hametner [a], Ernst Horkel [a], Bernhard Zachhuber [b], Bernhard Lendl [b], Johannes Fröhlich [a]

[a] Institute of Applied Synthetic Chemistry, Vienna University of Technology, 1060 Vienna, Austria
[b] Institute of Chemical Technologies and Analytics, Vienna University of Technology, 1060 Vienna, Austria

ARTICLE INFO

ABSTRACT

A convenient approach for the synthesis of monodisperse oligo(ethylene glycols) up to 12 units is described. A novel cleavage protocol replacing laborious hydrogenolysis is introduced to achieve a fast, inexpensive and widely applicable procedure. In addition to the synthetic part, Fourier transform infrared (FTIR) spectroscopy using a fibre optic attenuated total reflection (ATR) sensor was applied to monitor the formation of sensitive key intermediates, resulting in optimized reaction times. By applying this in-line technique, the possibility of real-time analysis under inert conditions was impressively demonstrated.

© 2009 Elsevier Ltd. All rights reserved.

Oligomers of ethylene glycol (PEGs) have a wide range of applications in many fields of science and industry. They can be applied as synthons for crown ether-type derivatives,[1] non-ionic surfactants,[2] templates for the synthesis of porous inorganic materials,[3] and more recently, functional mono-layers were used to develop biocompatible material.[4] In the field of biomedical engineering 'hydrogels' prevent unspecific adsorption of proteins from biological media. Another application field is bioconjugation of proteins, in order to increase the water solubility, which serves as one of the most effective drug delivery systems.[5] As a matter of fact, the physical and chemical properties of these modified materials often depend significantly on the number of repetition units of the PEG tether.

As part of our ongoing research on PEG-grafted polystyrene resins,[6] a series of novel polystyrene-oligo(oxyethylene) graft copolymers containing monodisperse PEG units (n = 2–12, even numbers) have been synthesized and examined regarding their applicability for gel-phase ^{13}C NMR spectroscopy.[7] A stronger correlation than expected between the graft length and the line widths in the gel-phase spectra was observed. As a consequence, the demand arose to synthesize monodisperse PEGs most efficiently.

For the preparation of the resins mentioned above, we required access to well-defined oligo(ethylene glycols) of up to 12 units.[6] Despite the widespread utility of PEGs, their synthesis remains a challenging task. The published synthetic methods for commercially unavailable or expensive representatives (n >4) are usually time-consuming or include extensive purification procedures.

To the best of our knowledge, the most promising approach was published by Keegstra et al.,[8] who applied bidirectional chain elongation. Taking this sequence as a starting point, we intended to optimize the key steps in order to shorten reaction times from periods as long as several days to more acceptable values. Eliminating this major disadvantage would result in an easy to handle, fast and low-cost synthetic procedure for well-defined oligo(ethylene glycols).

The first reaction step shown in Scheme 1 (deprotonation of mono-trityl protected glycols 1a–b) is reported to take at least 18 h to reach completion.

To verify this, it was necessary to monitor the conversion in an inert, anhydrous reaction medium. Encouraged by recent studies,[9] a mid-IR fibre optic probe was chosen for fast in-line monitoring of the chemical reaction under investigation. The ATR fibre system consisted of the FTIR spectrometer Bruker Matrix F® in connection with an ATR fibre probe (A.R.T. Photonics, Berlin; Ø 12 mm) and a MCT (mercury cadmium telluride) detector (Belov Technology, Co., Inc.). The probe was directly inserted through the ground neck of
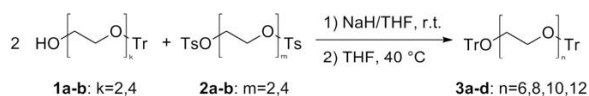
Scheme 1. Synthesis of glycols **3a–d**; monitoring via ATR–IR-sensor spectroscopy.

the reaction vessel and comprised two 1 m silver halide fibres (Ø 1 mm) connecting to a conical two bounce diamond ATR element housed in a rod of hastelloy. Using this set-up it was possible to follow the reactions to be studied in real-time covering a spectral range from 600 to 2000 wavenumbers.

The major advantage of in-line versus at-line ATR–IR-spectroscopy is that monitoring takes place inside the reaction system, thus eliminating steps such as workup of samples prior to analysis, which avoids the risk of contamination or a loss of inertness. In our work we focus on the deprotonation of the monoprotected glycols **1a–b**. The progress of these reactions can either be determined by tracking changes in absorbance values at selected wavenumbers or applying modern chemometric methods, which process the entire spectral information. Among these multivariate curve resolution, alternating least squares (MCR-ALS) needs to be mentioned.[10] This technique decomposes the recorded data set into smaller matrices containing information on the spectra and the concentration profiles of each component involved in the reaction. A recently available user friendly interface for Matlab facilitates this type of data analysis.

Indeed, measurements indicated a rapid conversion of glycols **1a–b** to the corresponding alkoxides. Absorbance values at characteristic wavenumbers for the substrate and the product, respectively, are plotted versus reaction time in Figure 1. The blue curve derives from substance **1b**, the green graph originates from deprotonated **1b**. Monitoring here did not employ the more complex MCR-algorithm, but just non-overlapped single band monitoring. The graph clearly shows that after 90 min no significant changes of absorption values can be observed, thus being an indicator for the end of the reaction.
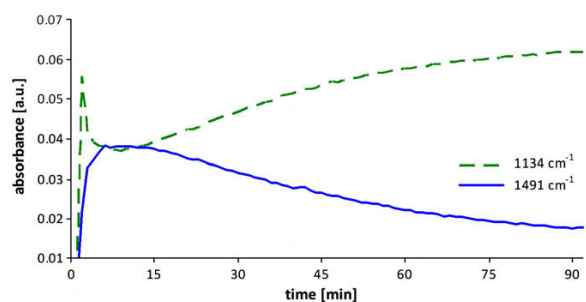
Figure 1. ATR–IR in-line monitoring for the deprotonation of monoprotected glycol **1b**. Distortions for $t \leqslant 10$ min are attributed to equilibration effects (temperature and concentration).

In fact, we could prove that this step is completed after a reaction time of 90 min for glycol **1b** and 210 min for **1a**, respectively.

According to the original procedure, the subsequent nucleophilic reaction of the alkoxide with the tosylated glycols **2a–b** has to be performed at room temperature. Refluxing the reaction mixture in THF as a solvent to increase conversion rates leads to products, which were dark in colour and contaminated by inseparable impurities. However, optimization studies showed that performing the reaction at 40 °C shortens the time from 96 h to 58–80 h avoiding the formation of unwanted by-products[11] (Table 1).

Table 1
Reaction times and yields for the preparation of **3a–d**

Entry	Glycol 1	Tosylate 2	Time[a] (h)	Product 3	Yield[b] (g)	Yield[b] (%)
1	**1a**	**2a**	4/84	**3a**	18.8	98
2	**1a**	**2b**	4/84	**3b**	165.4	97
3	**1b**	**2a**	2/60	**3c**	23.2	98
4	**1b**	**2b**	2/60	**3d**	24.6	95

[a] Times given refer to deprotonation and overall reaction time, respectively.
[b] Isolated yields.

To obtain the desired oligo(ethylene glycols) **4a–d**, the protecting groups have to be cleaved off. Virtually all published procedures use hydrogenolysis under high-pressure conditions in the presence of palladium for several days to achieve this final transformation (Scheme 2). Aside from long reaction time, this procedure suffers from some more disadvantages. The most serious one is the need for equipment allowing to perform gas reactions under high pressure, which might be a limiting factor. Furthermore, the reaction was never quantitative in our hands, always leaving small amounts of protected glycols in the product. Finally the use of halogenated organic solvents, for example, dichloromethane and transition metal catalysts might become troublesome, if the final product is intended to be used in the field of pharmaceutics or biology, especially when the procedure is performed on industrial scale.
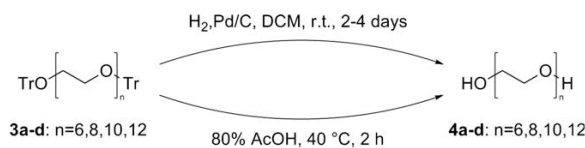
Scheme 2. Synthesis of glycols **4a–d**; hydrogenolysis versus acidic cleavage.

Our approach was to substitute this deprotection step against a safe, fast and inexpensive procedure. To the best of our knowledge, the well known acidic cleavage of trityl groups was not reported for this substance class until now. This is quite surprising, as we could show that the usage of aqueous acetic acid leads to pure products **4a–d** in nearly quantitative yields avoiding any tedious workup or implementation of chromatographic methods (Table 2).[12] It is worth mentioning, that it is necessary to stick to the given reaction conditions (time and temperature) to prevent the formation of the corresponding diacetates.[13]

Comparing this new protocol to hydrogenolysis, the advantages are clearly visible: dramatically shortened reaction times (2 h vs 4 days), easier workup and higher product quality (purity determined by ^{1}H NMR; compared to products synthesized in our lab according to literature). Moreover, nearly the theoretical amount of triphenylmethanol (pure according to combustion analysis) is isolated during workup and can simply be transformed to tritylchloride[14] enhancing the atom efficiency of the entire synthetic route.

In summary, we have reported an optimized protocol for the synthesis of monodisperse poly(ethylene glycols) up to 12 units. In contrast to other approaches described in literature, neither special equipment for high pressure hydrogenolysis nor any chromatographic purification is needed for the key steps of the sequence, making it attractive for especially large scale or industrial applications. In-line ATR–IR spectroscopy was shown to be a powerful analytical tool for the effective monitoring of 'problematic' processes. Due to the non invasive nature, this promising technology might arise as *the* solution for examining reactions

Table 2
Yields for the preparation of **4a–d**

Entry	Tritylate **3**	Product **4**	Yield[a] (g)	Yield[a] (%)
1	**3a**	**4a**	5.5	98
2	**3b**	**4b**	53.2	96
3	**3c**	**4c**	9.0	98
4	**3d**	**4d**	10.8	99

[a] Isolated yields; reaction conditions: 80% AcOH, 40 °C, 2 h.

under inert conditions. The scope of possible applications is widespread. In the field of organic chemistry one can imagine to apply this technique to, for example, metalation reactions, deprotonations, catalytic reactions under inert atmosphere (transition metal assisted coupling, olefin metathesis), etc. Experimental work covering some of these projects is already in progress. Furthermore, the possibility of elucidation of reaction mechanisms by monitoring transition states is clearly visible. This field of application is more sophisticated and will therefore be the aim of future projects.

Acknowledgements

Supplementary data

Supplementary data (experimental details and compound characterization data of substances **3a–d** and **4a–d**, copies of spectra (^{1}H NMR, ^{13}C NMR, IR)) associated with this article can be found, in the online version, at doi:10.1016/j.tetlet.2009.09.010.

References and notes

1. Huszthy, P.; Bradshaw, J. S.; Zhu, C. Y.; Izatt, R. M.; Lifson, S. *J. Org. Chem.* **1991**, *56*, 3330–3336.
2. Chu, B.; Zhou, Z.. In *Nonionic Surfactants: Polyoxyalkylene Block Copolymers, Surface Sciences Series*; Nace, V. M., Ed.; Marcel Dekker: New York, 1996; Vol. 60,.
3. Zhao, D.; Huo, Q.; Feng, J.; Chmelka, B. F.; Stucky, G. D. *J. Am. Chem. Soc.* **1998**, *120*, 6024–6036.
4. (a) Groll, J.; Amirgoulova, E. V.; Ameringer, T.; Heyes, C. D.; Roecker, C.; Nienhaus, G. U.; Moeller, M. *J. Am. Chem. Soc.* **2004**, *126*, 4234–4239; (b) Li, L.; Chen, S.; Jiang, S. *J. Biomater. Sci., Polym. Ed.* **2007**, *18*, 1415–1427; (c) Clare, T. L.; Clare, B. H.; Nichols, B. M.; Abbott, N. L.; Hamers, R. J. *Langmuir* **2005**, *21*, 6344–6355.
5. (a) Yamamoto, Y.; Yoshioka, H.; Takehana, T.; Yoshimura, S.; Kubo, K.; Nakamoto, K. *Polym. Prepr. (Am. Chem. Soc., Div. Polym. Chem.)* **2009**, *50*, 161–162; (b) Guiotto, A.; Canevari, M.; Pozzobon, M.; Moro, S.; Orsolini, P.; Veronese, F. M. *Bioorg. Med. Chem.* **2004**, *12*, 5031–5037; (c) Lee, L. S.; Conover, C.; Shi, C.; Whitlow, M.; Filpula, D. *Bioconjugate Chem.* **1999**, *10*, 973–981.
6. Braunshier, C.; Hametner, C.; Froehlich, J.; Schnoeller, J.; Hutter, H. *Tetrahedron Lett.* **2008**, *49*, 7103–7105.
7. Braunshier, C.; Hametner, C. *QSAR Comb. Sci.* **2007**, *26*, 908–918.
8. Keegstra, E. M. D.; Zwikker, J. W.; Roest, M. R.; Jenneskens, L. W. *J. Org. Chem.* **1992**, *57*, 6678–6680.
9. (a) Heise, H. M.; Kuepper, L.; Butvina, L. N. *Anal. Bioanal. Chem.* **2003**, *375*, 1116–1123; (b) Bentrup, U.; Kuepper, L.; Budde, U.; Lovis, K.; Jaehnisch, K. *Chem. Eng. Technol.* **2006**, *29*, 1216–1220; (c) Minnich, C. B.; Buskens, P.; Steffens, H. C.; Baeuerlein, P. S.; Butvina, L. N.; Kuepper, L.; Leitner, W.; Liauw, M. A.; Greiner, L. *Org. Process Res. Dev.* **2007**, *11*, 94–97.
10. Jaumot, J.; Gargallo, R.; de Juan, A.; Tauler, R. *Chemometr. Intell. Lab. Syst.* **2005**, *76*, 101–110.
11. Synthesis of 1,1,1,27,27,27-hexaphenyl-2,5,8,11,14,17, 20,23,26-nonaoxaheptacosane **3b**. Under argon, a 4-neck round bottom flask equipped with mechanical stirrer, reflux condenser, thermometer (and dropping funnel, respectively) and the ATR-IR Probe inlet was charged with sodium hydride (12.00 g, 500 mmol, 2.5 equiv) and dry THF (500 mL). To the well stirred suspension was added a solution of mono-trityl protected glycol **1a** (139.38 g, 400 mmol, 2.0 equiv) in dry THF (500 mL) at room temperature. After completion of the reaction according to IR-monitoring (4 h), the mixture was cooled to 0 °C and a solution of di-tosylated glycol **2b** (100.52 g, 200 mmol, 1.0 equiv) in dry THF (500 mL) was added. The temperature was adjusted to 40 °C and the suspension was stirred for 80 h. For workup, the reaction mixture was poured onto ice water (1200 mL)/chloroform (800 mL). The phases were separated and the aqueous phase was extracted with chloroform (500 mL). The combined organic layers were washed with brine (500 mL) and dried over sodium sulfate. After removing the solvent under reduced pressure, the title compound was obtained as a clear, slightly orange, viscous oil. Yield: 165.36 g (97%). ^{1}H NMR (200 MHz, DMSO-d_6) δ = 7.48–7.15 (m, 30 H), 3.67–3.39 (m, 28 H), 3.06 (t, J = 4.8 Hz, 4 H); ^{13}C APT NMR (50 MHz, DMSO-d_6) δ = 143.8 (s), 128.2 (d), 127.8 (d), 126.9 (d), 85.9 (t), 70.1 (t), 69.9 (t), 69.85 (t), 69.82 (t), 69.77 (t), 69.7 (t), 63.0 (t). Anal. Calcd for $C_{54}H_{62}O_9$ (855.09): C, 75.85; H, 7.31. Found: C, 76.15; H, 7.15; N, <0.05.
12. Synthesis of 3,6,9,12,15,18,21-heptaoxatricosane-1,23-diol **4b**. Compound **3b** (128.26 g, 150 mmol) was stirred with 80% acetic acid (1200 mL) at 40 °C. After 2 h the reaction was completed according to HPLC analysis. The mixture was allowed to cool to room temperature and poured onto ice water (600 mL). The precipitate was filtered off over a glass sinter funnel. The filtrate was concentrated under reduced pressure leaving a cloudy oil. The crude product was mixed with cold water (500 mL) and the suspension was again filtered over the same glass sinter funnel, still containing the bed of triphenylmethanol formed during the first filtration. The filter cake was washed with cold water, giving 77.02 g (99%) of pure triphenylmethanol after drying at 40 °C/15 mbar. The solvent of the filtrate was removed under reduced pressure (0.05 mbar) to afford the title compound as a clear, slightly orange oil. Yield: 53.20 g (96%). ^{1}H NMR (200 MHz, CDCl$_3$) δ = 3.62–3.38 (m, 32 H), 3.30 (br s, 2 H). ^{13}C NMR (50 MHz, CDCl$_3$) δ = 72.2, 70.15, 70.10, 69.9, 61.1. Anal. Calcd for $C_{16}H_{34}O_9$ (370.44): C, 51.88; H, 9.25. Found: C, 51.81; H, 9.34; N, <0.05.
13. Increasing reaction temperature from 40 °C to reflux and prolonging reaction times from 2 h to 3 d results in almost a quantitative formation of the corresponding diacetates. However, these can be converted into the desired glycols by sodium methanolate-catalyzed transesterification.
14. Bachmann, W. E. *Org. Synth.* **1943**, *23*, 100.

Synthesis and Application of Monodisperse

Oligo(oxyethylene) Grafted Polystyrene Resins for

Solid Phase Organic Synthesis

Daniel Lumpi, Christian Braunshier*, Ernst Horkel, Christian Hametner and Johannes Fröhlich

Institute of Applied Synthetic Chemistry, Vienna University of Technology,

Getreidemarkt 9/163, 1060 Vienna, Austria

Supporting Information

1

Gel-phase ^{13}C-NMR characterization of target PS-PEG resins (3a-f, 4a-f)

PS-PEG(2)-O-TBDMS 3a. ^{13}C gel-phase NMR (100 MHz, CDCl$_3$): δ = 72.8 (t), 69.9 (t), 67.3 (t), 62.8 (t, CH_2-O-Si), 26.0 (q, Si-C-(CH_3)$_3$), 18.4 (s, Si-C-(CH$_3$)$_3$), -4.9 (q, Si-CH_3) ppm.

PS-PEG(4)-O-TBDMS 3b. ^{13}C gel-phase NMR (100 MHz, CDCl$_3$): δ = 72.6 (t), 70.7 (t), 69.8 (t), 67.2 (t), 62.7 (t), 26.0 (q), 18.4 (s), -4.9 (q) ppm.

PS-PEG(6)-O-TBDMS 3c. ^{13}C gel-phase NMR (100 MHz, CDCl$_3$): δ = 72.6 (t), 70.7 (t), 69.8 (t), 67.2 (t), 62.7 (t), 26.0 (q), 18.4 (s), -4.9 (q) ppm.

PS-PEG(8)-O-TBDMS 3d. ^{13}C gel-phase NMR (100 MHz, CDCl$_3$): δ = 72.7 (t), 70.8 (t), 69.9 (t), 62.8 (t), 26.0 (q), 18.4 (s), -5.2 (q) ppm.

PS-PEG(10)-O-TBDMS 3e. ^{13}C gel-phase NMR (100 MHz, CDCl$_3$): δ = 72.7 (t), 70.6 (t), 69.9 (t), 62.8 (t), 26.0 (q), 18.4 (s), -5.2 (q) ppm.

PS-PEG(12)-O-TBDMS 3f. ^{13}C gel-phase NMR (100 MHz, CDCl$_3$): δ = 72.7 (t), 70.8 (t), 69.9 (t), 62.8 (t), 26.0 (q), 18.4 (s), -5.2 (q) ppm.

PS-PEG(2)-OH 4a. ^{13}C gel-phase NMR (100 MHz, CDCl$_3$): δ = 72.6 (t), 69.8 (t), 67.4 (t), 61.8 (t, $CH2$-OH) ppm.

PS-PEG(4)-OH 4b. ^{13}C gel-phase NMR (100 MHz, CDCl$_3$): δ = 72.5 (t), 70.7 (t), 70.6 (t), 70.4 (t), 69.9 (t), 67.3 (t), 61.7 (t) ppm.

PS-PEG(6)-OH 4c. ^{13}C gel-phase NMR (100 MHz, CDCl$_3$): δ = 72.5 (t), 70.6 (t), 70.3 (t), 69.9 (t), 67.3 (t), 61.7 (t) ppm.

PS-PEG(8)-OH 4d. ^{13}C gel-phase NMR (100 MHz, CDCl$_3$): δ = 72.6 (t), 70.6 (t), 70.3 (t), 69.9 (t), 67.3 (t), 61.7 (t) ppm.
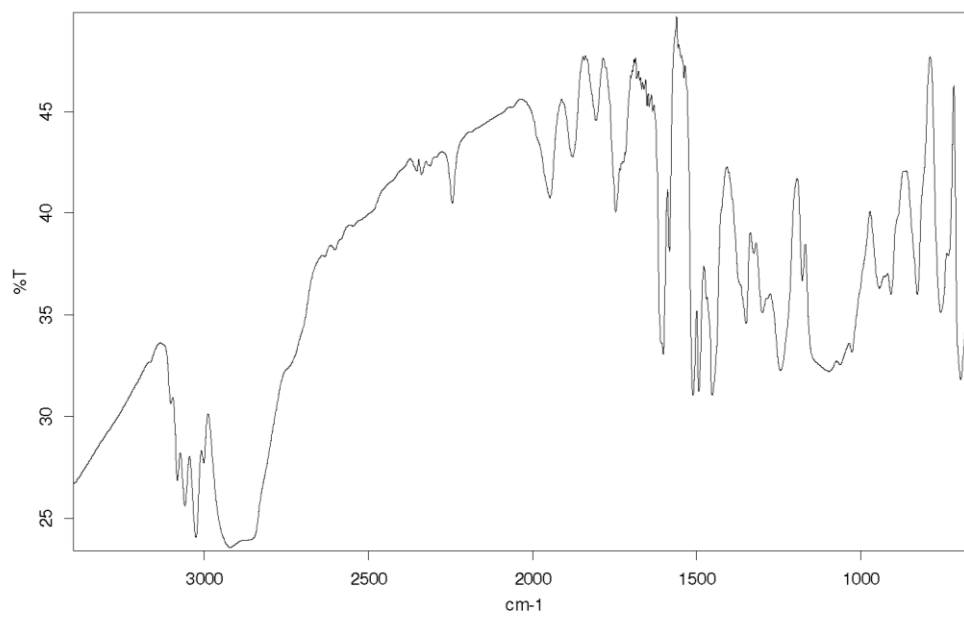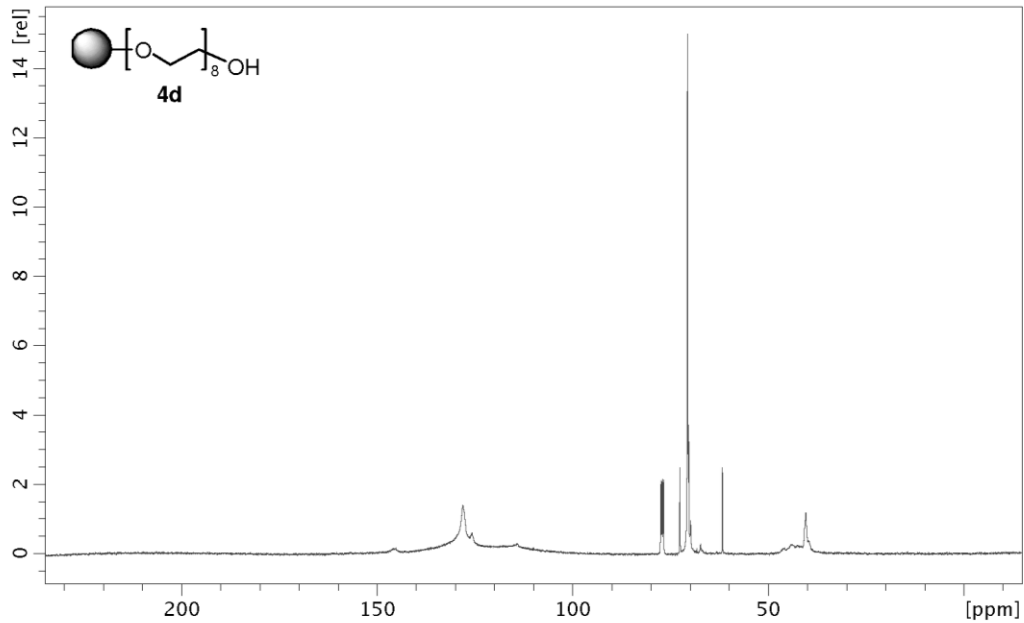
PS-PEG(10)-OH 4e. ^{13}C gel-phase NMR (100 MHz, CDCl$_3$): δ = 72.6 (t), 70.6 (t), 70.4 (t), 69.9 (t), 67.3 (t), 61.8 (t) ppm.
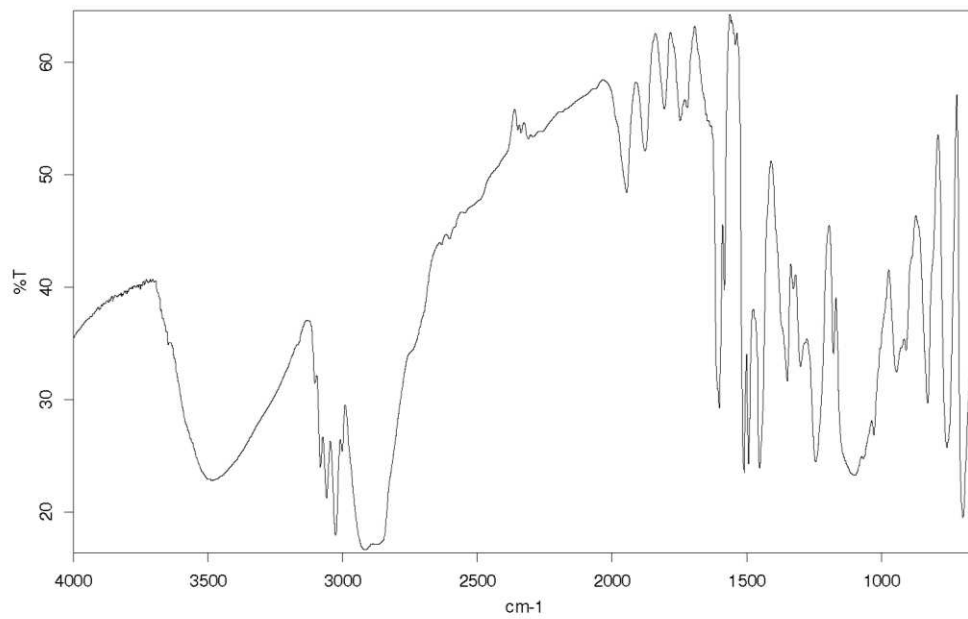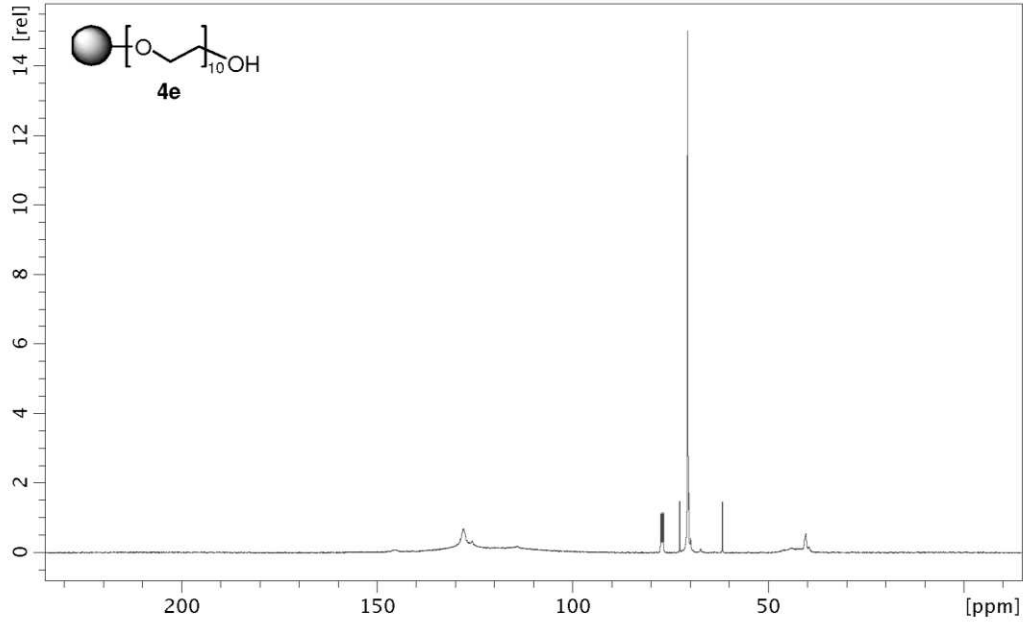
PS-PEG(12)-OH 4f. ^{13}C gel-phase NMR (100 MHz, CDCl$_3$): δ = 72.6 (t), 70.6 (t), 70.3 (t), 69.9 (t), 67.3 (t), 61.7 (t) ppm.
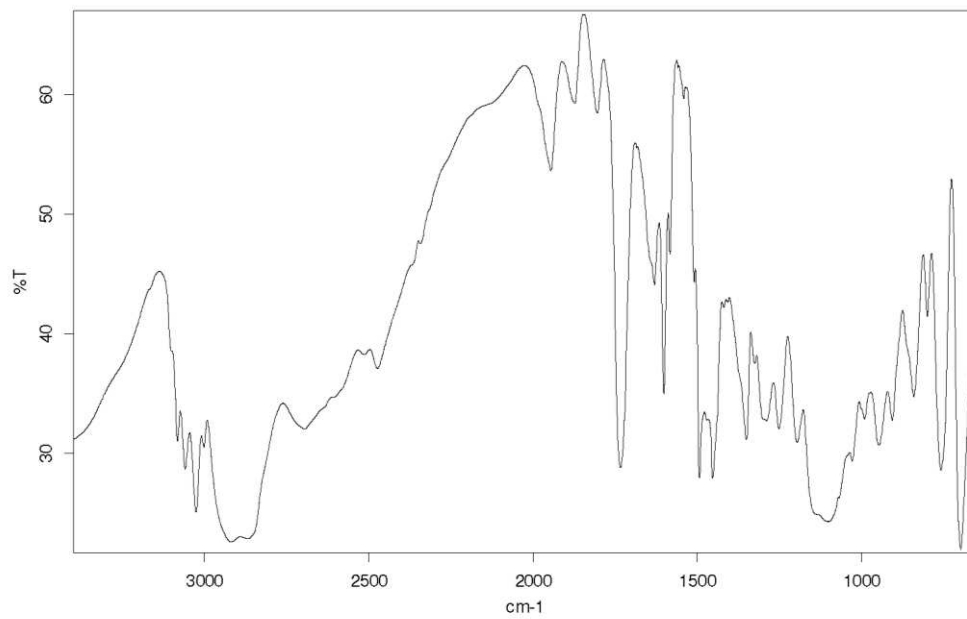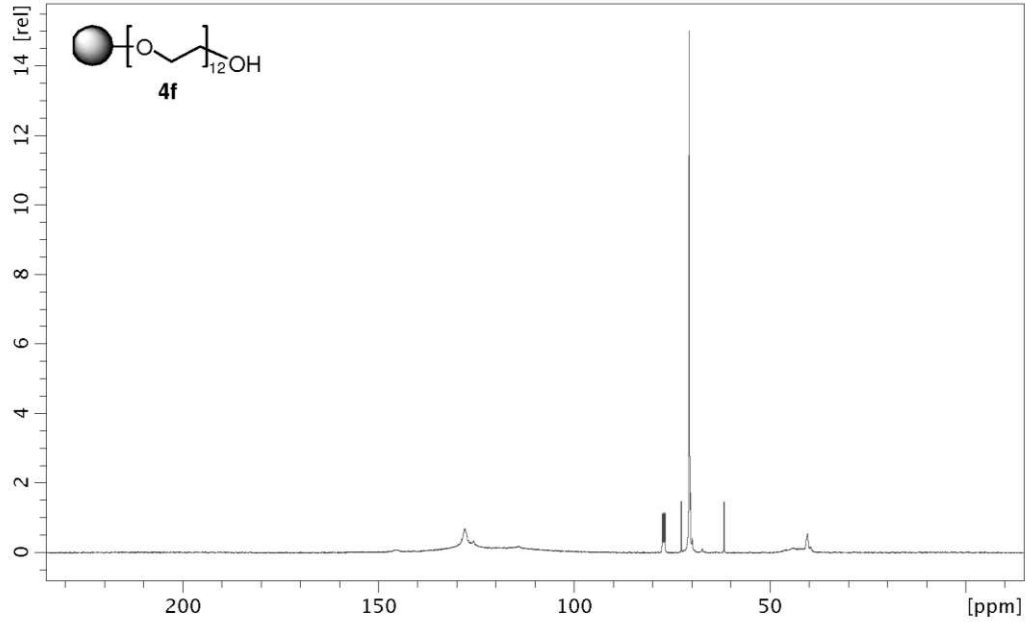
2

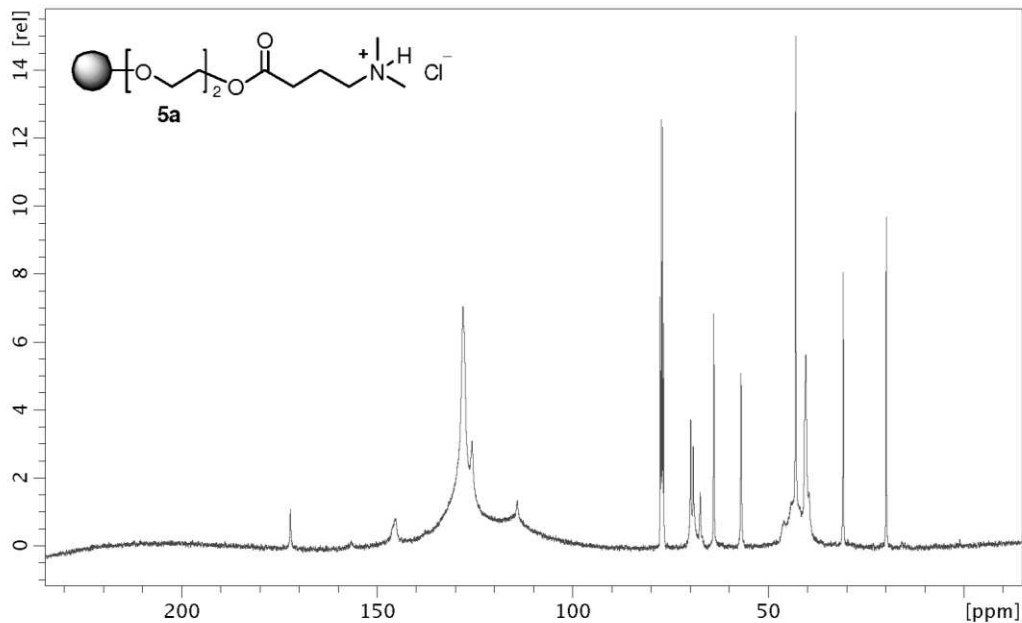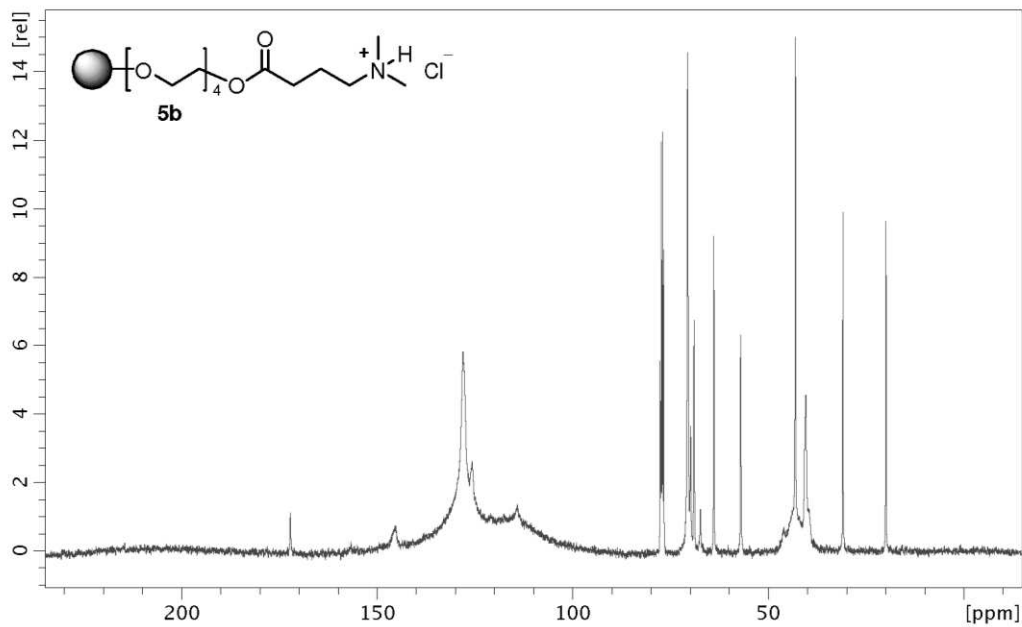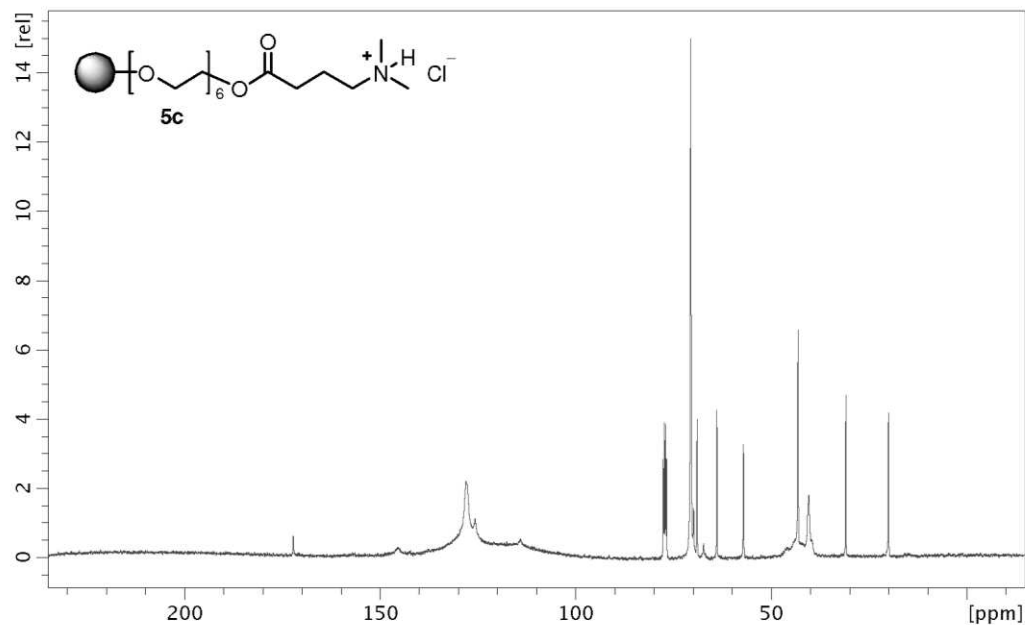## Gel-phase ^{13}C-NMR and IR spectra of PS-PEG-2-OH (4a)
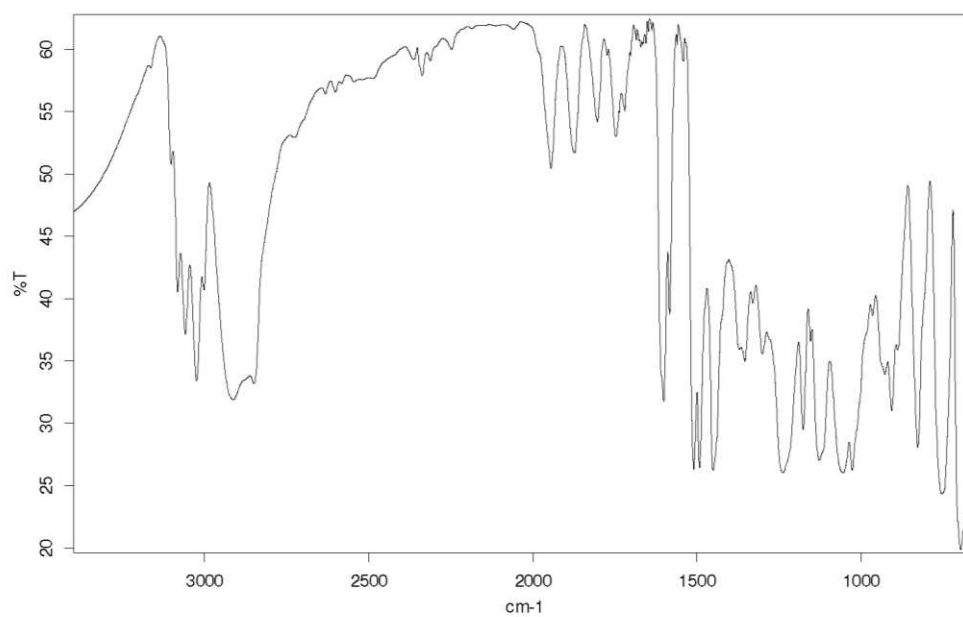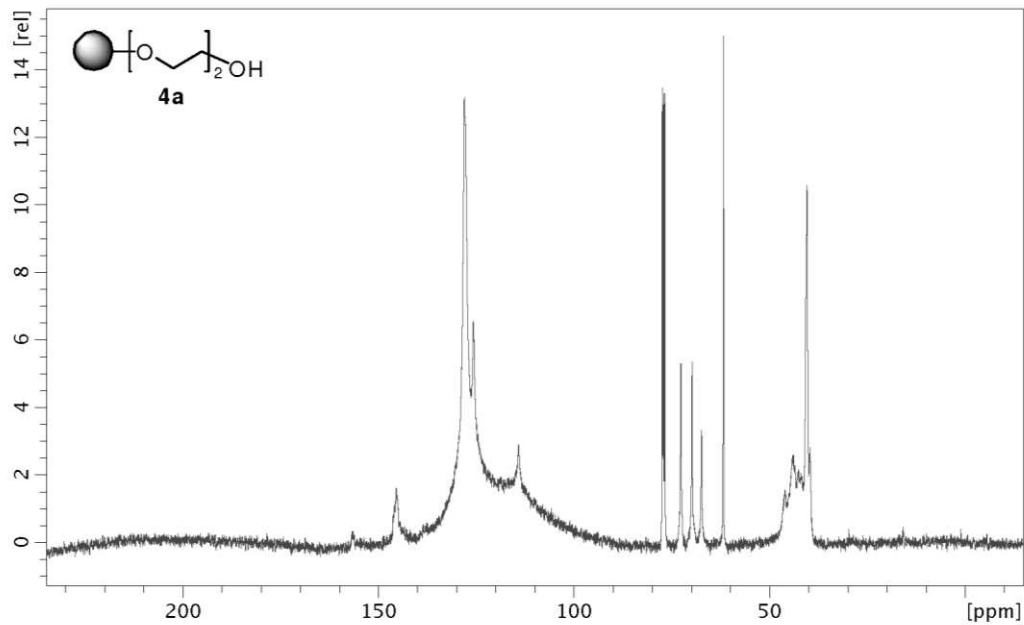
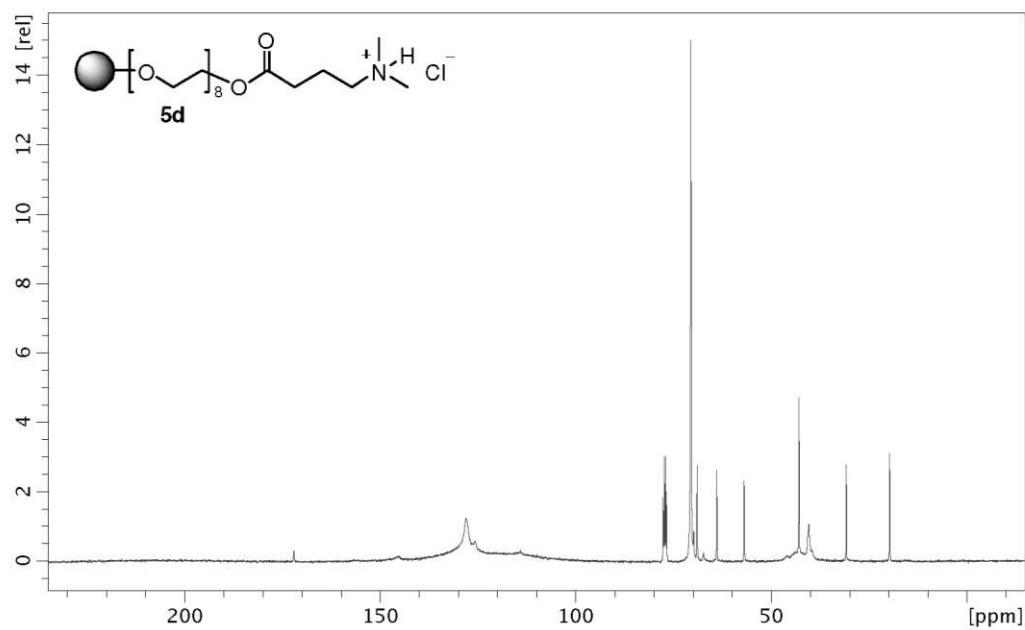## Gel-phase ^{13}C-NMR and IR spectra of PS-PEG-4-OH (4b)

4
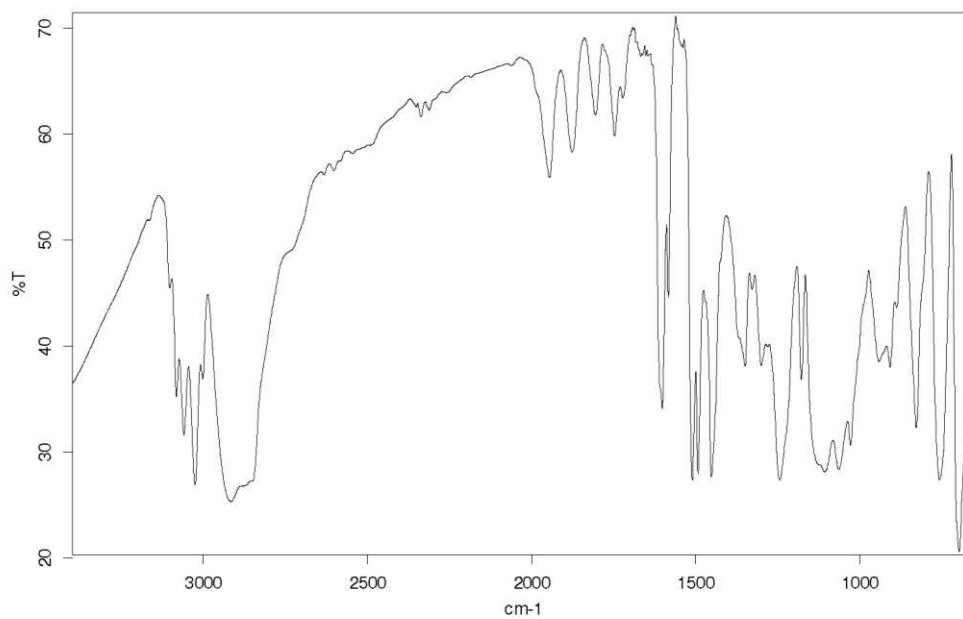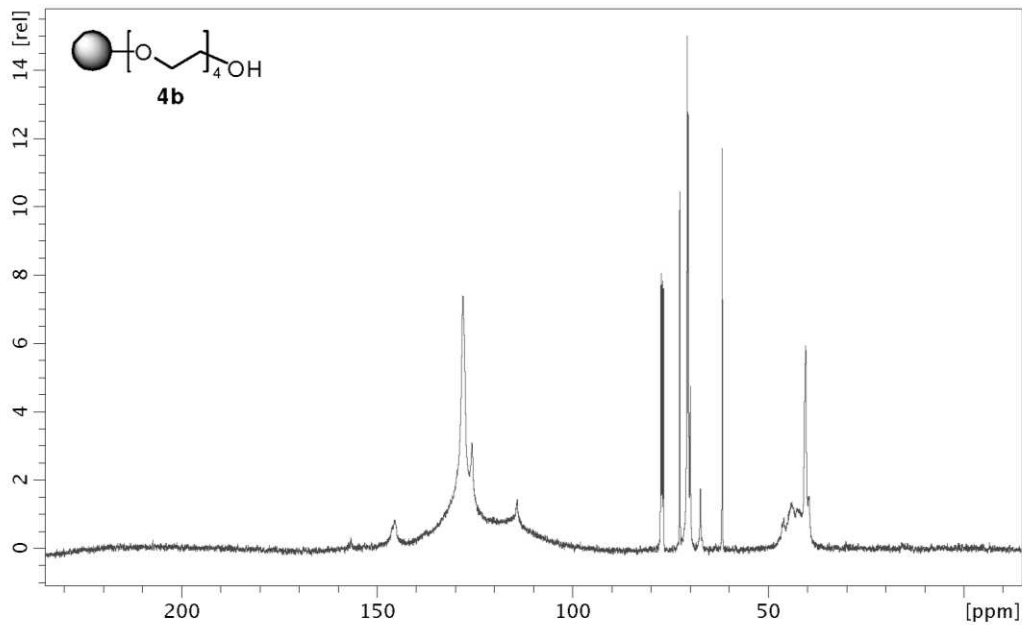
Gel-phase ^{13}C-NMR and IR spectra of PS-PEG-6-OH (4c)


5
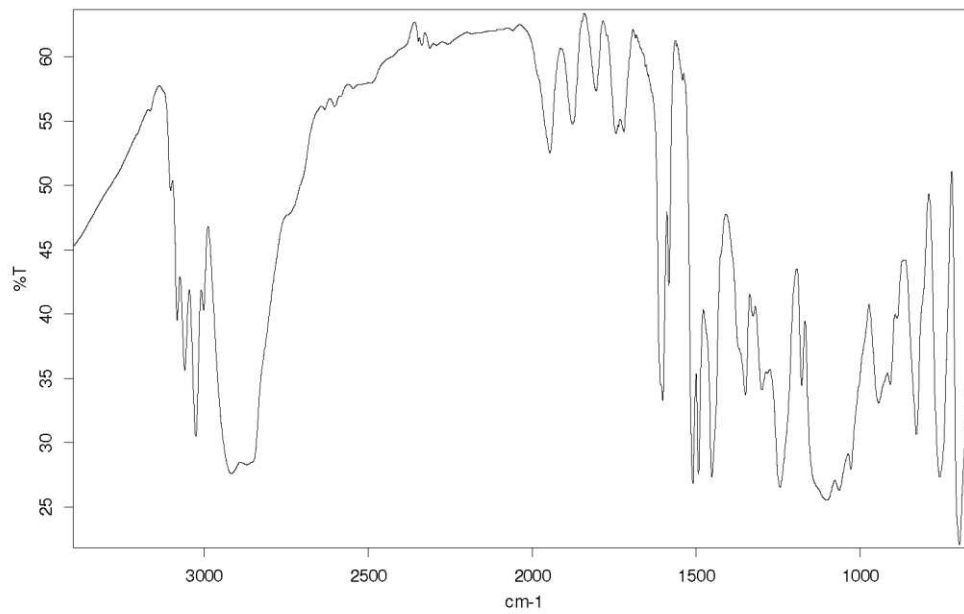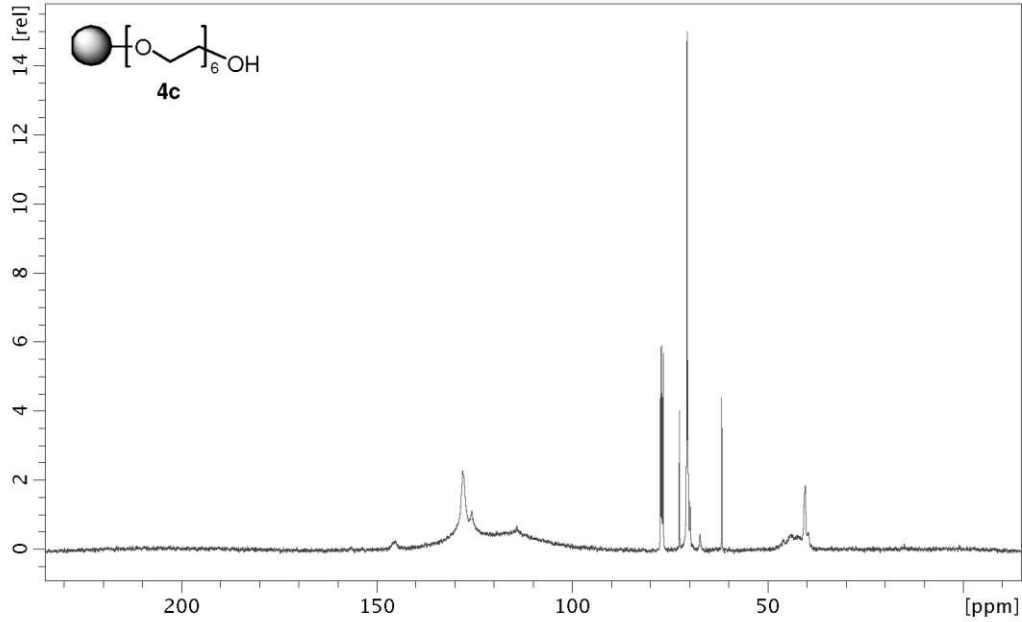
Gel-phase ^{13}C-NMR and IR spectra of PS-PEG-8-OH (4d)

6

Gel-phase ^{13}C-NMR and IR spectra of PS-PEG-10-OH (4e)

7

Gel-phase ^{13}C-NMR and IR spectra of PS-PEG-12-OH (4f)

8

Gel-phase ^{13}C-NMR spectrum of PS-PEG-2-N1-C3-HCl (5a)

Gel-phase ^{13}C-NMR spectrum of PS-PEG-4-N1-C3-HCl (5b)

9

Gel-phase ^{13}C-NMR spectrum of PS-PEG-6-N1-C3-HCl (5c)

Gel-phase ^{13}C-NMR spectrum of PS-PEG-8-N1-C3-HCl (5d)
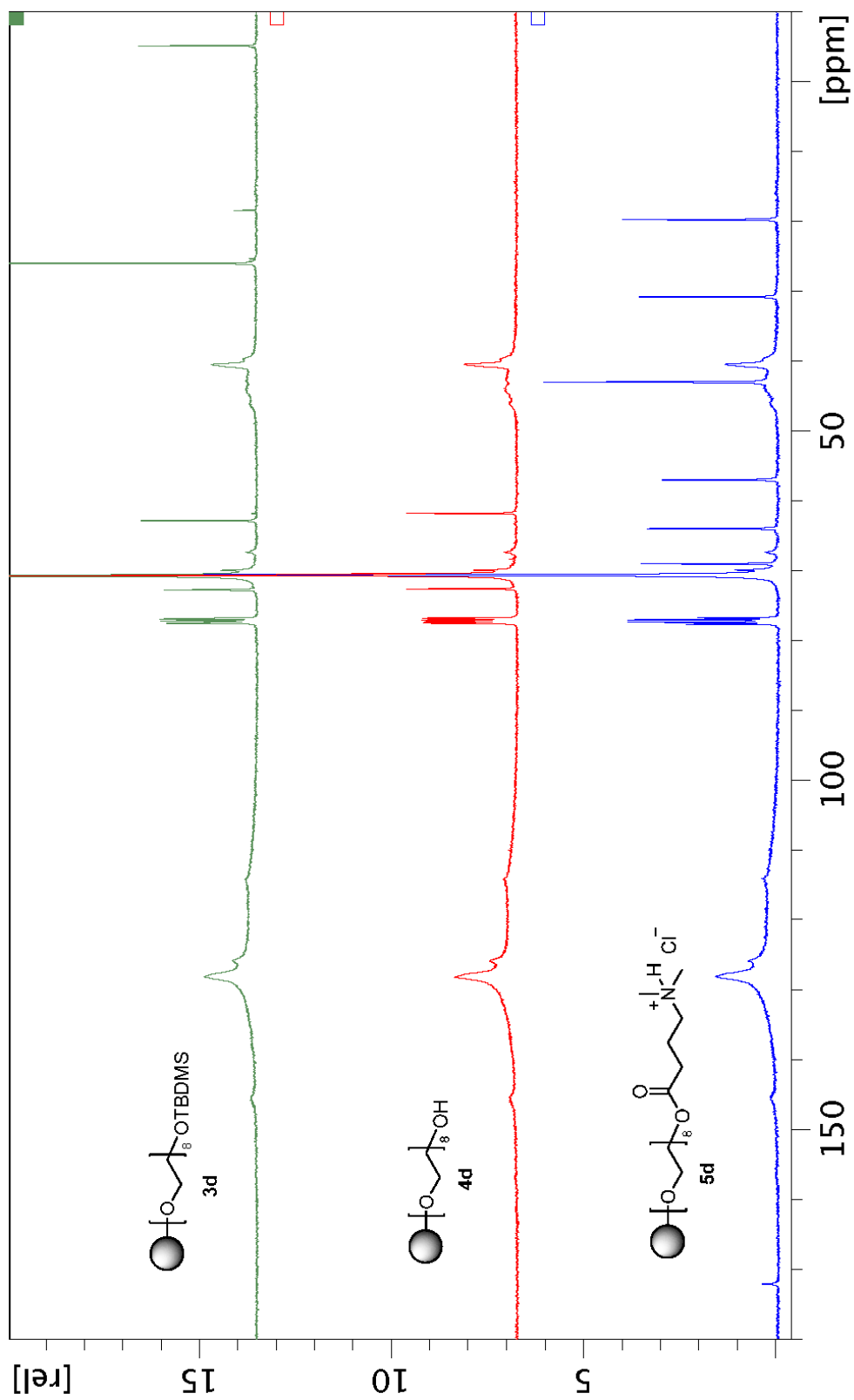

10

Gel-phase ^{13}C-NMR spectrum of PS-PEG-10-N1-C3-HCl (5e)
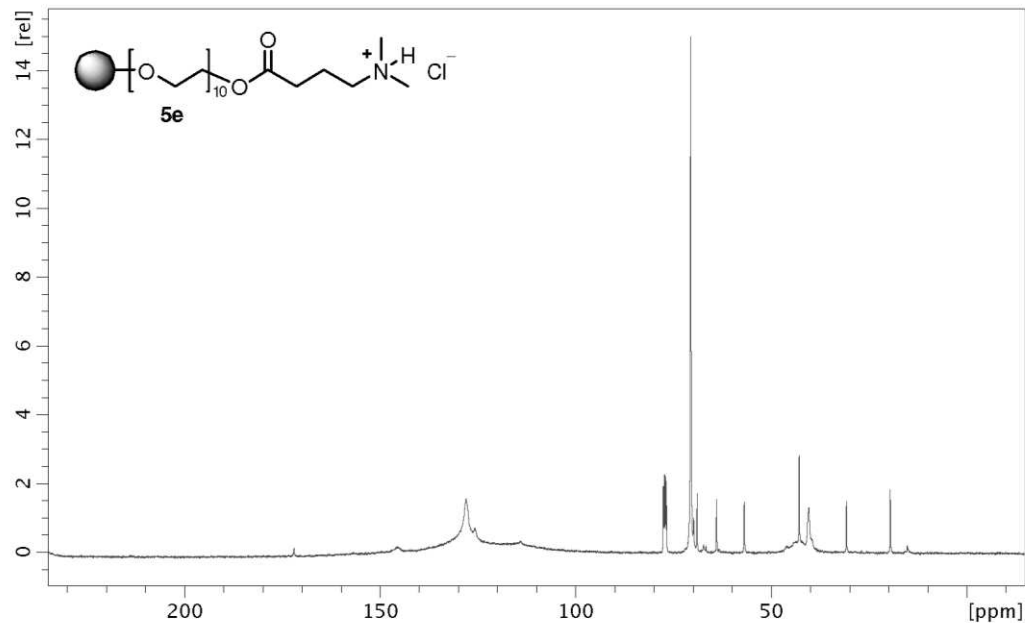
Gel-phase ^{13}C-NMR spectrum of PS-PEG-12-N1-C3-HCl (5f)

11
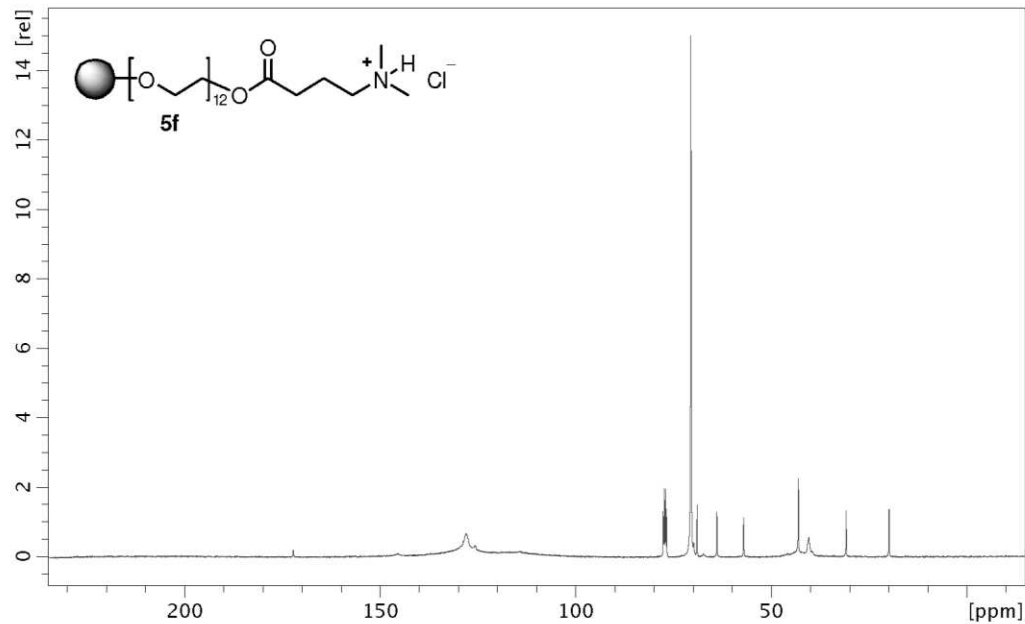
Gel-phase ^{13}C-NMR spectra of application example 2 (Heck coupling)

12
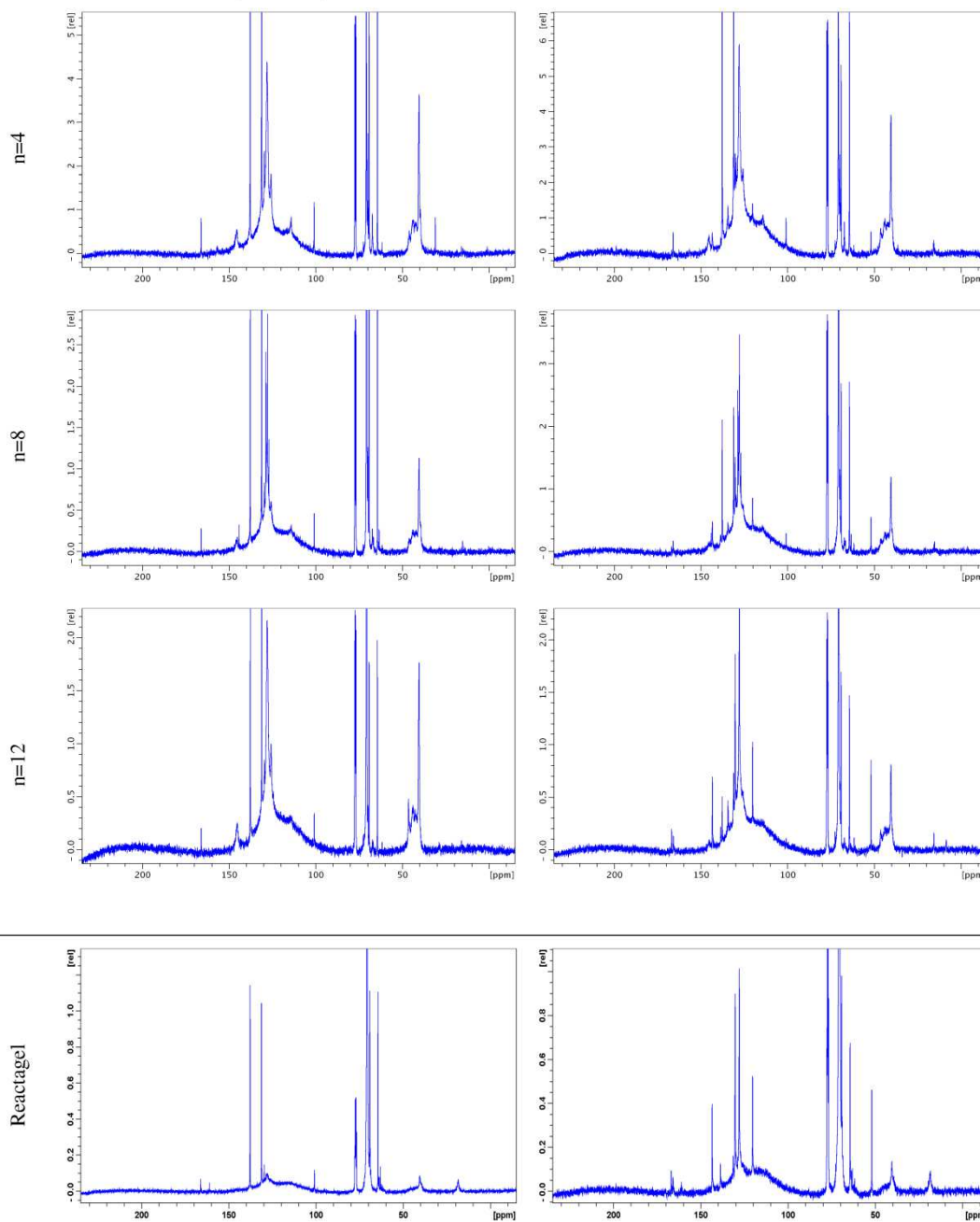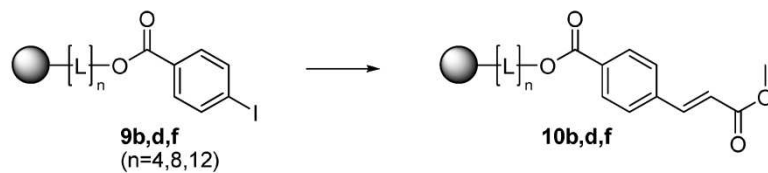
Gel phase ¹³C-NMR reaction monitoring of resins 3d-5d

6. REFERENCES

[1] Huszthy, P.; Bradshaw, J. S.; Zhu, C. Y.; Izatt, R. M.; Lifson, S. *J. Org. Chem.* **1991**, *56*, 3330.

[2] Chu, B.; Zhou, Z. In Nonionic Surfactants: Polyoxyalkylene Block Copolymers; Nace, V. M., Ed.; Surface Sciences Series; Marcel Dekker: New York, 1996; Vol. 60.

[3] Zhao, D.; Huo, Q.; Feng, J.; Chmelka, B. F.; Stucky, G. D. *J. Am. Chem. Soc.* **1998**, *120*, 6024.

[4] Groll, J.; Amirgoulova, E. V.; Ameringer, T.; Heyes, C. D.; Roecker, C.; Nienhaus, G. U.; Moeller, M. *J. Am. Chem. Soc.* **2004**, *126*, 4234.

[5] Li, L.; Chen, S.; Jiang, S. *J. Biomater. Sci., Polym. Ed.* **2007**, *18*, 1415.

[6] Clare, T. L.; Clare, B. H.; Nichols, B. M.; Abbott, N. L.; Hamers, R. J. *Langmuir* **2005**, *21*, 6344.

[7] Calo, E.; Khutoryanskiy, V. V. *Eur. Polym. J.* **2015**, *65*, 252.

[8] Parlato, M.; Reichert, S.; Barney, N.; Murphy, W. L. *Macromol. Biosci.* **2014**, *14*, 687.

[9] Yamamoto, Y.; Yoshioka, H.; Takehana, T.; Yoshimura, S.; Kubo, K.; Nakamoto, K.-i. *Polym. Prepr. (Am. Chem. Soc., Div. Polym. Chem.)* **2009**, *50*, 160.

[10] Guiotto, A.; Canevari, M.; Pozzobon, M.; Moro, S.; Orsolini, P.; Veronese, F. M. *Bioorg. Med. Chem.* **2004**, *12*, 5031.

[11] Lee, L. S.; Conover, C.; Shi, C.; Whitlow, M.; Filpula, D. *Bioconjugate Chem.* **1999**, *10*, 973.

[12] Braunshier, C.; Hametner, C. *QSAR Comb. Sci.* **2007**, *26*, 908.

[13] Braunshier, C.; Hametner, C.; Froehlich, J.; Schnoeller, J.; Hutter, H. *Tetrahedron Lett.* **2008**, *49*, 7103.

[14] Solid-Phase Organic Synthesis: Concepts, Strategies, and Applications, First Edition. Edited by Patrick H. Toy and Yulin Lam. 2012 John Wiley & Sons, Inc. Published 2012 by John Wiley & Sons, Inc.

[15] Elisseeff, J. *Nat. Mater.* **2008**, *7*, 271.

[16] Ahmed, E. M. *J. Adv. Res.* **2015**, *6*, 105.

[17]   Torgersen, J.; Qin, X.-H.; Li, Z.; Ovsianikov, A.; Liska, R.; Stampfl, J. *Adv. Funct. Mater.* **2013**, *23*, 4542.

[18]   Previously summarized by Lumpi, D. (2015) In Hydrogels in Tissue Engineering: Two-Photon Polymerization"; lecture report: (166.202) Introduction to Biomaterials and Tissue Engineering.

[19]   Tomatsu, I.; Peng, K.; Kros, A. *Adv. Drug Delivery Rev.* **2011**, *63*, 1257.

[20]   Young, C.-D.; Wu, J.-R.; Tsou, T.-L. *Biomaterials* **1998**, *19*, 1745.

[21]   Kobayashi, M.; Toguchida, J.; Oka, M. *J. Biomed. Mater. Res.* **2001**, *58*, 344.

[22]   Elisseeff, J.; McIntosh, W.; Anseth, K.; Riley, S.; Ragan, P.; Langer, R. *J. Biomed. Mater. Res.* **2000**, *51*, 164.

[23]   Melchels, F. P. W.; Feijen, J.; Grijpma, D. W. *Biomaterials* **2010**, *31*, 6121.

[24]   Nandy, J. P.; Prakesch, M.; Khadem, S.; Reddy, P. T.; Sharma, U.; Arya, P. *Chem. Rev. (Washington, DC, U. S.)* **2009**, *109*, 1999.

[25]   Vaino, A. R.; Janda, K. D. *J. Comb. Chem.* **2000**, *2*, 579.

[26]   Lumpi, D.; Braunshier, C "Effective Reaction Monitoring of Intermediates by ATR-IR Spectroscopy Utilizing Fibre Optic Probes"; In Infrared Spectroscopy - Materials Science, Engineering and Technology, T. Theophanides (ed.); InTech, Janeza Trdine 9, 51 000 Rijeka, Croatia, 2012, ISBN: 978-953-51-0537-4, 493 - 510.

[27]   Lumpi, D., PhD Thesis RG Fröhlich, Vienna University of Technology, 2013.

[28]   Bakeev, K. A. (Ed.). (2005). Process Analytical Technology - Spectroscopic tools and implementation strategies for the Chemical and Pharmaceutical Industries, Blackwell Publishing Ltd., ISBN 9781405121033, Oxford/UK.

[29]   Rubin, A. E.; Tummala, S.; Both, D. A.; Wang, C.; Delaney, E. J. *Chem. Rev. (Washington, DC, U. S.)* **2006**, *106*, 2794.

[30]   Wiss, J.; Fleury, C.; Onken, U. *Org. Process Res. Dev.* **2006**, *10*, 349.

[31]   Minnich, C. B.; Buskens, P.; Steffens, H. C.; Baeuerlein, P. S.; Butvina, L. N.; Kuepper, L.; Leitner, W.; Liauw, M. A.; Greiner, L. *Org. Process Res. Dev.* **2007**, *11*, 94.

[32]   Grunwaldt, J.-D.; Baiker, A. *Phys. Chem. Chem. Phys.* **2005**, *7*, 3526.

[33]   Marziano, I.; Sharp, D. C. A.; Dunn, P. J.; Hailey, P. A. *Org. Process Res. Dev.* **2000**, *4*, 357.

[34]   Zogg, A.; Fischer, U.; Hungerbuehler, K. *Chem. Eng. Sci.* **2004**, *59*, 5795.

[35]   Melling P. J. & Thomson M. (2002). Fiber-optic Probes for Mid-infrared Spectrometry, In: Handbook of Vibrational Spectroscopy, J. M. Chalmers & P. R. Griffiths (Eds.), John Wiley & Sons Ltd., ISBN 0471988472, Chichester.

[36]   Raichlin, Y.; Katzir, A. *Appl. Spectrosc.* **2008**, *62*, 55A.

[37]   Lendl, B. & Mizaikoff, B. (2002). Optical Fibers for Mid-infrared Spectrometry, In: Handbook of Vibrational Spectroscopy, J. M. Chalmers & P. R. Griffiths (Eds.), John Wiley & Sons Ltd., ISBN 0471988472, Chichester.

[38]   Mazarevica, G.; Diewok, J.; Baena, J. R.; Rosenberg, E.; Lendl, B. *Appl. Spectrosc.* **2004**, *58*, 804.

[39]   Brancaleon, L.; Bamberg, M. P.; Kollias, N. *Appl. Spectrosc.* **2000**, *54*, 1175.

[40]   Mizaikoff, B. & Lendl, B. (2002). Sensor Systems Based on Mid-infrared Transparent Fibers, In: Handbook of Vibrational Spectroscopy, J. M. Chalmers & P. R. Griffiths (Eds.), John Wiley & Sons Ltd., ISBN 0471988472, Chichester.

[41]   Harrington J. A. (2010). Infrared Fibres, In: Handbook of Optics (3rd Ed.), M. Bass (Ed.), 12.1-12.13, The McGraw-Hill Companies, ISBN 978-0-07-163314-7.

[42]   McGarrity, J. F.; Prodolliet, J.; Smyth, T. *Org. Magn. Reson.* **1981**, *17*, 59.

[43]   McGarrity, J. F.; Ogle, C. A. *J. Am. Chem. Soc.* **1985**, *107*, 1805.

[44]   McGarrity, J. F.; Ogle, C. A.; Brich, Z.; Loosli, H. R. *J. Am. Chem. Soc.* **1985**, *107*, 1810.

[45]   Keegstra, E. M. D.; Zwikker, J. W.; Roest, M. R.; Jenneskens, L. W. *J. Org. Chem.* **1992**, *57*, 6678.

[46]   Heise, H. M.; Kuepper, L.; Butvina, L. N. *Anal. Bioanal. Chem.* **2003**, *375*, 1116.

[47]   Bentrup, U.; Kuepper, L.; Budde, U.; Lovis, K.; Jaehnisch, K. *Chem. Eng. Technol.* **2006**, *29*, 1216.

[48]   Jaumot, J.; Gargallo, R.; de Juan, A.; Tauler, R. *Chemom. Intell. Lab. Syst.* **2005**, *76*, 101.

[49]   Lumpi, D.; Braunshier, C.; Hametner, C.; Horkel, E.; Zachhuber, B.; Lendl, B.; Froehlich, J. *Tetrahedron Lett.* **2009**, *50*, 6469.

[50]   Waldner, B., Internship report RG Fröhlich, Vienna University of Technology, 2007.

[51]   Lumpi, D. Internship report RG Fröhlich, Vienna University of Technology, 2007.

[52]   Bachmann, W. E.; Hauser, C. R.; Hudson, B. E., Jr. *Org. Synth.* **1943**, *23*, 100.

[53]   Bayer, E.; Hemmasi, B.; Albert, K.; Rapp, W.; Dengler, M. Peptides, Structure and Function, Proceedings of the 8th American Peptide Symposium; Hruby, V. J., Rich, D. H., Eds; Pierce Chemical Company: Rockford, IL, 1983; pp 87-90.

[54]   Dal Cin, M.; Davalli, S.; Marchioro, C.; Passarini, M.; Perini, O.; Provera, S.; Zaramella, A. *Farmaco* **2002**, *57*, 497.

[55]   Yan, B. *Acc. Chem. Res.* **1998**, *31*, 621.

[56]   Lumpi, D.; Braunshier, C.; Horkel, E.; Hametner, C.; Froehlich, J. *ACS Comb. Sci.* **2014**, *16*, 367.

[57]   Chen, Y.; Baker, G. L. *J. Org. Chem.* **1999**, *64*, 6870.

[58]   Lumpi, D.; Wagner, C.; Schoepf, M.; Horkel, E.; Ramer, G.; Lendl, B.; Froehlich, J. *Chem. Commun. (Cambridge, U. K.)* **2012**, *48*, 2451.

[59]   Svatunek, D., PhD Thesis RG Allmaier, Vienna University of Technology, 2016.